UNIVERSITY OF NAIROBI

SCHOOL OF ENGINEERING

DEPARTMENT OF ELECTRICAL AND INFORMATION ENGINEERING

Development of Optimized Under-Frequency Load-Shedding Scheme With Renewable-Energy Integration

Student Name: Paul Muia Musyoka

Reg. No: F56/6984/2017

A Thesis Submitted in Partial Fulfillment for the Degree of Master of Science (Electrical and Electronic Engineering) in the Department of Electrical and Information Engineering in the University of Nairobi.

August 2020

Declaration

Name of student: Paul Muia Musyoka
Registration: F56/6984/2017
College: Architecture and Engineering
Faculty/School/Institute: School of Engineering
Department: Electrical and Information Engineering
Course Name: Master of Science (Electrical and Electronic Engineering)
Title of work: Development of Optimal Under-Frequency Load Shedding Scheme with Renewable Energy

1) I understand what plagiarism is and I'm aware of the university policy in this regard
2) I declare that this research proposal is my original work and has not been submitted elsewhere for examination, award of a degree or publication. Where other works or my own work has been used, this has properly been acknowledged and referenced in accordance with the University of Nairobi's requirements
3) I have not sought or used the services of any professional agencies to produce this work
4) I have not allowed , and shall not allow anyone to copy my work with the intention of passing it off as his/her work
5) I understand that any false claim in respect of this work shall result in disciplinary action in accordance with University of Nairobi anti-plagiarism policy

Name: Paul Muia Musyoka: Signature 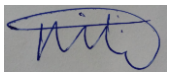 Reg. No: F56/6984/2017

Date: 19/ 06/ 2020

Supervisor's Approval

This thesis has been submitted for examination with our approval as university supervisors:

Dr. Peter Moses Musau: Signature:  Date: ....24th June, 2020.....

Dr. Abraham Nyete: Signature_____  _____ Date_____24th June 2020_____

Dedication

First and Foremost, I express my deepest of gratitude and an overflow of heartfelt love and joyful tears to Almighty God. You are 100% faithful in the way you keep a promise; how I wish I could be equally faithful.

Next, I dedicate this research to my Mum, Dad and Aunt Margret, who kept on asking me “Have you finished your project?” and I would just tell them, am halfway done. Next time you ask me I say “well, it has been a sweet melody each time you ever asked” vote of thanks.

Most important, I would like to thank my classmates Benson, Naomi and Wycliffe, for their grouping, team working and keeping together attitudes and admirable working attributes; showers of blessings.

Acknowledgement

I'm forever indebted to Dr. Peter Musau, for his patience, encouragement, unwavering support and more so, the prayer. Your immense technical expertise and contributions all along the due process are highly regarded. I must say, I was either fortunate or lucky to have you as my lead supervisor. I may not pay you back for your precious time, which you took out of your busy schedule, to ensure this research was moving forward and making weekly and monthly progress. I hope you find a kind satisfaction in the contents of this thesis.

Paramount to actualization of this thesis is Dr. Nyete's guidance, support and helpful suggestions, for organizing the seminars in which I presented the progress every other time, improved my presentation skills considerably. Your contributions are highly regarded.

Specifically to Ojwang Benson Onyango, I would not have come this far, and I know not where I would be right now, if you had not edited my many mistakes in formats, grammar and neatness, its brought me thus far.

My deepest gratitude to the chairman, department of electrical and information engineering, dean, school of engineering and director, graduate school for the administrative support that you have accorded this work throughout the research process.

Table of Contents

List of Tables

List of Figures

List of Appendices

List of Symbols, Abbreviations and Nomenclature

BPSO----------Binary Particle Swarm Optimization

EA----------Evolutionary Algorithm

EAPP----------East Africa Power Pool

EMTDC --------Electro Magnetic Transient Design and Control

E-VIEW---------Econometric analysis, forecasting and Simulation tool

GA----------Genetic Algorithm

KOSAP----------Kenya Off-grid Solar Access Project

KPLC----------Kenya Power and Lighting Company

NEPLAN--------Network planning Tool

NL----------Network Losses

PLCs----------Programmable Logic Controller

PSCAD----------Power Systems simulation tool

PSO----------Particle Swarm Optimization

REA----------Rural Electrification Authority

ROCOF----------Rate of Change of Frequency

TD----------Transmission and Distribution Network

UFLS----------Under Frequency Load Shedding

VD----------Voltage Deviations

ABSTRACT

Name: Paul Muia Musyoka

Registration No: F56/6984/2017

Development of Optimal Under-Frequency Load-Shedding with Renewable Energy

Under-frequency load shedding maximizes the performance of a power system at times of severe power imbalance. It involves trading off the total amount of load shed versus required frequency stability level, in order to prevent frequency collapse of the grid. For reliable power supply to consumers, renewable energy powered off-grid systems complement the main grid supply. Renewable energy micro-grids experience adverse frequency instabilities due to intermittent nature of the generation sources, and thus requiring load shedding. This comes at a loss of load and reduces operator's revenue, in pursuit of power system security and stability levels that comply to grid codes. Given the unpredictable consumer behavior, and the fact that shedding loads leads to economic losses for the utility, and a blackout to consumers, an optimal process of load shedding that disconnects the least load from the grid was developed in this research. The developed load shedding attains the grid code frequency stability levels and only applies as the option of last resort, towards securing the network from frequency collapse. A hybrid particle swarm – genetic algorithm, coded in MATLAB, is utilized to optimize the load shedding process given the conditions and constraints surrounding the modeled micro-grid, which is powered purely by renewable energy sources. Results from this study ascertain the optimization of load shedding process for the studied micro-grid. Though load shedding restores the micro-grid back to its stable operation, 100% optimization was not achieved. For instance, a maximum power imbalance of 269MW, has an optimum load combination constituted of 12 loads and falls in the second stage/ second priority of load shedding i.e. combines loads in domestic/ agricultural and commercial categories and spares industrial category of loads as per the prioritization. The total load disconnected for this imbalance is 295MW, consisting of 5MW, 6MW, 8MW, 10MW, 14MW, 16MW, 18MW, 23MW, 25MW, 31MW, 42MW and 97MW feeders. Hence a difference of 26MW (295-269) is disconnected unnecessarily since there is no single combination that adds up to 269MW. In conclusion, this research improves the design and practices of load shedding processes, lowers the Incidence of blackouts in off-grid areas and offers a solution for recovering the frequency stability of renewable energy islanded micro-grid networks, at times of severe power deficiency.

Keywords: ***Under-Frequency Load Shedding, Renewable Energy Islanded Micro-Grid, Frequency Stability, Kenya Off-Grid Systems, Frequency Recovery.***

CHAPTER ONE

INTRODUCTION

1.1. Background Information

Frequency of power supplied to consumers by a utility company needs to be regulated within specified standard range. If the demand is higher than the supply, the frequency falls while higher supply leads to higher frequency. Load shedding/ demand control is a process of disconnecting part of the load from the grid and is usually occasioned by severe deficits of power, in which the load demand is higher than the power supply [1]. Generation reserves are suitable solutions to provide the power balance during high demands, but are usually designed according to the peak demands in the load duration curve. Once the demand exceeds the total generation capacity, the utility's network is unable to support the load.

Load shedding is a measure taken by utility companies to curb voltage collapse and or frequency collapse, once other techniques such as automatic generation control, frequency compensation and or voltage compensation are unable to restore the health of the grid [2]. However, the shedding comes at a loss, either by loss of power not supplied or if the utility company is contracted to supply reliable source of power to a client, failure to which they pay them for loss of production and thus a disadvantage to the utility company too.

Mainly, the advantage of load shedding is that it maintains the health of the network in terms of frequency, voltage, active and reactive power capacity limits, hence avoids cost of replacements for equipment resulting from faulty operation. Load shedding is therefore an emergency operation by utility company, for security of their generation, transmission and distribution equipment [18-22].

The disadvantage of load shedding is that it results in blackouts that are not friendly to end users. Also the utility company loses revenue. Due to the fact that most of the economic (commercial, manufacturing etc.) and life-support activities rely on electricity; consumers demand and are ready to pay for reliability, security, reserve and availability of power and thus warrantying development of frequency recovery schemes with higher expectations from the utility company.

Micro-grid systems are usually brought into play, in order to supplement the main grid in such times of power imbalance and can be operated online or offline [3]. Kenyan grid system is majorly powered by renewable energy sources such as hydro, geo-thermal and wind turbines, which provide the bulk power sources at lower costs. Diesel generators are usually called to service at times of high demand and for stability reasons. The transmission grid code has therefore been affected by recent developments in the sector such as East Africa Power Pool (EAPP) [4] and more so by the Kenya Off-Grid Solar Access Projects [5]

Emergency and growth rate of renewable energy powered micro-grids (both online and islanded), in Kenya is very high. With current government policies in favor of the same, the trend will last for long. The main concern of a micro-grid, especially the ones powered by the intermittent sources of renewable energy, is the stability of the system at times of insufficient power. The ambitious Kenya national grid strategy for last-mile connections has further widened the gap between energy supplied from generation sources and the demand by consumers, since the out-stretched distribution networks experience extreme power losses due to their extreme low voltages and high currents.

This research optimizes the load shedding method of achieving power system stability, borrowing largely from specifications of the Kenya National Grid Transmission Code for the distribution and load profile model and from IEEE 9 Bus power system for the generation and transmission model. The strategy can be deployed optimally as the option of last resort, when preferable techniques such as automatic generation control and frequency compensation have failed to meet the power system stability threshold.

1.2. Problem Statement

Deficiency of power and faults on the grid is a major problem that results once the demand exceeds the total generation capacity of the power system, stretching the generation systems beyond their specified capacity, a fatal operation, which can result in destruction of equipment and components in the network. Most a times, utility companies respond to this deficiency by shedding the load, which results in blackouts, a disgusting experience on the consumers, loss of revenue and a breach of quality of service as per the contractual agreements[12-20].

in pursuit for a solution to this challenge, micro-grids have been invented to carry the loads that have been shed by the main grid or to supply to off-grid areas and vice-versa. These micro-grids can operate in either interconnected mode or in island mode; however they experience frequency fluctuations due to varying nature of load demand. The main grid in the interconnected mode of operation caters for, the frequency fluctuations. In the islanded mode, the instability persists and may lead to frequency collapse of the micro-grid[7-13].

With insistence on renewable energy for environmental safety, a challenge of intermittent nature of these energy sources is imposed on the micro-grid, which leads to necessity of load shedding in these networks. This thesis therefore finds an optimal solution to the under-frequency instability problem of an islanded micro-grid, which operates purely on renewable energy generators (hybrid wind/solar, hydro and geo-thermal). These generations are selected due to set up of the Kenyan micro-grid systems, in off-grid areas, where these generations are most available and majorly utilized as the main power sources [26-29].

The problems addressed in this thesis include load vs. generation prioritization and optimization of frequency stability through minimization of voltage deviations, frequency fluctuations, effect on renewable energy storage, amount of load shed and network losses. The UFLS strategy is applied as the option of last resort towards securing the micro-grid system from frequency collapse [6]. The constraints imposed on the optimization function include intermittent nature due to environmental constraints for the generations/ power sources, transmission/ distribution power loss limits and maximum and minimum generation capacities of the considered plants.

1.3. Objectives

1.3.1 Main Objective

Develop an optimized under-frequency load-shedding scheme for the model micro-grid, which economically dispatches generators, prioritizes the loads and optimally sheds the load during times of severe power deficiency

1.3.2 Specific objectives

i) Model an islanded renewable energy micro-grid

ii) Develop different scenarios the generation constraints imposed on each generator by the energy source

iii) Carry out a simulation of the micro-grid and carry out optimization of the frequency stability, for a steady operation of the renewable energy micro-grid with the formulated constraints

1.4. Research Questions

i) How does under-frequency load shedding affect the utility operator profitability, the power system network stability and the reliability of power?

ii) What are the key under-frequency load shedding implications in terms of frequency fluactuations and voltage deviations?

iii) Which is the most optimal load shedding strategy that balances cost of load shedding, stability level and power system reliability?

iv) Why is it necessary to do load shedding, given that it leads to loss of revenue to the utility operator and the power users are deprived of a reliable source of power?

1.5. Justification

[22-23]Renewable distributed generations are the driving forces behind the recent developments and higher indices of researches in this topic. Integrating the renewable energy sources in to the grid, especially solar farms, reduces the system stability, security and reliability at once. However, it's desirable to integrate the renewables, in order to reap the benefits of cheap energy sourcing and save the environment from adverse effects of thermal and diesel power plants.

Power system stability and security issues addressed in this thesis include effects of frequency fluctuations, voltage deviations, cost of load shedding and cost of renewable energy storage and network losses during power imbalance. Load shedding strategy is deployed to restore the system back to stability considering these aspects.

The study develops an improved frequency stability model of a purely renewable energy powered micro-grid, operating in an island mode, for use as option of last resort. The study provides minimal environmental effect, since the renewable energy source constraints are imposed on the objective function.

1.6. Scope of Work

A model of renewable energy sources micro-grid has been developed and simulations conducted in the MATLAB platform to optimize the multi-objective function, where hybrid particle swarm optimization-genetic algorithm (PSO-GA) is used.

The problems encountered in micro-grids, especially those regarding intermittency of renewable energy sources is covered in depth, with the developed solution based on load shedding only applying as a measure of last resort. The data utilized to simulate the system is outsourced from the Kenyan case study to depict applicability of the solution in the Kenya energy sector. The stability levels are also measured against the Kenya National Grid Transmission Code 2016.

The PSO-GA method has been selected and utilized in this research, due to its capabilities to optimize objective functions with non-linear functions, for optimum load shedding; when applied to deficit contingencies and losses for medium, small and large systems, and due to fact that, it adapts well with the system dynamics.

However, this research is limited to islanded micro-grids only and does not address effect of load shedding on the mechanical stability of the network components. More so, system stability formulations do not consider effect of temperature changes associated with losses and faults.

1.7 Research Contributions

The research explored and exploited five effects of load shedding strategies i.e. frequency fluctuations, voltage deviations, amount of load shed, renewable energy storage effects and network losses on the model renewable energy micro-grid. The national transmission grid code/ procedure for demand control is applied for the stabilization of rotor angle, based on the developed load shedding scheme.

The problem has been solved using a new technique, i.e. Hybrid PSO-GA, which had not been used previously by the presiding researchers. The mathematical modeling provides a unique processing of data and measurements from the model grid to realize highly reliable results in the simulation.

1.8 Thesis Organization

This thesis is organized into six chapters. Chapter one introduces the research topic and gives a detailed background, explains the problem statement, outlines objectives, justifies the research and offers an overview of the scope of work carried out. Chapter two is a literature review of the previous research works related to the topic, deriving the research gap and formulates the problem multi-objective function. Chapter three describes the methodology employed in solving the formulated problem and sources of the data used to model the renewable energy micro-grid. Chapter four illustrates the results realized from the research in plotted graphs and in tables forms. Chapter five analyses the results explaining and qualitatively interpreting the results. Chapter six concludes the thesis and recommends new areas of research in the under-frequency load shedding studies, with a key focus on multi-machine dynamic equivalents.

CHAPTER TWO

LITERATURE REVIEW

2.0 Introduction

UFLS is meant to balance the load demand vs. generation in periods of severe frequency drops that threaten the stability of the interconnected or islanded off-grid system. UFLS is a measure of last resort that is taken by utility operators at the expense of their revenue, where all other system stability measures have failed to yield desirable results. The number of activations of this strategy and total interrupted MW of load are two clear indicators of the system reliability, in an inverse proportionality relationship. The significance of UFLS can be assessed comparatively over time, to total load loss, once the strategy is activated.

2.1 Under Frequency Load Shedding With Renewable Energy

In order to find a solution to system setting uncertainty, fuzzy systems were used for load shedding to achieve the standard frequency stability of the grid, for optimal system operation and least cost of load shedding. Gray MK and Morsi WG [2] studied under frequency load shedding relay setting parameters such as input frequency and rate of change of frequency was carried out. Determination of these parameters was achieved by the use of particle swarm optimization as per the specifications of the design model In this study, the generation constraints and cost of load shedding are not addressed, however, load prioritization can suitably be achieved through this technique.

The crucial parameters of a relay setting such as shedding stages and shed loads, were determined prior to the scheme engagement and thus optimizing the shedding process. Hong Ying and Wei Shih [3] minimized the percentage of load that has to be disconnected and optimized the frequency shift by use of under-frequency load shedding relay. The method used to carry out these operations was the hierarchical genetic algorithm. An autonomous system of wind and diesel powered generation was constituted in the simulation, and used to demonstrate the application of the developed technique. The opportunity presented in this research is to

consider a variety of renewable energy sources which are currently the most common sources of power for practical micro-grids.

Guilherme P Borges et al [7] presented research results of a load shedding that achieves the desired grid stability, verified on a PSCAD simulation. MATLAB was used to model the islanded micro-grid, in which the particle swarm optimization based under frequency load shedding technique, to solve the power imbalance, was developed and demonstrated. The frequency stabilization was achieved by use of this technique. The weakness of this strategy was the failure to formulate the frequency fluctuations, prior to shedding and no considerations were made to ensure stable power flow.

Scenario based method is utilized in a research, where the frequency fluctuations and cost of storage of renewable energy are constituted in a multi-objective function. Musau Peter et al [8] considered the effect of wind and solar on power system frequency stability, investigating the loss of 180MW hydro plant generation that caused a total blackout for 3 hours The combined approach for frequency stability and energy storage cost function are presented for more precise results. However, the research does not consider the sensitivity factors for the power flow, and fails to address contingency and operational transients, which are key considerations for restoration of power balance. These effects result upon loss/connection of major generation or connection/ loss of large load that causes power imbalance.

Bayhan Sertac [9] used predictive under frequency load shedding algorithm based on the hardware in the loop test for load shedding. The algorithm was tested and validated. An AC islanded micro-grid is modeled and operated, applying the strategy to restore system stability, where the reliability is maximized amid unpredicted faults in the grid. The study fails to address the network losses and voltage changes that occur during power imbalance.

In a two stage load shedding scheme, the first stage ceases rapid decline in frequency, in which frequency deviations are measured locally and deployed in the process of load shedding, achieving a steady state condition. Quan Zhou et al [10] found a solution in a scaled down islanded micro-grid, which possess severe deficits of power, presenting a 2 –stage load shedding

scheme. The resulting power flow re-distribution upon load shedding is estimated, through distributed energy resources with high response inverters. Upon steady state condition, the load prioritization based second stage is activated to shade the load. Electro Magnetic Transient Design and Control (EMTDC) and PSCAD based time domain simulations are deployed to verify the developed scheme in a small-scale grid.

Musau P [11] carried out a review and formulation of the effect of renewable energy on frequency, voltage and rotor angle stabilities. The economic dispatch problem was solved by use of scenario based method. Optimal load shedding scheme using harmony search method was explored and an algorithm developed for the same. However the method didn't consider all the load shedding factors such as prioritization of loads and minimization of voltage deviations.

A thyristor switched lag compensator was used for improvemennts of frequency stability and optimization of the process was carried out using fire-fly algorithm. Musau P et al [12] considered parameters such as settling time, frequency deviation, nadir frequency and rate of change of frequency, in modeling the response of renewable energy power plants and developing frequency stabilization strategies. The results from this study indicate that frequency of parralled generation plants falls out of sychronism upon disturbance and low inertia turbine plants have least settling time and experience huge Rate of Change of Frequency (ROCOF) and high frequency fluctuations.

Digisilent software was used in simulation of Programmable Logic Controller (PLCs), in which the functions are embedded. Ali Parizard et al [13] demonstrated the operation of an islanded mode micro-grid, using intelligent load-shedding for power imbalances to stabilize voltage and frequency levels. The results affirm an efficient demand control for contingencies that are severe.

Muhammad Usman et al [14] formulates a multi-objective function for restoration of voltage, considering cost of demand control, voltage deviations and power losses.

A summary of the literature review is tabulated in Table 2.0, in which the contribution made in each of the reviewed works to under frequency load shedding is indicated. The methods used to

address the problems are presented and the opportunities recommended in each research work are shown for the 7 major research works that have been explored widely.

Table 2.0: Summary of Literature Review

Ref.	Title of the refered research	Contribution	Method/s Used	Recommended opportunties
[2]	Frequency Control and Under frequency load shedding in the isolated area of Sharorah	developed a design model, which determines UFLS setting parameters (rate of change of frequency and input frequency), to solve the uncertainty associated with the system setting.	Particle swarm optimization,	Didn't focus on the load shedding scheme based on using heuristic methods but conventional relaying
[3]	Multi-objective Under frequency load shedding in an autonoumous system using hierarchical genetic algorithms	Developed a method for determination of under frequency relay crucial parameters such as delay time, number of stages and percentage of load that needs to be shed to achieve the standard frequency.	Hierarchical genetic algorithm	Failed to address the renewable energy storage challenges.
[7]	Use of genetic Algorithm for Evalaution and control of Technical problems due load shedding in Power systems	Power imbalance is considered for load shedding in a micro-grid operated in the island mode, modeled using MATLAB	PSO based optimization technique	Ignores the effect of frequency deviations due to power imbalance
[8]	Effects of renewable energy on Frequency stability: A proposed case study of Kenya Grid	A renewable energy-based frequency instability mitigation method is developed in this research, considering storage cost function for renewable energy, in a combined approach with frequency stability model.	Scenario based method	Didn't address the issues of voltage deviations associated with deficiency of power on the main grid
[9]	Predictive Load shedding method for islanded AC	Hardware in the loop tests validates an	Hardware in the loop	The scheme failed to tackle the problems

	microgrid with limited generation sources	algorithm for predictive shedding of the load in an AC micro-grid operating in islanded mode	validated Predictive algorithm	resulting from frequency deviations
[10]	Two stage load shedding for secondary control in Hierachical operation of islanded micro-grids	Found a solution in a scaled down islanded micro-grid, which possess severe deficits of power, presenting a 2 –stage load shedding scheme.	Two-stage load shedding Scheme	developed technique shades more load than optimal before the grid stabilizes and thus expensive in terms of costs
[11]	Security and Stability Aspects of Multi objective Dynamic Economic Dispatch with renewable energy and HVDC transmission lines	Reviewed and formulated the effect of renewable energy on frequency, voltage and rotor angle stabilities	Scenario based method and Harmony search algorithm	The work didn't formulate or address the voltage deviations and cost of load shedding
In this Thesis	Development of Optimized Under-Frequency Load-Shedding Scheme With Renewable-Energy Integration	Formulated and simulated the five major effects of load-shedding on the transient stability of the micro-grid	Hybrid PSO-GA algorithm	Did not adress temperature related changes and mechanical components stability effects, resulting from load-shedding

2.2 Research Gap

While power systems/ grids are dynamic networks, recent developments in research have not fully addressed under-frequency load shedding problem in renewable energy micro-grid-based system. This is necessary for frequency stability and appropriate inertia constant, which dwindles with high rates of renewable energy penetration. With growth in generation technologies, more efficient plants and new energy sources are likely to grow and affect the timing and prioritization of loads, which will require re-configuration of the load shedding schemes to achieve optimal results [21-25].

Considering the constraints for the micro-grids such as generation constraints for different power plants, i.e. operation and maintenance costs of the micro-grids, energy storage and renewable energy frequency fluctuations and power flow, this thesis provided an optimized load shedding technique. The load shedding technique caters for the power deficiency and prevents frequency collapse in the islanded micro-grid system.

The key issues addressed in this thesis include frequency fluctuations, voltage deviations, amount of load shedding, cost of renewable energy storage and network losses. A multi objective function is formulated to factor the under frequency load shedding operation costs, fuel constraints, power imbalance, network losses and frequency deviations, for islanded micro-grids in isolated areas. The optimal load shedding algorithm based on hybrid PSO-GA method is utilized to shed the load for the modeled case, in order to achieve the required frequency stability levels, with a high penetration of inertia-less solar power sources.

2.3. Renewable Energy Generation Models and Effects on Stability

The generation characteristics of the various plants in the modeled islanded micro-grid i.e. PV panels, wind turbines, mini hydro-plants and Geo thermal power are formulated as follows;

PV Panels:

Solar PV generation model considered a number of factors. These generation factors included global irradiance and active area of the solar PV. The I- V characteristic of the solar cell is given by Equation (2.1), while the power generation characteristic for the PV solar system is given by Equation (2.2), where I_{ph} is the PV output current generated by cells, V_{ph} is PV terminal voltage and A is the active area of the solar panel. T is temperature, K is a solar constant,Ns denotes series connection, I_{pv} represents the net output current of the panel. R_{sh} indicates parallel resistance, R_s is series resistance, P.R represents AC power output in KW, P_{nom} is the nominal power in the nameplate in KW, Gs is sunlight condition in kW per MW and G_{ag} is the global irradiance in kW per MW. E_{pv} is the AC energy output for the evaluation period in kWh and H_{ag} is the total global irrandiance at the plane of PV module

$$I_{PV} = N_{PP}\left\{I_{PH} - I_D\left[exp\frac{q\left(\frac{V_{PV}}{N_S N_{SS}} + \frac{I_{PV}R_S}{N_{PP}}\right)}{AKT} - 1\right] - \frac{\frac{V_{PV}}{N_S N_{SS}} + \frac{I_{PV}R_S}{N_{PP}}}{R_{SH}}\right\} \quad (2.1)$$

$$P.R = \frac{\sum P_{PV}}{P_{nom}} * \frac{G_s}{G_{ag}} = \frac{E_{pv}}{P_{nom}} * \frac{G_s}{H_{AG}} \quad (2.2)$$

Wind Turbines:

The amount of power generated from a wind turbine depends on velocity of wind, radius of the rotor, tip speed ratio and density of air flow. Equation (2.3) inter-relates the power generation analytical model of the wind turbine, adopted in this thesis:

$$P = \frac{1}{2}\pi\rho R^2 C_P\left(\frac{\omega R}{V}, \beta\right)V^3 \quad (2.3)$$

Where ρ is density of air flow, R is radius of the rotor, v is velocity of wind, Cp (ωR / v, β) is a function for power coefficient based on pitch angle of the blade (β) and the tip speed ratio, i.e. (ωR / v) in which ω is the angular speed of rotor.

Geo-thermal generators:

Geo-thermal generators are stable renewable energy sources. The specific work output of this generator is given in Equation (2.4); Kenya derives more than 20% of the total electricity from Geo-thermal sources. The Geo-thermal plants have been modeled in this thesis as base load carriers.

$$w = \frac{W_{tatol}}{m_1} : \; W_{tatol} = W_{lpt} + W_{hpt} \quad (2.4)$$

In which w is the specific work output, W_{total} is the sum of low pressure turbine power output (W_{lpt}) and high pressure turbine output (W_{hpt}), while m_1 is the mass flux/ mass flow rate of the steam

Hydro plants:

Kenya generates over 40% of their electricity from Hydro power plants. Equation (2.5) characterizes the real power generation of an hydropower plant, where f is the 737.5 foot pounds to kW conversion factor, H is net head, θ is reservoir elevation, Q is total release from all sources, qi is generator release, ε_I is efficiency factor, γ is 62.4 specific weight of water and pi is the generated electric power

$$P_i = \frac{H(Q,\theta)\varepsilon_I \gamma q_i}{f * 1000} \quad (2.5)$$

Effect of Renewable Energy on system stability:

Renewable energy sources affect three main components of stability in a grid. This includes the rotor angle stability which is dependent on real power flow, voltage stability which depends on the reactive power flow and frequency stability that is determined by the inertia of the rotating machines in the system. Considering a total network resistance (R), rate of change of frequency (df/dt), effective reactacne (X), reactive power (Q), real power (P), system standard frequency (f0), inertia constant (H) and a receiving end voltage (V^R); the voltage drop and thus stability is given by Equation (2.6), for a constant voltage source. Rotor angle and thus the power factor of the system are given by Equation (2.7), and the stability of the frequency is highly dependent on the inertia of the system as illustrated by Equation (2.8).

$$\Delta V = \frac{RP}{V^R} + \frac{XQ}{V^R}\ ; since\ R \ll X; then\ \Delta V = \frac{XQ}{V^R} \tag{2.6}$$

$$\delta = \frac{XP}{V^R} + \frac{QR}{V^R};\quad since\ R \ll X;\ then\ \delta = \frac{XP}{V^R} \tag{2.7}$$

$$f_o = \frac{2 * H * \frac{df}{dt}}{\Delta P} \tag{2.8}$$

Renewable energy sources have low or zero inertia, and thus frequency fluctuations are high. These sources exhibit generation characteristics that are stochastic in nature and thus are unable to retain a constant voltage and power at generation, which leads to deviations in voltage and rotor angle.

2.4.Problem Formulation

2.4.1. Multi-objective Function

The Multi-objective under-frequency load shedding function is formulated as shown in Equation (2.9), which is a constitution of weighted sub-functions.

$$Min\ F = \{\varphi_1 LS + \varphi_2 VD + \varphi_3 NL + \varphi_4 FF + \varphi_5 RE\} \tag{2.9}$$

The non-linear equation (2.9), is composed of five sub-functions i.e.

i) Amount of load shed to restore system stability (LS),

ii) Network power losses (NL),

iii) Effect of frequency fluctuations (FF),

iv) Effects of voltage deviations (VD),

v) Renewable energy storage required to supply power during power imbalance (RE).

Weighting coefficients i.e.$\varphi_1, \varphi_2, \varphi_3, \varphi_4$ and φ_5 are constants ranging between 0 to 1, that determines the extent to which the individual factors are co-related to the system stability.

2.4.2. Sub-functions

The sub-functions constituting multi-objective function are formulated as follows:

i) Amount of load shed to restore system stability (LS)

An amount of load will have to be shed, as a measure of last resort, in order to restore the system stability, once power demand/load exceeds the total generation capacity. Total power imbalance of the system can be calculated by adding the individual imbalances for the n generators in the system, according to Equation (2.10).

$$\sum_{n=1}^{n} Pm_n - \sum_{n=1}^{n} Pe_n = \frac{2\sum_{n=1}^{n}\left\{H_n \frac{df_n}{dt}\right\}}{f_0} = \Delta P_{ls} \qquad (2.10)$$

In equation (2.10), ΔP_{ls} is the total load that should be shed to eliminate generation vs. consumption power imbalance, Hn is the inertia constant of n^{th} generator, and n is total number of generators in the system. Multiplying this equation with per unit cost of power gives the cost function of Equation (2.11), for shed loads to attain frequency stability.

$$CLS = C_i \left[\sum_{j=1}^{n} Pm_j - \sum_{j=1}^{n} Pe_j = \frac{2\sum_{j=1}^{n}\left\{H_j \frac{df_j}{dt}\right\}}{f_0}\right] \qquad (2.11)$$

In which Ci is per unit cost of load shedding, P_m is available mechanical power at the prime mover and P_e is the required electrical power at the generator terminals/ load demand

ii) Voltage deviations (VD)

Power imbalance (resulting from abrupt disconnection or connection of large machines) causes voltage deviations, which in turn would violate network equipment voltage range specifications, and lead to destruction of utility or consumer equipment. These effects should be minimized. The sum of squared voltage deviations is given in Equation (2.12), where VD is the squared voltage deviation, M is total number of nodes in the system, V_j and V_m are the voltage magnitudes of the jth bus and swing bus respectively.

$$VD = \sum_{j=1}^{M} \frac{\left(V_j - V_m\right)^2}{V_m^2} \tag{2.12}$$

The cost function for destructions caused by voltage deviations on network machines/ equipment and control/electronic loads is formulated in Equation (2.13). Where, CVD is cost of destruction of network devices, n is total number of devices whose voltage range specifications have been violated by the deviation, C is per unit cost of the network/consumer device and D is rating of the network/ consumer device.

$$CVD = \sum_{i=1}^{i} \sum_{j=1}^{j} \left(C_i D_j\right) \tag{2.13}$$

iii) Network power losses (NL)

Power imbalance and load shedding processes result in to power losses in the network that must be minimized. The mathematical representation considered in this research for cost function of the network power losses, both reactive and active power losses, is formulated as shown in Equation (2.14). In this equation, NL is the power losses associated with power imbalance load shedding measures, M is number of network nodes, G is conductance and B is susceptance as per the model power system specifications.

$$NL = \sum_{j=1}^{M} \sum_{i=1}^{M} \left\{V_j V_i \left(G_{ji} \cos\theta_{ji} + B_{ji} \sin\theta_{ji}\right)\right\} \tag{2.14}$$

iv) Frequency fluctuations (FF)

Frequency fluctuations during loss of generation, connection or disconnection of large network machines or large consumer loads may violate the frequency specifications of consumer devices or network equipment. The frequency fluctuations are formulated from swing equation, and are given in Equation (2.15), where *nrm* denotes normal operation period, f denotes faulty operation period, PG is total generation, PD is total demand, H_n is inertia constant of n^{th} generator and f is given by Equation (2.16).

$$FF = 2\left[\left(\frac{H_{nrm}\frac{df_{nrm}}{dt}}{PG_{nrm} - PD_{nrm}}\right) - \left(\frac{H_f\frac{df_f}{dt}}{PG_f - PD_f}\right)\right] \tag{2.15}$$

$$f = \frac{\sum_{n=1}^{N_g} H_n f_n}{H} \tag{2.16}$$

The cost of network equipment and consumer loads/devices destroyed due to violations of frequency specifications is mathematically represented by Equation (2.17). This formula accounts for a possible error that could result from double counting of devices destroyed as a result of both voltage and frequency deviations.

$$CFF = \sum_{i=1}^{n}\sum_{j=1}^{m}\left(C_i\{D_j - D_{nm}\}\right) \tag{2.17}$$

In Equation (2.17), CFF is the cost of destructions resulting from frequency fluctuations, C_i is per unit cost of n^{th} equipment, D_j is destroyed device power rating and Dm_m represents the doubly counted, destroyed network nodes.

v) Renewable energy conservation and storage cost (CRE)

The annual cost of equipment associated with renewable energy generation, power conversion and battery storage are given by Equation (2.18). where: CRE is cost of renewable energy generation, conversion and storage; T is the time period of study; P_i is the units of power generated, C_{PGi} is generation fuel cost, C_{EAi} is equipment and accessories costs and C_{RESi} is the cost reduction due to storage

$$CRE = \left\{ \sum_{i=1}^{T} P_i (C_{PGi} + C_{EAi} - C_{RESi}) \right\} \quad (2.18)$$

The multi-objective function of equation (2.9) is optimized subject to the load shedding constraints i.e. load flow condition, generator reactive and active capacities, node voltages, feeder current limits, load shedding limits, allowable frequency range, load priorities and fuel cell/ battery storage capacity, which are formulated in Equations (2.19) to (2.28).

2.4.3. Constraints

i) Load flow equations

The convergence criterion (allowable power loss), will be the maximum limit for the network loss cost function of Equation (2.14). The load flow equations are given in Equation (2.19) and (2.20), where the symbols carry their normal meanings in load flow studies.

$$Q_{DGi} = Q_{Li} + V_j \sum_{i=1}^{M} V_i \left(G_{ji} \cos \theta_{ji} + B_{ji} \sin \theta_{ji} \right) \quad (2.19)$$

$$P_{DGi} = P_{Li} + V_j \sum_{i=1}^{M} V_i \left(G_{ji} \sin \theta_{ji} + B_{ji} \cos \theta_{ji} \right) \quad (2.20)$$

ii) Generator reactive and active Capacities

The generators in the model micro-grid and hence power generation is subjected to maximum and minimum reactive and active powers of each generator, as per Equation (2.21) and (2.22), in which P is active power, Q is reactive power and mn denotes minimum while mx denotes maximum values for n generators.

$$P_{RGn}^{mn} \leq P_{RGn} \leq P_{RGn}^{mx} \;\; n = 1, 2, 3, \ldots n \quad (2.21)$$

$$Q_{RGn}^{mn} \leq Q_{RGn} \leq Q_{RGn}^{mx} \;\; n = 1, 2, 3, \ldots n \quad (2.22)$$

iii) Node Voltages

The range of voltages for various nodes are given according to Equation (2.23), and any violations triggers load shedding as the measure of last resort

$$V_n^{mn} \leq V_n \leq V_n^{mx} \quad n = 1, 2, 3, \ldots M - 1 \tag{2.23}$$

iv) Feeder Current limits

Flow of current in the model micro-grid is subjected to specified maximum and minimum limits as per Equation (2.24).

$$\left|I_{ji}\right| \leq I_{ji\,mx} \quad j, i = 1, 2, 3, \ldots M \tag{2.24}$$

v) Load Shed Limits

The cost function for load shed to attain the required system frequency stability of equation (2.11), is within the range specified, in order to ensure certain prioritized loads remain connected. The load shedding priority condition is applied according to Equation (2.25).

$$P_{lsn}^{mn} \leq P_{lsn} \leq P_{lsn}^{mx} \quad n = 1, 2, 3, \ldots M \tag{2.25}$$

vi) Allowable frequency range

A standard frequency range specified as per the network equipment specifications shall apply to the cost of frequency fluctuation caused destructions of Equation (2.17). The expression of the frequency range is given in Equation (2.26).

$$f_{ls}^{mn} \leq f \leq f_{ls}^{mx} \tag{2.26}$$

vii) Load Priorities

During UFLS, its necessary to consider the loads connected to the micro-grid and the consumer preferences. For n loads (feeders from a distribution power station) powered by the modeled micro-grid, the prioritization is given by Equation (2.27), in which P is the allocated load priority, where P1 has the highest priority while Pn has the least priority.

$$P_1 > P_2 > P_3 > P_4 \ldots > P_{n-1} > P_n \tag{2.27}$$

viii) Fuel cells storage capacity

Charging and discharging the fuel cells are limited to the capacities/ battery ratings for the system, as formulated in Equation (2.28), where T = discharge time, t= instantaneous time, P_{gt}= battery rating and E= total energy.

$$\sum_{t=1}^{T} \Delta t P_{gt} \leq E \qquad (2.28)$$

ix) Assumptions for coherence and dynamic equevalencing

The complexity of multi-machine transient stability requires reduction for faster analysis. By assuming that model micro-grid, a multi-machine system is coherent, it is reduced into a single machine, infinite bus bar system using Equation (2.29), in which the inertia constants of individual machines are ramped together.

$$H_{eq} = \frac{H_1 G_1}{G_S} + \frac{H_2 G_2}{G_S} + \cdots + \frac{H_N G_N}{G_s} \qquad (2.29a)$$

$$H_{eq} = \sum_{i-1}^{N} \frac{H_i G_i}{G_s} \qquad (2.29b)$$

Where Heq is equivalent inertia constant, H1 is inertia constant of machine 1, G1 is MVA rating of machine 1 and Gs is base rating and N denotes the number of machines.

2.5.Review of Micro-Grid Modeling and Simulation Tools

NEPLAN, PSS/E, DSA power tools, MATLAB, ETAP, CYME, Risk A, PSCAD/ EMTDC are some of the simulation software available commercially for the analysis, modeling and optimization of micro-grids with severe generation constraints. The tools include;

PSCAD/EMTDC

This tool is highly suited in the simulation of AC transients, power quality, transformer saturation, wind power, protection and faults and FACTs. Using automation libraries, the PSCAD can be called through scripts to make the necessary simulations.

CYME

The main package comprises of transmission modules, industrial module and power distribution module. Additional packages in this platform include cable ampacity calculations, ground grid analysis and design, electromagnetic transients analysis and simulation, among others.

NEPLAN

NEPLAN is a power system planning tool, with modules such as electricity (generation, industrial, transmission and distribution) modeling, Heating/gas/water (networks planning, analysis and optimization tool for heating, gas and water) and asset management (budget planning, operation, structures and supply reliability). NEPLAN 360 cloud offers the packages through cloud computing, while XGS lab (EN and IEEE standardized analysis of EMI), NEPLAN research (Modeling new power systems, control strategies and algorithms) and NEPLAN RACH for connection of loads to LV and MV networks.

MATLAB/ SIMULINK (Utilized in this Research)

MATLAB was selected for simulation of the model, due to its ability to use symbolic computation, and offered larger database of in-built algorithms. Most importantly, the student version license of MATLAB is a cheaper compared to other simulation platforms, some of which are purely commercial products.

A code written in MATLAB platform is used to simulate the formulated model. With graphs and tabulated output data after applying the different system constraints. The optimum stability level for the micro-grid model was searched by use of the hybrid PSO-GA technique and plots generated, indicating the changes in stability with respect to the five effects of load shedding.

2.6. Chapter Conclusion

This research solves a multi-objective under-frequency load shedding problem, as formulated in equation (2.9). The multi-objective function is subject to constraints outlined in equations (2.19) to equation (2.28).

From the literature review, there is no existing research that has formulated and addressed a multi-objective function under-frequency load-shedding, considering the five effects of UFLS i.e. frequency fluctuations, voltage deviations, cost of load shedding, renewable energy storage

cost and network losses. This gap has been addressed in this thesis, in which intelligent search hybrid PSO-GA method was deployed to optimize the non-linear function.

A model micro-grid was simulated and the load shedding strategy applied to optimize the effects resulting from this measure of last resort. Imposing constraints on the formulated function provided a practically applicable solution that optimally sheds loads on a grid with minimum effects on the system stability in terms of the five factors considered.

CHAPTER THREE

METHODS AND MATERIALS

3.1. Method Statement

This research involved power flow analysis of model micro-grid system using IEEE 9 bus system, with modifications to provide for adherence to Kenya National Grid Transmission Code. A computer code in MATLAB was developed and simulations carried out on the same platform. This code provided the functions and data structures for taking up varied data from table files/ arrays, processing the input data using hybrid particle swarm - genetic algorithm and displaying the output inform of text or table files and 2-D graphics. Fig. 3.1 illustrates the methodology in a flow chart. Results realized from these simulations were analyzed and compared with other research works that have been done before, and a conclusion drawn, illustrating the achievements and drawbacks of the model and techniques used to arrive at the solution.

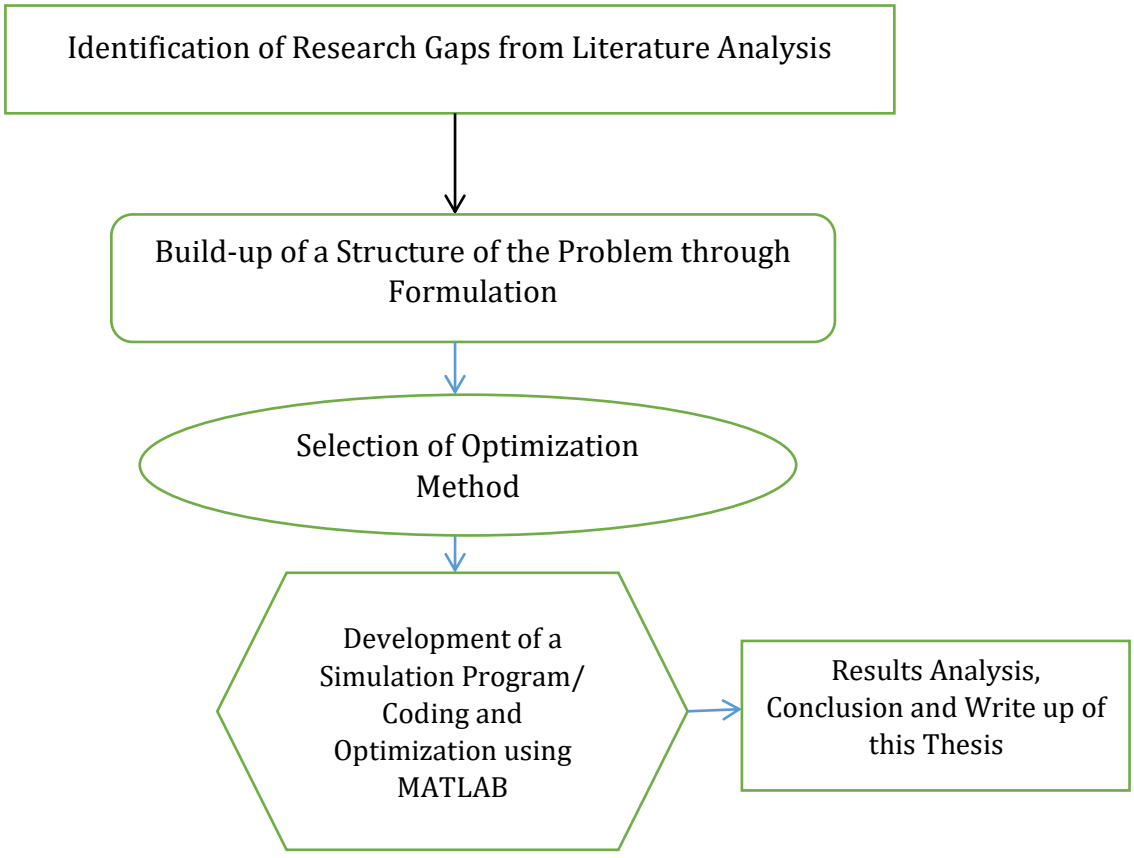

Fig. 3.1: Flow chart of the adopted methodology

3.2. Modified IEEE 9 Bus Transmission System (Secondary Data)

Relevant data for this section is attached in appendix C, with four main sections:

Section 1: Machine Data

Section 2: Exciter Data

Section 3: Governor Data

Section 4: Layout Diagram

3.3.Kenya National Grid Transmission Code (Secondary Data)

From Kenya National Grid Transmission Code, which incorporates East Africa Power Pool specifications data. The sets of data include: frequency regulation; voltages (i.e. steady state, transient and flicker); turbine and voltage controls; controllable wind turbine/ solar plants' (fault ride through, frequency range and ramp rates) and demand control (operation, methods of demand control, load shedding procedure and demand restoration), were obtained and utilized to develop the load shedding scheme with prioritized loads. These facts are outlined in the following sub-sections 3.4.1 through to 3.4.6.

3.3.1 Frequency

When operating within the normal conditions, the grid is operated within a range of ±1%, about the nominal frequency of 50Hz, ranging between 49.5Hz to 50.5Hz. This frequency band is expanded to ±2% i.e. a range of between 49.0Hz to 51.0Hz about the nominal frequency, upon occurrence of disturbance in the network. Once a major disturbance such as disconnection of large loads, failure of a major element in the transmission network or tripping of generating unit occurs, the frequency band can be expanded further up to ±2.5%, to range between 48.75 Hz to 51.25Hz.

Extreme operational measures allow extreme condition operation such as simultaneous occurrence of 2 or more major disturbances happening with frequency ranges of -5%/+3% of the nominal frequency for a maximum of 20 seconds before extreme measures such as load shedding

are taken. These operational conditions and respective frequency limits are shown in Table 3.3.1 (a).

Table 3.3.1 Frequency Limits for Grid operations

Operating condition	Freq. Limits (Hz)
Extreme fault operation	f>51.50 or f<47.75 for up to 20 sec.
Max. Band for system large fault	48.75 to 51.25
System disturbance	49 to 51
Normal operation	49.5 to 50.5

3.3.2 Voltage

a) Steady State Voltage

Avoiding excessive reactive power demand/transmission on the system and thus lower voltage drop levels requires location of reactive power generators close to reactive power consumers. For the nominal voltages used in the EAPP, i.e. 66kV, 132kV, 230kV, 110kV, 220kV, 400kV and 500kV, three operating conditions are specified with different ranges of voltage fluctuations/ drops as shown in Table 3.3.2 (a). The voltages can fluctuate between the lower and upper limits about the unit point.

Table 3.3.2(a): Steady State voltages for Model Micro-grid

Operational condition	Allowed Limits of voltage (p.u) swings
Multiple Contingency	0.85 to 1.20
Contigency (N-1)	0.90 to 1.10
Normal Operation	0.95 to 1.05

Power system operators are required to pursue their customers for power factors compliances such that during off-peak periods, the power factor is either lagging or unit and during peak demand, power factor should be at least 0.95.

b) Insulation Levels against Transient Voltages

Transient over voltages resulting from long transmission line switching or lighting surge, must be accounted for through insulation levels according to IEC 60071-1. For the Kenyan case, these insulation levels are provided in Table 3.3.2 (b),

Table 3.3.2(b): Insulation Levels against transient voltage limits

Nominal/Rated Voltage	50 Hz, 1 minute WV	Lighting Surge	Highest operating voltage
220kV	395kV	950kV	245kV
132kV	275kV	650kV	145kV
66kV	140kV	325 kV	72.5kV

c) Voltage Flicker

When a connection point experiences infrequent voltage flicker, it should not exceed 2.0. ± 3% while those connection points with repetitive voltage flicker, should not exceed 1.0 ± 1% p.u. of the steady state level of voltage.

3.3.3 Turbine controller

Turbine speed control should have a damping coefficient above 5 percent in steam turbines and above 3 percent in gas turbines, under any operating condition, and the speed of a generating unit shall not exceed 103 percent, which corresponds to 51.5Hz for a time period more than 20 seconds.

3.3.4 Voltage controller

Damping coefficient of the voltage control loop shall be at least or above 0.25 for entire operating range

3.3.5 Controllable wind turbine/ solar plants

a) Fault Ride Through

The plants provide active power that's proportional to retained voltages and maximizes reactive current supply during voltage dip while operating within its declared limit for at least 600 milliseconds or until voltage recovery to normal operating range. The plant will provide 90 percent of its max. active power within 1 second upon voltage recovery.

b) Frequency Ranges

These RES generating units must remain connected for limits of:

i) 0.5 Hz, rate of change of frequency.
ii) 20 seconds for frequency range of 47.0 to 47.5 Hz
iii) 60 minutes for frequency ranges of 49.0 to 51.0 Hz
iv) Continuously operate at frequency range of 49.5 Hz to 50.5 Hz

c)Ramp Rates

Ramp rate settings for the wind turbine shall be in MW per minute, for averages of 10 and 1 minute, with independent setting options for varying each of the two, over ranges of 1MW and 30MW.

3.3.6 Demand Control/ load shedding

a) Demand Control Operation

Rather than risk cascading outages, uncontrolled failure for apparatus or plants, the network operator, after exhausting all alternative remedy action, shall disconnect loads from the power system, since demand control is only necessary as a measure of last resort.

b) Methods of Demand Control

The security of the micro-grid can be preserved through application of either of the following three types of demand control

i) Planned load shedding (manual) which includes rota load disconnection and voltage reduction
ii) Emergency manual load shedding
iii) Automatic under frequency/ under voltage relays load shedding

c) Adopted Kenya National Grid/ EAPP Load Shedding Scheme Procedure guidelines

a) For automatic load shedding, each operator avails 60% of their annual peak demand for demand control

b) Dynamic performance of the system determines the shedding schemes through probable demand vs. generation imbalance simulation

c) Analysis carried out to determine and eliminate over-voltage, over-frequency and transmission overloads that are unacceptable

d) Loads on the network section subject to shedding are divided in blocks, whose under voltage/ frequency settings, block size, location and number is non-discriminatory and considers constraints of the power system for automatic shedding

e) If automatic load shedding fails to clear out the critical condition, manual disconnection of extra loads is permitted to restore the system

f) Upon stabilization, the disconnected demand can be restored as per the instruction of control center

g) Relay settings for low voltage/ frequency should be in coordination with plans for emergency procedures and operations

h) The levels of disconnected loads and under frequency/ voltage relay settings should be reviewed annually

d) Demand Restoration

Black start and system restoration procedures should be applied during restoration, after partial or total shutdown in practically equitable stages

3.4. Renewable Energy Micro-Grid Modeling

A modified IEEE 9 bus system has been considered. The network constitutes of 3 power plants i.e. Hydropower plant, a hybrid wind/ solar plant and geothermal plant. The transmission of the power is provided by the 12 buses, according to the architecture of Figure 3.4.0. There are 3 loads with different number of feeders, labeled Load 1, Load 2 and Load 3. These loads are specified in section 3.4.3. The islanded micro-grid in this dissertation is an “island” isolated from within the national grid and hence its maximum power ranges on the higher side above the normal assumptions of average power for a stand-alone micro-grid.

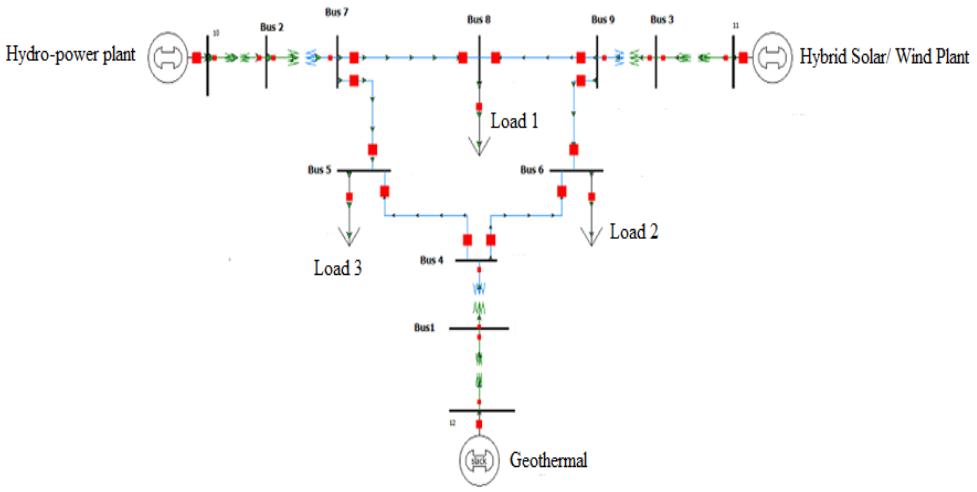

Figure 3.4.0: Layout plan of the model power system

3.4.1 Generation Model

a) Hydro power Generation

A hydro plant modeled based on quation (2.5) is developed, with the input and output parameter constraints as tabulated in Table 3.4.1 (a)

Table 3.4.1 (a): Hydro-turbine power generation

Input Parameter	*Output Parameter*	*Data Type*
Gravitational Acceleration in M^2 per second	Hydro-Power (MW)	constant
Density of water in K/M^3		constant
Hydraulic Head in M		Variable
Volumetric Flow rates		Variable
Efficiency of Hydro-turbine		Variable

b) Hybrid Wind Turbine/ Solar farms Model

Wind turbine generation model is developed in the simulation code, with input and output parameters as shown in Table 3.4.1 (b), the model is based on equation

Table 3.4.1 (b): Wind Turbine Generation Model

Input Parameter	*Output Parameter*	*Data Type*
The average density of air at		constant

NTP (20 Degs and 1 atm) is 1.204 kg/m3	Wind-Power (MW)	
Standard power coefficient range of a wind turbines		Variable
Diameter size of wind turbines in the wind farm in ft.		Variable
velocity of wind in miles per hour varying from 11 to 27 miles per hour		Variable
Number of wind turbines in the farm		Constant

Solar PV farm model is established per equation (2.2), with the input and output parameters indicated in Table 3.4.1 (c).

Table 3.4.1 (c): Solar PV farm model parameters

Input Parameter	*Output Parameter*	*Data Type*
Solar PV efficiency range	Solar PV-Power (MW)	constant
Range of performance ratio co-efficient dependent on temp and losses		Variable
Solar radiation in kWh/sq.m according to EPRA and Global Solar atlas		Variable
Area covered by Solar PV farm in sq. Meter		Constant

A base load carrier geothermal flash steam generation unit is provided in the micro-grid, as a base carrier with an output capacity of 175MW, hence the input parameters/ constraints are assumed.

3.4.2 Transmission and Distribution Power Losses Model

Using the modified IEEE 9 Bus system with the constraint three generators of section 3.4.1, a power flow solution based on equations 2.19 -2.24, is carried out for power loss using NR method for transmission system. An additional distribution system and non-technical power loss provided for, ranging between 15 to 18 percent as per the world bank 2019 report on energy efficiency for Kenya national grid systems.

3.4.3 Distribution Feeders Switching/ Loading Profile Model

The three distribution stations are constituted of feeders as illustrated in Table 3.4.3 (a). The islanded micro-grid in this dissertation is an "island" isolated from within the national grid and hence its maximum power ranges on the higher side above the normal assumptions of average power for a stand-alone micro-grid.

Table 3.4.3 (a): Loading profile for the renewable micro-grid

Name of Substation Feeder Relay	SS1 (Central Rift)			SS2 (North Rift)			SS3 (West Kenya)		
	OPL	AAL	PL	OPL	AL	PL	OPL	AL	PL
Baringo	3.4	6.4	9.8	X	X	X	X	X	X
Nakuru	69.9	132.8	202.7	X	X	X	X	X	X
XNarok	4.9	9.3	14.2	X	X	X	X	X	X
Elgeyo Marakwet	X	X	X	5.2	3.4	5.2	X	X	X
Nandi	X	X	X	18.2	11.9	18.2	X	X	X
Tranzoia	X	X	X	10.6	20.0	30.6	X	X	X
Uasin Gishu	X	X	X	33.5	63.5	97.0	X	X	X
West Pokot	X	X	X	2.0	3.7	5.7	X	X	X
Bomet	X	X	X	X	X	X	3.4	6.4	9.8
Bungoma	X	X	X	X	X	X	7.9	15.1	23.0
Busia	X	X	X	X	X	X	6.3	11.9	18.2
Homabay	X	X	X	X	X	X	4.9	9.3	14.2
Kakamega	X	X	X	X	X	X	13.9	26.5	40.4
Kericho	X	X	X	X	X	X	10.5	19.8	30.3
Kisii	X	X	X	X	X	X	14.5	27.4	41.9

Kisumu	X	X	X	X	X	X	37.9	72.0	109.9
Migori	X	X	X	X	X	X	8.6	16.2	24.8
Nyamira	X	X	X	X	X	X	2.8	5.4	8.2
Siaya	X	X	X	X	X	X	6.1	11.6	17.7
Vihiga	X	X	X	X	X	X	5.7	10.7	16.4

An ideal daily load curve is generated from the data provided in table 3.5.3 (a), considering off-peak total load from 2200Hours to 0400Hours; Actual/ Average Load from 0500Hours to 1800Hours and Peak Load from 1900Hours to 2100Hours, depicting a typical week day load profile.

3.4.4 Coherence and Dynamic Equivalency

The complexity of transient stability is reduced for faster analysis. By assuming a coherent multi-machine system which reduces into a single machine, infinite bus bar system using equation (2.29), in which the inertia constants of individual machines are ramped together.

3.4.5 Prioritized Load Shedding Scheme Development

Either the above distribution feeders are classified into three categories, as industrial loads, commercial loads or domestic / agricultural loads as indicated in Table 3.4.5. The islanded micro-grid in this dissertation is an "island" isolated from within the national grid and hence its maximum power ranges on the higher side above the normal assumptions of average power for a stand-alone micro-grid.

Table 3.4.5 (a): Grouping and Prioritization of loads

Group	Priority	Name of the feeder/ Load			
Industrial Load	High	Nakuru	Kakamega	Kericho	Kisumu
Commercial Loads	Mid	Bungoma	Nandi	Homabay	Narok
		Transnzoia	Kisii		
Agricultural/ Domestic Load	Low	Baringo	Marakwet	West pokot	Busia
		Migori	Nyamira	Siaya	Uasin Gishu
		Bomet	Vihiga		

Once power imbalance is detected and a measure of last resort is deemed necessary, the system searches through domestic loads for a suitable combination of loads that add up to approximately

equal the power imbalance, since this is within optimal points. Iterations are made, computing sum total of the possible load combinations (particle population) and checking system stability to select the most effective (stable) solution according to equation 2.9 i.e. the objective function.

3.5.Under-frequency Load Shedding Optimization Techniques

A summary of the methods that have been used to address single or multi – objective under frequency load shedding optimization problems are illustrated in Table 3.5, indicating their advantages and disadvantages in solving the UFLS problems.

Table 3.5 Summary analysis of Techniques for Solving UFLS

Method	**Advantages**	**Disadvantages**
PSO algorithm	Faster convergence or low computation time	Getting trapped in a local minima Premature convergence
Hierarchical genetic algorithm	Takes less number of iterations to find fit solutions Guarantees wide range of solution due to mutation	Lacks a clear stop creterion Tends to converge at local Optima
Scenario based method	Erroneous solutions may result from penalties given by tracking models	Solution performs well in different possible scenarios
Hardware in the loop test algorithm	Assumptuions made in transfer function may be inaccurate	-Suitable for multi input – multi-output systems
2- stage load shedding scheme	Lower damping in the second stage results into osscilations	Stops rapid frequency decline and restores suystem to intial state if generation is available
Harmony search method	Repetition of solution vector Use of fixed values for both bandwidth generation and pitch adjustment rate	Fast convergence Low running time per iteration
Hybrid PSO-GA *(Selected and utilized in this thesis)*	*Advantages include:* Avoiding Stagnation of particles Convergence in sub-optimal, local optima and minima is to be eliminated The number of iterations reduce	*Demerits:* Each iteration take longer time to evalaute the particle position and or new velocity.

3.6. Justification of Hybrid PSO-GA Optimization Algorithm

The utilized hybrid methods, whose flow chart is shown in Figure 3.1, i.e. hybridized genetic algorithm with particle swarm optimization techniques were considered for solving the multi-objective optimization problem formulated in equation (2.9) . These methods have not been used previously as far as the literature reviewed is concerned. The following characteristics adapt this method to the problem formulated in the multi objective function in chapter two, equation (2.9):

a) Application of PSO ensures optimized load shedding scheme with minimum number of iterations is constituted to achieve the convergence criterion
b) Cross over and mutation operations suitably adapts to the system dynamics, for large, small and medium power systems with considerations for losses and contingencies
c) Escaping local minima traps provides ability to deliver high power quality solution for the constraint grid during the load shedding process
d) Swarm and individual confidence adjustment constants guarantees the capability to optimize this objective function with non-linear functions for optimum load shedding

3.7.Hybrid PSO – GA method Flow Chart

Hybrid PSO-GA benefits from three main components i.e. first, escaping from local minima traps or premature convergence as a result of mutation operation in the whole population. Second, reduction of dimensionality achieved through application of crossover in partitioned sub-populations for a diverse population. Third, exploitation and exploration process balancing due to application of PSO. The algorithm for this method adopts the flow chart shown in Figure (3.7), and whose steps are outlined as follows;

Step 1: Initialization of population (size of population, swarm and individual acceleration constants, probability of mutation and crossover, number of partitions, partition variables and solutions etc.)

Step 2: Fitness function evaluation for search agents

Step 3: Application of PSO on the whole population

Step 4: Genetic Algorithm selection operator is applied on the population

Step 5: Partitioning of the whole population in Sub partitions/ sub-populations

Step 6: Arithmetical cross over is then applied to each sub-population

Step 7: Mutation operator of genetic algorithm is applied to the swarm

Step 8: Update the global best and individual best positions and iterate until the convergence criteria is met

The position and velocity of each particle is updated in every iteration according to Equations (3.1) and (3.2). In these equations, x represents the position of the particle, v represents the particle velocity, pb is the best position achieved by the particle, gb is the global best position, j denotes the iteration number, 0 denotes the previous iteration and 1 denotes the current iteration.

$$x_j^1 = x_j^0 + v_j^1 , \quad j = 1, 2, 3, 4 \dots P \tag{3.1}$$

$$v_j^1 = v_j^0 + \in_1 r_{jl}\left(pb_j^0 - x_j^0\right) + \in_2 r_{j2}\left(gb - x_j^0\right) \tag{3.2}$$

The crossover operation is done by first choosing a random set of β such that;

$$\beta \in (0,1) \tag{3.3}$$

2 offspring are generated from parents such that;

$$OS_j^1 = \beta pop_j^1 + (1-\beta) pop_j^2 \tag{3.4}$$

$$OS_j^2 = \beta pop_j^2 + (1-\beta) pop_j^1 \tag{3.5}$$

In Equations (3.3), (3.4) and (3.5) OS represents offspring, pop is population and j denotes the iteration.

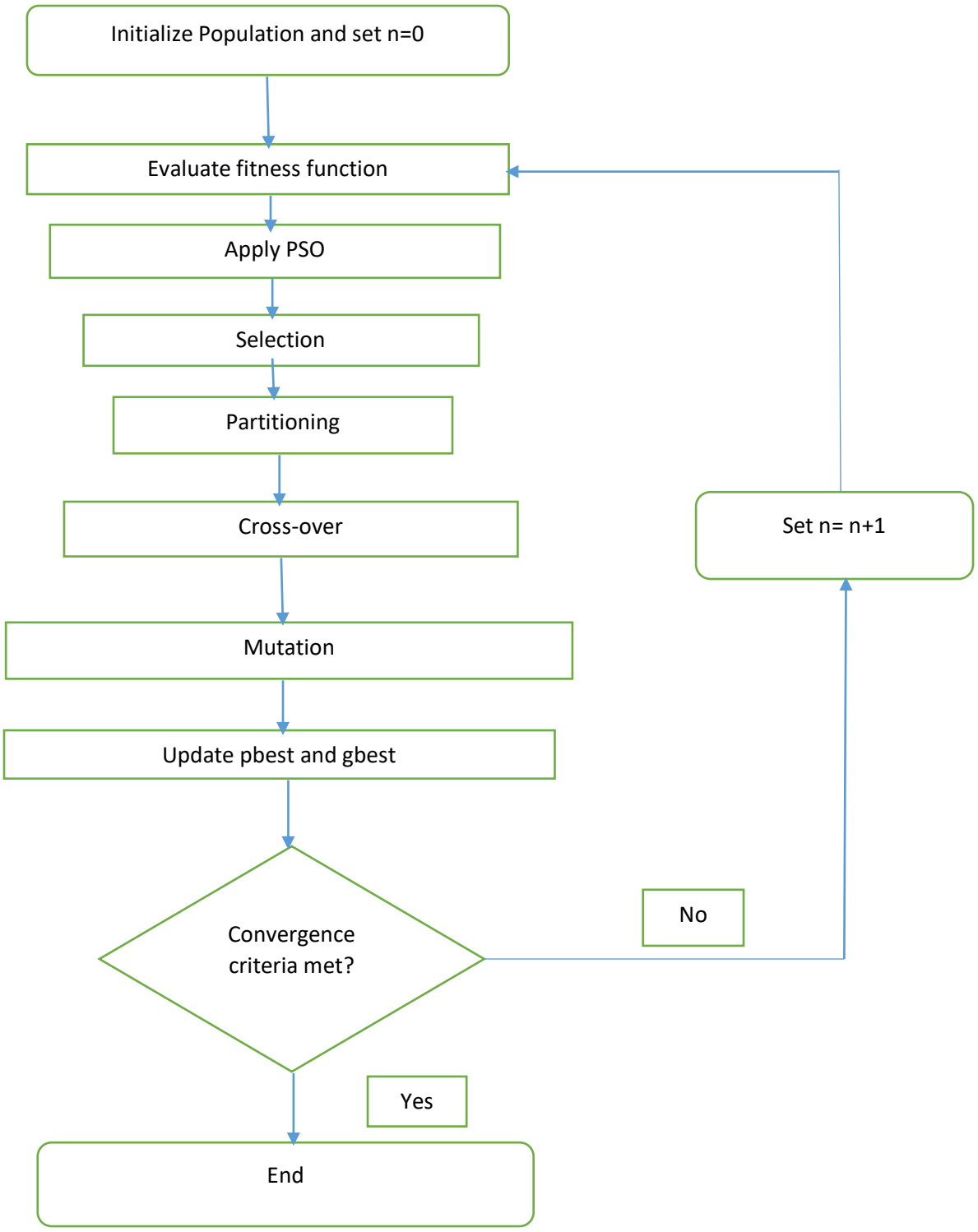

Figure 3.7 Hybrid PSO – GA method flow chart

3.8.Mapping of the Hybrid PSO-GA Method to the Multi-Objective Problem Formulation

Table 3.8 illustrates the mapping of the various parameters in the PSO-GA algorithm, in which a population of 1500 possible load shedding schemes are searched through, evaluated and optimum solution derived according to the objective function of equation (2.9). The mapped parameters are coded in a MATLAB platform, in which the simulation runs.

A population of 1500 was the highest number of possible combinations for a single value of power imbalance and was generated from the code. Gene sizes of 32 bits were considered necessary since there are 5 weights in the multi-objective function (2^5 = 32). The cross-over probability and mutation probabilities were selected from general recommendations applicable to the technique. However, to encourage cross-over and hence population variability for new generations, a high value of cross-over probability (above 0.6) was considered i.e. 0.75. On the other hand, mutation is discouraged, since it leads to a generation that doesn't constitute original characteristics of the species and hence a value below 0.2 was considered i.e. 0.1.

Table 3.8. Mapping of the hybrid PSO-GA method to the multi-objective function

No.	Hybrid Method Variable/ operator	Multi-objective variable description	Limits/ Specifications
1.	Population/ particles/ chromosomes	(CLS, CVD, CFF, CNL, CRE) possible solutions (combinations of loads optimal for shedding)	1500
2.	Genes	32bits	32
3.	Cross-over	Probability	0.75
4.	Mutation	Probability	0.01
5.	Selection	Minimum Calculated Value of chromosomes	Optimal point
6.	gbest	Global best position	A variable
8.	Velocity	Rate of change of positions	Updated in each iteration
9.	Positions	Values assumed by particles	Updated in each iteration
10.	pbest	Individual Particle best position	A variable
11.	Fitness Function	Multi-objective function	Eqn 2.9
12.	Number of Partitions	As per size of sub-populations	3
13.	Number of Possible Solutions per partition	Sub-populations	500 individuals per sub-population
14.	Convergence Creterion	After 50 iterations	50 iterations
15.	Time counter (t)	1/t = execution speed	Speed of execution

3.9.MATLAB Based Simulation Code

A code written in the MATLAB language is used to simulate the under-frequency load-shedding in the model micro-grid, and derive the optimal swing curves for populated possible shedding schemes, depending on the size of power imbalance. This code is availed in appendix A of this thesis.

3.10 Chapter Conclusion

In order to model the renewable energy micro-grid, secondary data was sourced according to section 3.2 and 3.3. This data is utilized to develop a model renewable energy micro-grid constituting generation, transmission/distribution, load profile and a load shedding scheme based on the formulated objective. The model micro-grid is coded in Matlab language for simulations as per Section 3.9 and Appendix A. Load shedding is applied only as a measure of last result to stabilize the grid. The developed load shedding scheme prioritizes the loads through classification into industrial, commercial and agricultural/ domestic load blocks. This classification ensures discrimination during shedding process, according to different levels of reliability required for different load sizes by the Kenya electricity transmission code.

CHAPTER FOUR

RESULTS ANALYSIS

4.1 Generation Models (GenMod)

4.1.1 Generation Model Findings

Power supply of the model renewable energy micro-grid varies with variation in mechanical power sources such as wind, hydro-head, solar radiation and highly depends on power harvesting equipment design and efficiencies. Considering these parameters, the simulation adopted a total generation varying from 175.55 to 1316.24, for economical unit commitments during hours of the day as shown in Table 4.1.

Table 4.1 Generation model power outputs variations based on intermittent sources

wtcp	wtd	wv	wtg	hth	htq	hte	htg	h	opc	a	pvg	gtg	TG
.25	43	11.0	0.22	10	1	.8	.079	.33	.075	10	.25	175	175.55
.27	49	12.6	1.55	24	20.9	.82	4.01	.35	.083	109	3.15	175	183.72
.29	54	14.2	5.07	38	40.8	.83	12.62	.36	.091	208	6.9	175	199.60
.31	60	15.8	12.87	52	60.7	.85	26.16	.38	.099	307	11.6	175	225.63
.33	66	17.4	28.3	66	80.6	.86	44.88	.40	.107	406	17.36	175	265.54
.35	71	19.0	56.5	80	100.5	.87	69.01	.41	.116	505	24.30	175	324.82
.37	77	20.6	105.0	94	120.4	.89	98.81	.43	.124	604	32.54	175	411.37
.39	83	22.2	184.5	108	140.3	.91	134.52	.45	.133	703	42.19	175	536.18
.41	89	23.8	309.5	122	160.2	.92	176.39	.46	.143	802	53.40	175	714.25
.43	94	25.4	499.6	136	180.1	.93	224.67	.48	.152	901	66.29	175	965.55
.45	100	27.0	780.7	150	200.0	.95	279.59	.50	.162	1000	81	175	1316.24

Key

wtcp	wind turbine coefficient	htg	hydro-turbine power output from the hydro-power generation model
wtd	wind turbine diameter	h	solar radiation
wv	wind velocity	opc	solar pv performance coefficient/ efficiency
wtg	wind turbine power output for the constituted wind turbine generation model	a	area covered by solar panel in 1000 M^2
hth	hydro-turbine head	pvg	solar panel power output from the solar PV generation model
htq	hydro-turbine flow rate	gtg	geothermal base load carrier generator
hte	hydro-turbine efficiency	TG	total generation for the renewable energy micro-grid

4.1.2. Discussion of Generation Model Results

Four different generation technologies are considered for powering the micro-grid. A wind turbine generation farm with 3 variable input parameters i.e. standard power coefficient of 0.25 to 0.45, turbine diameter of 130 to 300 ft. and wind velocities varying between 11 to 27 miles per hour was considered. It generates 0.22 MW at its worst (operating at the lower limits of its input variables) and 780.7MW when wind speeds hit the upper limit. Since the velocity of wind flow is stochastic, the power output from this plant is also stochastic, necessitating adaptable grid stabilization measures for frequency and voltage.

A hydropower plants farm model, whose input variables include hydraulic head ranging between 10 to 150 meters, volumetric flow rates of 1 to 200 cubic meters per second and turbine efficiency of 0.8 to 0.95, generates at its best 279MW and 0.079 MW when operated at its worst. The unpredictability of rainfall and annual seasons provides a pattern for hydropower generation that is unreliable during off-seasons, when the levels of water are below limits for generation.

Solar PV generation farm whose input parameters include efficiencies of 0.15 to 0.18, performance ratio of 0.5 to 0.9, covering an area of 10000 to 100000 sq. m and a solar radiation of 0.333 to 0.5 kwh/sq.m has capacity to produce 0.25MW at its worst and 81MW at its best. Expected generation from these plants is much unpredictable since solar radiation varies with variation in cloud cover, making it a stochastic generation system.

The geothermal flash steam power plant is a more stable source of renewable energy, whose carbon footprint is low and has a stable source of mechanical power. It's therefore suitable for use as a base load carrier in a renewable energy micro-grid.

4.2 Transmission and Distribution (TD) Losses

4.2.1 TD Loss Results

The transmission and distribution losses model considers load flow studies for the transmission network using the IEEE 9 Bus system, and considers distribution losses of about 14 to 18 percent of the generation, according to distribution distances and voltage levels, as per the World Bank energy efficiency survey 2019. The resultant power loss profile is illustrated in the graphs of Figure 4.1.

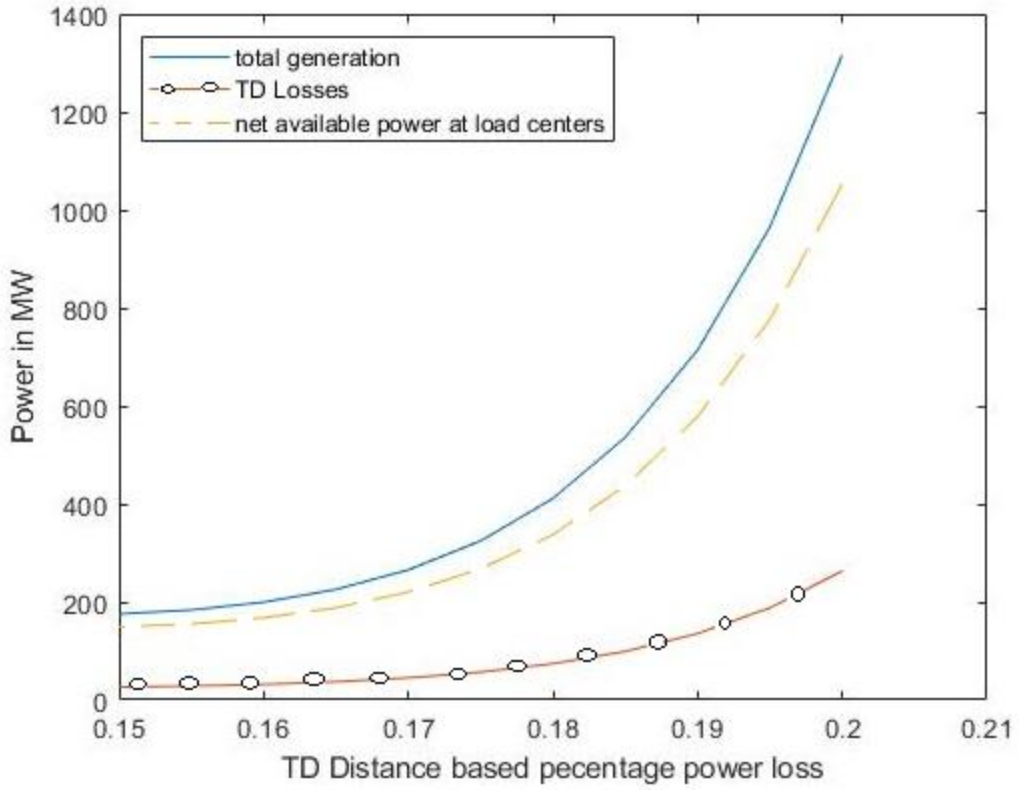

Figure 4.1. Resultant power loss for the micro-grid TD network

4.2.2. Evaluation of TD Loss Findings

Considering IEEE 9 bus system, a load flow study is carried out to derive the percentage transmission losses averaging at 2%, since the transmission voltage are higher. Distribution losses are accounted for, considering last mile connection distances and voltage levels, which indicate a total loss of 14% to 18% percent of the generated/ evacuated power, according to World Bank energy efficiency report 2019. These losses further contribute to the power deficiency and unmet demand, which in turn makes the grid unstable.

4.3 Power Demand/ Load Profile

4.3.1 Power Demand/ Load Profile Findings

The loads constituted in this section are isolated from the Kenya Distribution Master Plan (KDMP) report, composed by Kenya Power and Lighting Company for 2011 to 2031 load forecasting and distribution expansion for the western region. Since the islanded micro-grid in

this dissertation is an “island” isolated from within the national grid, its maximum power ranges on the higher side above the normal assumptions of average power for a stand-alone micro-grid. The ideal curve is obtained by summation of actual loads and calculation of peak and off peak loads from recorded load factors and is illustrated in Figure 4.2.

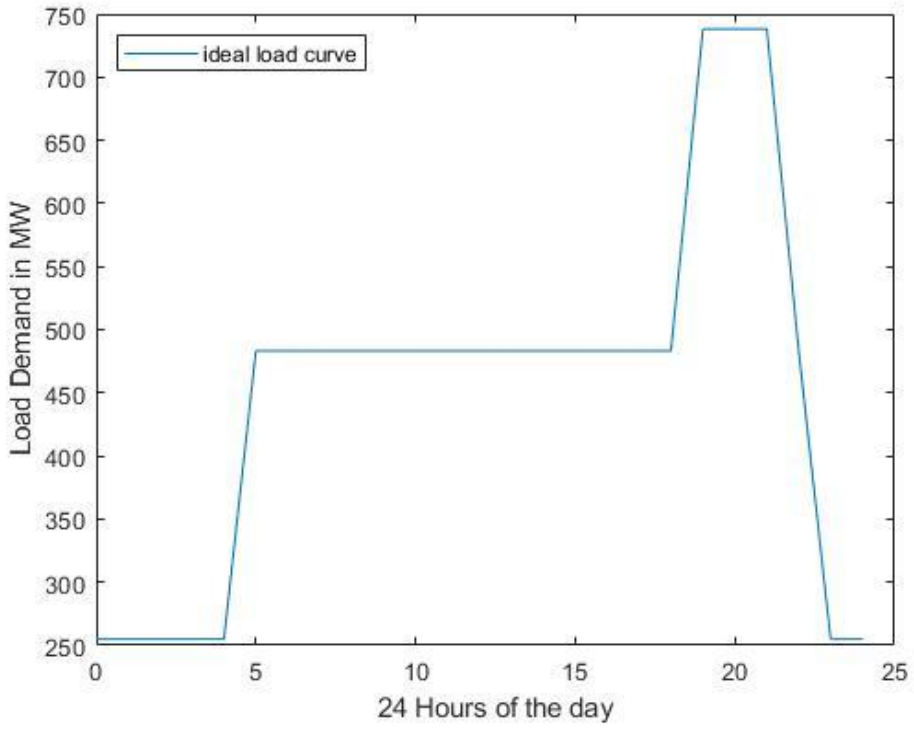

Figure 4.2 Ideal load curve model for the Renewable Energy Micro-grid.

4.3.2. Evaluation of Power Demand/ Load Profile

Isolated from KPLC distribution master plan report, the three main power stations with feeders for 20 loads are modeled, using load factor and actual loads to determine the peak demand. The ideal load curve depicts only average behaviors fitting to the real curve. Since consumers keep on switching loads on and off, the resulting load curve exhibits a stochastic behavior within limits of peak and off-peak demands.

The unpredictable behavior of the load curve further complicates the system stability, with peak demand occurring at night, when the solar PV is at its worst generation. The renewable energy micro-grid ends up with stochastic inputs parameters for power generation, whose output must

meet the stochastic behavior of the loading profiles. The stability of the system is thus plunged into a last resort measures space frequently for continued operational security.

4.4 Power Imbalance Curve

4.4.1 Power Imbalance Results

Two model unit commitment/ dispatch plans are constituted from the available generations dependent on the source intermittence for the renewables. For each commitment model a different reserve percentage is allowed for borrowing or purchasing power during times of power imbalances. Net power imbalances are obtained by deducting power losses from the dispatched generations and allowing for borrowing from the spinning reserves during times of deficiency. This gives rise to the four curves illustrated in Figure 4.3

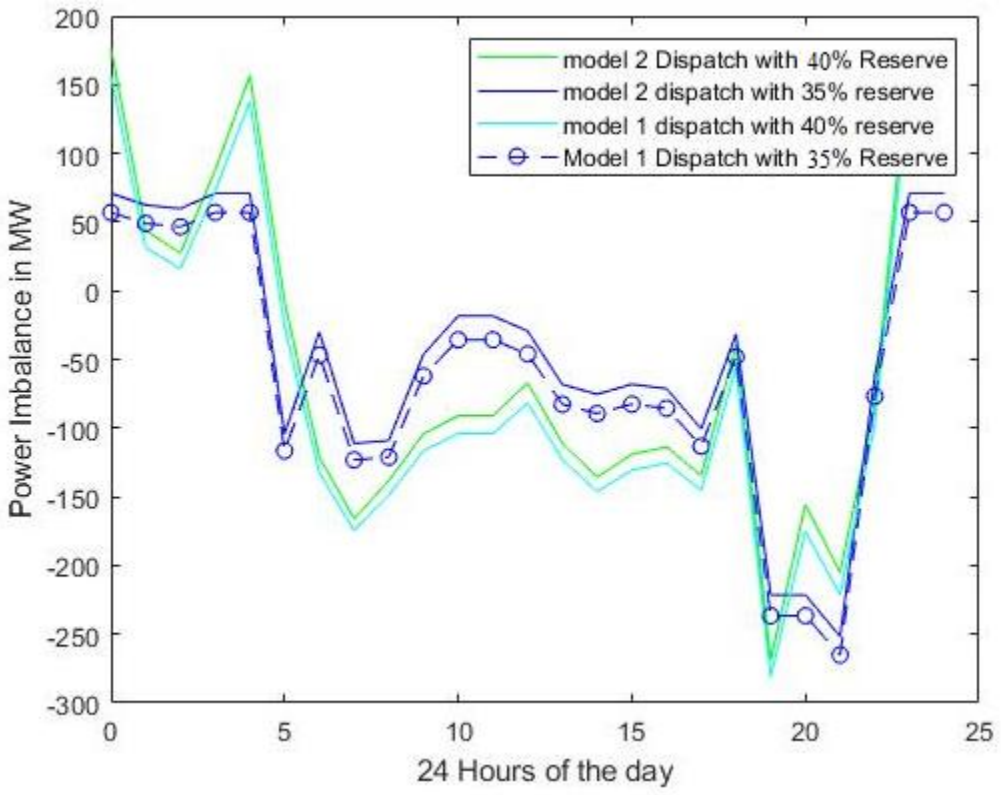

Figure 4.3 Power imbalance curves for the model micro-grid at times of deficiency

4.4.2. Power Imbalance Curve Analysis

A net power imbalance is eminent, as a result of unpredictable renewable energy source generation and probable load switching by consumers. The renewable energy micro-grid remains resilient for short periods of low net power imbalances, since the inertia constant of the wind, geothermal and hydro plants provides the self-restoration although with larger swings in the swing curve. A positive power imbalance is economically desirable since the operator will not incur the cost of energy not supplied.

For large negative net power imbalances, which occur majorly at the peak demand periods, it's necessary to take remedial measures of the last resort such as load shedding, by treating the loads as faults and disconnecting the feeders. This leads to losses on both sides of network i.e. to consumers and to operator in pursuit for a secure grid.

4.5 Transient Stability Swing Curve before Load Shedding

4.5.1. Findings on transient swing curve before load shedding

Examining the transient stability of the renewable micro-grid with power imbalances as the key system disturbances, the swing curves of Figure 4.4 are derived. These swing curves indicate severe instability that needs immediate load shedding to secure the system from frequency collapse.

4.5.2. Discussion of transient swing curve before load shedding

Investigation of the transient frequency stability is carried out, for the largest power imbalances, at intervals of 30 seconds, which shows that the system is unstable with swing curve increasing its swing amplitudes continuously. Each of the 4 unit commitment models with different reserve percentages, results in a different swing curve, with rotor angle swinging within a range of 0.4 to 1.5 electrical radians. Measures of last resort for restoration of system stability are therefore necessary to prevent frequency collapse of the renewable energy micro-grid.

4.6 Prioritized Load Shedding Scheme

4.6.1 Findings on Prioritized Load Shedding Scheme

After simulation, there are about 1500 possible combinations of loads, forming the population for optimization. These population of possible solutions are evaluated using PSO-GA and that

has best swing curve is selected and implemented. These possible solutions can be accessed after running the MATLAB code and prompting an array variable named “loadshed”. For example, a maximum power imbalance of 269MW, has an optimum load combination constituted of 12 loads and falls in the second stage/ second priority of load shedding i.e. combines loads in domestic/ agricultural and commercial categories and spares industrial category of loads as per the prioritization. The total load disconnected for this imbalance is 295MW, consisting of 5MW, 6MW, 8MW, 10MW, 14MW, 16MW, 18MW, 23MW, 25MW, 31MW, 42MW and 97MW feeders.

4.6.2 Evaluation of the Prioritized loads shedding Scheme

A load-shedding scheme has been developed, prioritizing loads as per the Kenya national grid transmission code. Industrial loads, who are majorly large consumers, are given first priority, such that their loads will be the last to be affected. Commercial loads are second in priority, while domestic and agricultural loads are least in priority and thus are disconnected from the grid if the optimal search finds a suitable combination within the group.

If the total power imbalance of the micro-grid is larger than the total sum of all domestic loads, the second stage is considered where commercial and domestic/ agricultural loads are availed for an optimal combination of the load shedding scheme. In this stage, some domestic loads might remain connected while commercial loads are disconnected depending on the optimal stability realized through the PSO-GA algorithm. Lastly, if the power imbalance is greater than commercial and domestic/ agricultural loads, then all loads will be availed for load shedding in the third / last stage and none is favored or discriminated. This stage can a times result into a total shutdown of the grid. For every possible load combinations, the frequency stability is investigated before disconnecting the loads to ensure selection is made for the best scheme.

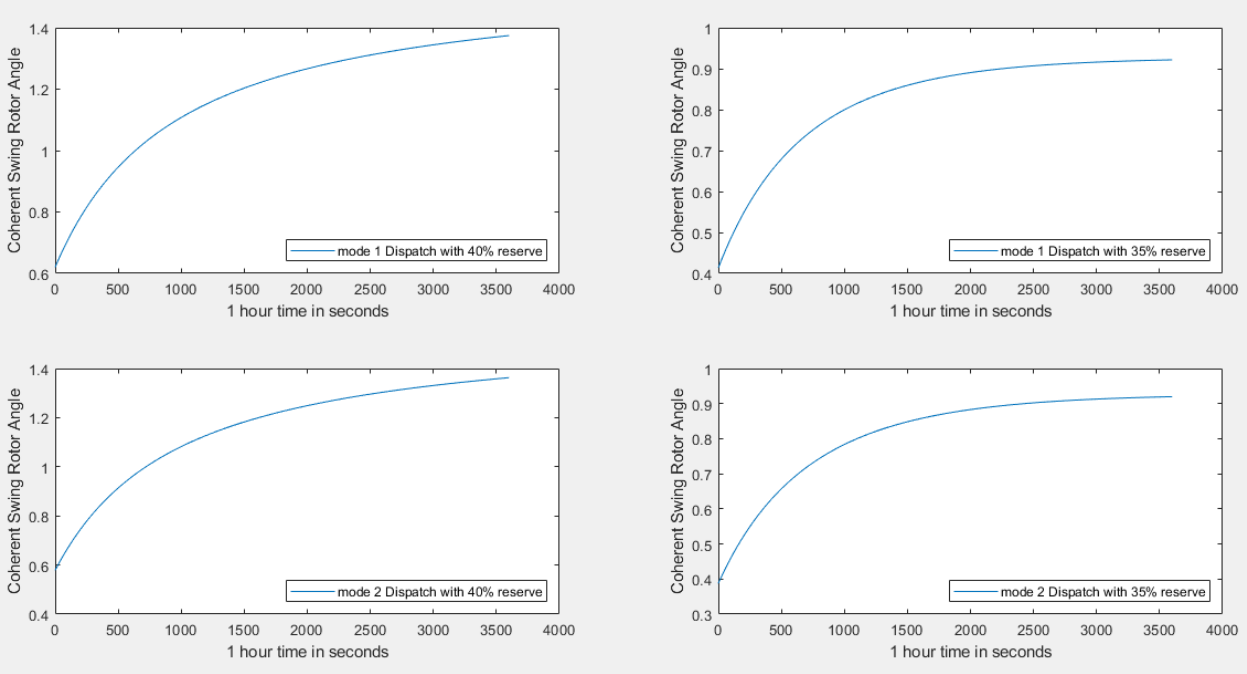

Figure 4.4 Transient stability swing curve before load shedding

4.7 Optimal Recovery Transient Stability Swing Curve after Load Shedding

4.7.1. Optimal Recovery Transient Stability Swing Curve after Load Shedding Results

The PSO-GA method is utilized to find the most optimal load shedding combinations for rotor angle recoveries. These optimal load combinations are then treated as faulty feeders and disconnected by switching off respective relays, thus relieving the micro-grid from adverse effects. The restored stable system swing curves are indicated in Figure 4.5.

4.7.2. Discussion of Optimal Recovery Transient Stability Swing Curve, after Load Shedding

After disconnecting the loads from the micro-grid, a transient stability study is carried out to investigate the state. The swing amplitudes start reducing until the original rotor angle is attained, or a better position. Disconnected loads remain off until the time when generation is available to power then, during which the scheme priority works on a reverse process, where industrial loads are connected first, followed by commercial and lastly domestic/ agricultural loads. However if the available generation can only support a domestic load, the priority for industrial loads is by-passed/ violated.

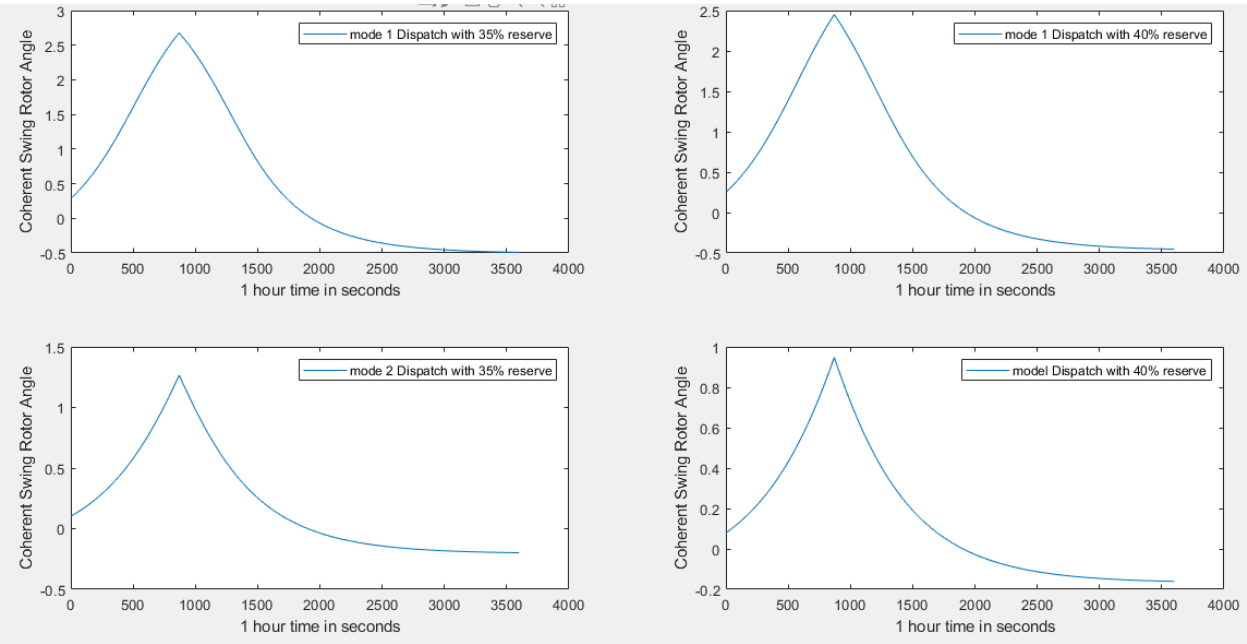

Figure 4.5 Optimal Recovery transient stability swing curve after load shedding

4.8. Validation of Results

Each of the results outlined in this chapter are analyzed and interpreted. Majorly a stable micro-grid is realized at times of severe power imbalances, only after shedding the loads. 20 loads (distribution feeders) are optimally combined using the PSO-GA techniques in order to achieve, each of the possible combination is evaluated as per the objective function, and the best suited combination is selected and disconnected from the micro-grid.

After disconnection, plotted swing curves are investigated for frequency stability, ensuring it meets all specifications outlined in the Kenya Electricity Transmission Code. The swing curves indicate that high reserve capacity renewable energy micro-grids would stabilize with minimal load disconnection as compared to micro-grids with smaller reserve capacities. However, energy reserves are costly and therefore optimal load shedding management is achieved via a compromise of the two strategies.

4.9. Chapter Conclusion

This chapter demonstrates various results realized from simulations based on the MATLAB code of the model micro-grid. The outputs include; generation capacities, transmission and distribution losses, load profile curve, net power balancing curve, load shedding scheme operational schedule, under-frequency swing curve before load shedding and stabilized swing curves after load shedding. The tendency of the load curves towards the zero point indicates level of stabilities achieved for the system after load shedding.

Power imbalance curves are obtained by finding the difference between available generation and the load profile at that time. Such a difference can be either positive or negative. The positive power imbalance is discarded since it results into over-frequency, while the research interest is in under-frequency that occurs only during the negative net power imbalance. After load shedding the swing curves end up to a point very close to the zero point indicating low swings and hence high stability.

Smaller magnitudes of the power imbalance can be accommodated without adverse effects on the quality, reliability and security of the micro-grid, depending on the inertia constant of the generation and compensation strategies employed. However, large magnitudes results into generators falling out of synchronism and thus immediate measures of last result (in this case load shedding scheme) is deployed.

CHAPTER FIVE

CONCLUSION AND RECOMMENDATIONS

5.1. Conclusion and Implications of the findings

Highly penetrated renewable energy grids or purely renewable energy micro-grids exhibit higher frequencies of network instabilities due to stochastic nature of loading and chaotic generation of power from unpredictable sources. These system instabilities are solvable by compensation techniques for voltage and frequency, which only apply when the available generation is capable of powering the connected loads without violating the limits thereof. In cases where the generation is insufficient and power imbalances lead to violation of voltage and frequency limits, demand control is deployed as a measure of last resort. Key findings in this research include;

- ✓ Optimization of demand control in renewable energy micro-grids involves developing load shedding schemes and searching for the most optimum by investigating the stability for combinations of loads whose summation is in the space around the power imbalance. With climate change campaign in favor of renewable energy micro-grids or integration to national grids, the stability of the power systems become more unpredictable.
- ✓ Its therefore necessary to optimize both unit commitment plans to track the load curve closely and design load-shedding schemes that attain the voltage and frequency limits, while retaining maximum load on the grid.
- ✓ The study shows that through load-shedding, renewable energy micro-grids can be operated in the stable state at the expense of loads during times of severe power imbalances.
- ✓ Optimization of the load-shedding using PSO-GA technique ensures optimum amount of load is shed from the grid with each possible load shedding scheme getting evaluated first and selection of most optimum scheme with priority for loads is accomplished.
- ✓ Though load shedding restores the micro-grid back to its stable operation, 100% optimization was not achieved

5.2. Recommended Applications

Adoption of the optimized load shedding scheme developed in this thesis, will definitely assure operators of off-grid systems, of a full exploitation of opportunities and options available in a load shedding process. These opportunities are composed of the five objective components, i.e. frequency fluctuations, voltage deviations, battery storage, amount of loads shed and power losses. Once adopted in power systems operation, the optimized load shedding scheme will provide minimal interruptions/ blackouts, for minimal periods, while maintaining a secure operational margin, for a highly profitable power network operation during severe power imbalance. It is therefore necessary for off-grid operators to adopt the developed optimal load shedding scheme.

An ideal solution for renewable energy micro-grids stability is to provide energy reserves sufficient enough to take up loads immediately after shedding, to avoid violation of consumer rights to universal access to energy for long periods. However, these reserves will increase cost of energy even during times of sufficient renewable energy supply. A compromise is therefore required to ensure forecasting for availability of energy is integrated with reserve schemes/ power purchase agreements and contracts in form of time and amount of energy with a trade-off for load-shedding in short periods of power generation scarcity.

Combined load forecasting and renewable energy source forecasting for approximation of power imbalances and hence network planning and operational schedule drafting for highly penetrated or pure renewable energy micro-grids is inevitable.

Intelligent search using PSO-GA algorithm for optimal load shedding scheme results into minimum load sheds to attain required transient stability levels. However the amount of load disconnected from the grid may be slightly larger due feeder sizing. Loads tapping from a feeder are uncontrolled from the power station and only the whole feeder can be switched on or off.

5.3. Areas of Further Study

Two main areas of study are further recommended for more effective demand control operations of RE micro-grids. These include:

i). **Dynamic Equivalency for Multi-machine stability studies**

Reducing multi-machine networks into smaller number (1, 2 or 3) machine network is quite useful in providing approximate overall stability behavior of the whole systems. Such equivalent networks reduce time of stability study and are necessary for operational planning. However, in such a study the equivalent network consists of "virtual" machines whose stability may not reflect the real behavior of the multi-machine system, where some machines will retain synchronism and others fall out of step, in times of power imbalances. More accurate equivalent networks that can be extended backwards to tell the behavior of each machine's transient stability according to individual inertia constants is necessary.

ii). Comparative Rota and Automatic Load shedding relays

Rota load-shedding as opposed to priority based load shedding is non-discriminatory, where every consumer remains connected to the grid for an equal amount of time regardless of their category. Automatic load shedding relays disconnect loads as per the SCADA system commands and is rarely optimal, sometimes disconnecting less and other times disconnecting more feeders from the grid since its operation is based on real time measurements. A comparative study can be carried out to establish the frequency stability implications of either of these load shedding methods.

REFERENCES

[1] Bargaan B, Bukhari B, Cabigao A, Depierreux F, and Khursheed A, "Frequency Control and Under frequency load shedding in the isolated area of Sharorah," in *Saudi Arabia Smart Grid (SASG)*, Saudi Arabia, 2017.

[2] Gray MK and Morsi W.G, "Application of PSO and Fuzzy Logic for Under frequency load shedding," in *IEEE Electrical Power and Energy Conference (EPEC)*, 2013.

[3] Hong Ying and Wei Shih-Fan, "Multi-objective Under frequency load shedding in an autonoumous system using hierarchical genetic algorithms," in *IEEE transactions on power delivery*, 2010.

[4] Zelalem Gebrehiwot, "East Africa Power Pull," 2010.

[5] Kenya Power and Lighting Co. and Rural Electrification Authority, "Kenya off-grid solar access project (KOSAP) for underserved counties," 2017.

[6] Nygaard Ivan et al, "Market for Integration of Smaller Wind Turbines in Mini-grids in Kenya," 2018.

[7] Guilherme P. Borges et al, "Use of genetic Algorithm for Evalaution and control of Technical problems due load shedding in Power systems," in *International conference on power generation systems and renewable energy technologies*, 2017.

[8] Musau Peter Chepkania Terry, Odero Nicodemus and Wekesa Cyrus, "Effects of renewable energy on Frequency stability: A proposed case study of Kenya Grid," in *IEEE PES- IAS power Africa*, 2017.

[9] Bayhan Sertac , "Predictive Load shedding method for islanded AC microgrid with limited generation sources," in *IEEE 12th International conference compatibility, Power electronics and power engineering*, 2018.

[10] Quan Zhou, Li Zhiyi, Wu Qiuwei and Shahidehpour Mohammad , "Two stage load shedding for secondary control in Hierachical operation of islanded micro-grids," in *IEEE Transactions on smart grid*, 2018.

[11] Musau M.P, "Security and Stability Aspects of Multi objective Dynamic Economic Dispatch with renewable energy and HVDC transmission lines," *Journal of Power and Energy Engineering*, 2018.

[12] Musau P.M, Ojwang B.O and Kiprotich M, "Improving Frequency Stability for Renewable Energy Power Plants with Disturbances," in *Proceedings of the 2019 IEEE PES GTD Asia*, GTD Asia, 2019.

[13] Ali Parizad Khoshkhoo Hamid, Dehghan Shahab and Moradtalab Rasoul, "An Intelligent Load and Generation Shedding Procedure in an Islanded Network Using a Smart Power Management System," in *Smart Grid Conference*, SGC, 2017, pp. 4279-5386.

[14] Muhammad Usman, Amin Adil, Azam Muneer and Mokhlis H, "Optimal Under Voltage Load Shedding Scheme for a Distribution Network Using EPSO Algorithm," in *Energy conference*, Malaysia, 2018, pp. 5386-5482.

[15] Energy regulatory commission of kenya, "Kenya national grid transmission code," Nairobi, 2013.

[16] Ardash TV, and HL Suresh , "PLC based Load Shedding Mechanism using Battery SOC in Micro Grids," in *IEEE International Conference on Power, Control, Signals and Instrumentation*

Engineering, India, 2017, pp. 386-0814.

[17] Hazlie Mokhlis, JA Laghari, Abu Bakar and Karimi Mazaher "A Fuzzy based load shedding scheme for an islanded distribution network," in *Power and Energy Systems (AsiaPES 2013)*, Thailand, 2013, pp. P2013/800-088.

[18] Karimi M, Mohamad H, Mokhlis H, and Bakar A.H.A, "Under-Frequency Load Shedding scheme for islanded distribution network connected with mini-hydro," *Electrical Power and Energy Systems*, pp. 127-138, 2012.

[19] Kumar Manoj and Swarup Shanti, "Particle Swarm Optimization based Corrective Strategy to Alleviate Overloads in Power System," in *World Congress on Nature & Biologically Inspired Computing*, India, 2009, pp. 4244-5612.

[20] Mohamad H, Isa A.I, Yasin Mat, Salim N.A and Rahim Mohd N.N.A, "Optimal Load Shedding Technique for an Islanding Distribution System by Using Particle Swarm," in *Energy Conference*, Pakistan, 2017

[21] Andre Richter and Martin Wolter, "Under-Frequency Load Shedding in the European Interconnection System," in *Energy Conference*, uk, 2018

[22] Kenya Power and Lighting Company, "KPLC Distribution Master Plan Study," Nairobi, 2011.

[23] M.K Gray and W.G Morsi, "Application of PSO and Fuzzy Logic for Under frequency load shedding," in *IEEE Electrical Power and Energy Conference (EPEC)*, 2013.

APPENDICES

Appendix A: Matlab Based Simulation Code

```
clear all
clc
ch = input('Enter the bus system no.: (6 or 9 or 14 or 26 or 30 or 57): ');
while ch ~= 6 && ch ~= 14 && ch ~= 26 && ch ~= 30 && ch ~= 57 && ch ~= 9
   fprintf('Invalid Input try again\n');
   ch = input('Enter the bus system no.: (6 or 9 or 14 or 26 or 30 or 57): ');
end
switch ch
   case 6
      data6
   case 14
      data14
   case 26
      data26
   case 30
      data30
   case 57
      data57
   case 9
      data9
end
met = input('Enter the method for load flow (1 - GS, 2 - NR, 3 - Fast Decouple): ');
while met ~= 1 && met ~= 2 && met ~= 3
   fprintf('Invalid Input try again\n');
   met = input('Enter the method for load flow (1 - GS, 2 - NR, 3 - Fast Decouple): ');
end
switch met
   case 1
      maingauss
   case 2
      mainnewton
   case 3
      maindecouple
end
%Power Imbalances Model
%GENERATION TURBINE MODELS
% Wind Turbine Generation Model
K=0.000133;%Horse power to KW conversion constant
Ad= 0.075; %The average density of air at NTP (20 Degs and 1 atm) is 1.204 kg/m3 i.e. 0.075 pounds per cubic foot.
WTCp=0.25:0.02:0.45;% standard power coefficient range of a wind turbine,no units
WTd=130:17:300;%Diameter size of wind turbines in the wind farm in ft
Wv=11:1.6:27;%velocity of wind in miles per hour varying from 11 to 27 miles per hour, EPRA
WTa=pi*WTd.*WTd/4;%swept area of wind turbine in sq. ft
NWTs=10:24:250;%Number of wind turbines in the farm
WTG=0.5*K*WTCp.*Ad.*WTa.*Wv.*Wv.*Wv.*NWTs/1000;%MW output of the wind turbine
WvP=1./Wv;
WTaP=1./WTa;
figure (1)
subplot(2,2,1)
plot3(WTa,Wv,WTG)
subplot(2,2,2)
plot3(WTaP,Wv,WTG)
subplot(2,2,3)
plot3(WTa,Wv,WTG)
subplot(2,2,4)
plot3(WTaP,WvP,WTG)
% Hydropower Turbine Generation Model
```

```
g=9.81; %gravitational acceleration in M/sq.sec.
Wd=1000; %Density of Water in Kg/cubic Meter
HTh=10:14:150; %Hdraulic head in meters
HTQ=1:19.9:200; %Volumetric Flow Rates
HTeff=0.8:0.015:0.95;%Efficiency of hyropower turbine generation
HTG=g*Wd*HTh.*HTQ.*HTeff/1000000;%MW output of the Hydroturbine
HTQP=1./HTQ;
HThP=1./HTh;
figure (2)
subplot(2,2,1)
plot3(HTG,HTQ,HTh)
subplot(2,2,2)
plot3(HTG,HTQP,HTh)
subplot(2,2,3)
plot3(HTG,HTQ,HThP)
subplot(2,2,4)
plot3(HTG,HTQP,HThP)
% Solar PV Generation Model
SPVeff=0.15:0.003:0.18; % Solar PV efficiency range
PR=0.5:0.04:0.9; %Range of performance ratio co-efficient dependent on temp and losses
OpCoef=SPVeff.*PR;% Output coefficient
H=0.3333:0.01667:0.5; %Solar radiation in kWh/sq.m according to EPRA and Global Solar atlas
A=10000:99000:1000000;% Area covered by Solar PV farm in sq. Meter
PVG=A.*H.*OpCoef/1000; %MW output of the PV Solar farm
PRP=1./PR;
AP=1./A;
figure (3)
subplot(2,2,1)
plot3(PVG,PR,A)
subplot(2,2,2)
plot3(PVG,PRP,A)
subplot(2,2,3)
plot3(PVG,PR,AP)
subplot(2,2,4)
plot3(PVG,PRP,AP)
% Geothermal Steam Turbine Generation model
GT=ones(1,11); %Stable Generation for the Base Load
GTG=175*GT; % Assumed base load of 175MW
%Total Power Generation
TotalGen=WTG+HTG+PVG+GTG;
%Generation Model Output Table
GenModel=[WTCp;WTd;Wv;WTG;HTh;HTQ;HTeff;HTG;H;OpCoef;A;PVG;GTG;TotalGen];
GenModelOutput=GenModel.';
[fileID,message]= fopen('C:\Users\paulm\Desktop\mscwork\mscwork\Sem 4\code\GenerationModelsOutput.m','w');
fprintf(fileID,'%6s %4s %8s %6s %4s %6s %6s %6s %6s %5s %7s %7s %5s
%5s\r\n','WTCp','WTd','Wv','WTG','HTh','HTQ','HTeff','HTG','H','OpCoef','A','PVG','GTG','TotalGen');
fprintf(fileID,'%5.4f %3.1f %6.4f %5.4f %3.1f %6.4f %5.4f %6.4f %6.4f %5.4f %6.1f %7.4f %3.1f %7.4f\r\n',GenModel);
fclose(fileID);
%Transmission and Distribution Model
SLT = 0;
fprintf('\n')
fprintf('                    Line Flow and Losses \n\n')
fprintf('    --Line--  Power at bus & line flow    --Line loss--  Transformer\n')
fprintf('    from  to    MW      Mvar     MVA       MW      Mvar      tap\n')

for n = 1:nbus
busprt = 0;
   for L = 1:nbr;
      if busprt == 0
      fprintf('   \n'), fprintf('%6g', n), fprintf('      %9.3f', P(n)*basemva)
      fprintf('%9.3f', Q(n)*basemva), fprintf('%9.3f\n', abs(S(n)*basemva))

```

```
        busprt = 1;
        else, end
        if nl(L)==n      k = nr(L);
        In = (V(n) - a(L)*V(k))*y(L)/a(L)^2 + Bc(L)/a(L)^2*V(n);
        Ik = (V(k) - V(n)/a(L))*y(L) + Bc(L)*V(k);
        Snk = V(n)*conj(In)*basemva;
        Skn = V(k)*conj(Ik)*basemva;
        SL  = Snk + Skn;
        SLT = SLT + SL;
        elseif nr(L)==n  k = nl(L);
        In = (V(n) - V(k)/a(L))*y(L) + Bc(L)*V(n);
        Ik = (V(k) - a(L)*V(n))*y(L)/a(L)^2 + Bc(L)/a(L)^2*V(k);
        Snk = V(n)*conj(In)*basemva;
        Skn = V(k)*conj(Ik)*basemva;
        SL  = Snk + Skn;
        SLT = SLT + SL;
        else, end
          if nl(L)==n | nr(L)==n
          fprintf('%12g', k),
          fprintf('%9.3f', real(Snk)), fprintf('%9.3f', imag(Snk))
          fprintf('%9.3f', abs(Snk)),
          fprintf('%9.3f', real(SL)),
             if nl(L) ==n & a(L) ~= 1
             fprintf('%9.3f', imag(SL)), fprintf('%9.3f\n', a(L))
             else, fprintf('%9.3f\n', imag(SL))
             end
        else, end
  end
end
SLT = SLT/2;
fprintf('   \n'), fprintf('    Total loss                    ')
fprintf('%9.3f', real(SLT)), fprintf('%9.3f\n', imag(SLT))
clear Ik In SL SLT Skn Snk
PPL=0.15:0.005:0.2;%The range of Percentage power losses according to World Bank Report 2019
TDL=TotalGen.*PPL;%Power Losses in MW due to transmission and distribution networks
NP=TotalGen-TDL;%Net power available at secondary distribution transformer
figure (4)
plot(PPL,TotalGen)
xlabel('TD Distance based pecentage power loss')
ylabel('Power in MW')
hold on
plot(PPL,TDL)
xlabel('TD Distance based pecentage power loss')
ylabel('Power in MW')
hold on
plot(PPL,NP)
xlabel('TD Distance based pecentage power loss')
ylabel('Power in MW')
legend({'total generation','TD Losses','net available power at load centers'},'location','northwest')
%DAILY LOAD PROFILE MODEL:
%There are three main substations (CR,NR and WK) with 3, 5 and 12 loads respectively in their feeders
%CR Substation Daily Loading Profile
Bar=[3.4 6.4 9.8];Nak=[69.9 132.8 202.7];Nar=[4.9 9.3 14.2]; %3 loads in the first substation consisting off peak, actual and peak values
CR=Bar+Nak+Nar;% Total load on first substation with offpeak, actual and peak values
%NR Substation Daily Loading Profile
ElgM=[1.8 3.4 5.2];Nan=[6.3 11.9 18.2];TraZ=[10.6 20.0 30.6];UasN=[33.5 63.5 97.0];WesP=[2.0 3.7 5.7]; %5 loads of the second substation
NR=ElgM+Nan+TraZ+UasN+WesP;%Total load on second substation considering offpeak, actual and peak values
%WK Substation Daily Loading Profile
Bom=[3.4 6.4 9.8];Bun=[7.9 15.1 23.0];Bus=[6.3 11.9 18.2];Hom=[4.9 9.3 14.2];
Kak=[13.9 26.5 40.4];Ker=[10.5 19.8 30.3];Kii=[14.5 27.4 41.9];Kisu=[37.9 72.0 109.9];
```

```
Mig=[8.6 16.2 24.8];Nyam=[2.8 5.4 8.2];Sia=[6.1 11.6 17.7];Vih=[5.7 10.7 16.4];
WK=Bom+Bun+Bus+Hom+Kak+Ker+Kii+Kisu+Mig+Nyam+Sia+Vih;%Total of 12 loads on the third substation
%Off Peak, Actual and Peak Load Profile Models
OL=CR(1)+NR(1)+WK(1);%Off peak load on the micro-grid
AL=CR(2)+NR(2)+WK(2);%Actual or Average load on the micro-grid
PL=CR(3)+NR(3)+WK(3);%Peak Load on the micro-grid
%Daily Load Curve for the micro-grid
Time=0:1:24;
DLPM=[OL OL OL OL OL AL AL AL AL AL AL AL AL AL AL AL AL AL AL PL PL PL AL OL OL];
figure (5)
plot(Time,DLPM)
xlabel('24 Hours of the day')
ylabel('Load Demand in MW')
legend({'ideal load curve'},'location','northwest')
%Constraint Generation units comittment plan Models
WTGFJ=[WTG(9) WTG(7) WTG(7) WTG(8) WTG(9) WTG(9) WTG(5) WTG(4) WTG(6) WTG(5) WTG(5) WTG(5) WTG(6)
WTG(4) WTG(4) WTG(4) WTG(6) WTG(6) WTG(8) WTG(7) WTG(9) WTG(8) WTG(7) WTG(9) WTG(9)];
WTGAO=[WTG(5) WTG(4) WTG(6) WTG(5) WTG(5) WTG(5) WTG(6) WTG(4) WTG(4) WTG(4) WTG(6) WTG(6)
WTG(5) WTG(4) WTG(6) WTG(5) WTG(5) WTG(5) WTG(6) WTG(4) WTG(4) WTG(4) WTG(6) WTG(5) WTG(5)];
HTGFJ=[HTG(8) HTG(7) HTG(6) HTG(7) HTG(7) HTG(6) HTG(8) HTG(6) HTG(6) HTG(8) HTG(8) HTG(8) HTG(8)
HTG(7) HTG(6) HTG(7) HTG(7) HTG(6) HTG(8) HTG(7) HTG(7) HTG(8) HTG(8) HTG(8) HTG(8)];
HTGAO=[HTG(10) HTG(10) HTG(9) HTG(10) HTG(10) HTG(9) HTG(11) HTG(9) HTG(9) HTG(11) HTG(11) HTG(11)
HTG(11) HTG(10) HTG(9) HTG(10) HTG(10) HTG(9) HTG(11) HTG(11) HTG(11) HTG(10) HTG(10) HTG(10) HTG(10)];
PVGFJ=[PVG(1) PVG(1) PVG(1) PVG(1) PVG(1) PVG(1) PVG(4) PVG(4) PVG(5) PVG(8) PVG(10) PVG(10) PVG(11)
PVG(11) PVG(10) PVG(10) PVG(7) PVG(6) PVG(2) PVG(2) PVG(2) PVG(2) PVG(2) PVG(1) PVG(1)];
PVGAO=[PVG(1) PVG(1) PVG(1) PVG(1) PVG(1) PVG(1) PVG(2) PVG(2) PVG(3) PVG(5) PVG(6) PVG(6) PVG(7) PVG(7)
PVG(6) PVG(5) PVG(4) PVG(3) PVG(1) PVG(1) PVG(1) PVG(1) PVG(1) PVG(1) PVG(1)];
GTGFAJO=[GTG(1) GTG(2) GTG(3) GTG(4) GTG(5) GTG(6) GTG(1) GTG(2) GTG(3) GTG(4) GTG(5) GTG(6) GTG(1)
GTG(2) GTG(3) GTG(4) GTG(5) GTG(6) GTG(1) GTG(2) GTG(3) GTG(4) GTG(5) GTG(6) GTG(6)];
GFJHB=WTGFJ+PVGFJ;
GFJ=GFJHB+HTGFJ+GTGFAJO;
GAOHB=WTGAO+PVGAO;
GAO=GAOHB+HTGAO+GTGFAJO;
%Constraint Generation on selected days
figure (6)
plot(Time,GFJ)
hold on
plot(Time,GAO)
xlabel('24 Hours of the day')
ylabel('Optimum Genearation Capacity in MW')
legend('Model 1','Model 2')
%Net power considering lower limit of the TD model
NPFJLL=0.85*GFJ;
NPAOLL=0.85*GAO;
%Net Power considering upper limit of the TD model
NPFJUL=0.80*GFJ;
NPAOUL=0.80*GAO;
%Power Imbalance
PIFJLL=NPFJLL-DLPM;
PIAOLL=NPAOLL-DLPM;
PIFJUL=NPFJUL-DLPM;
PIAOUL=NPAOUL-DLPM;
%Resultant Daily Power Imbalance Curves (micro-grid disturbances)
figure (7)
plot(Time,PIFJLL,'b')
hold on
plot(Time,PIAOLL,'g')
hold on
plot(Time,PIFJUL,'c')
hold on
plot(Time,PIAOUL,'b--o')
%Net power imbalance after allowng for 35 percent reserve capacity, for
```

```
%normal frequency/voltage control, compensation or regulation
NPIFJLL=0.65*PIFJLL;
NPIAOLL=0.65*PIAOLL;
NPIFJUL=0.65*PIFJUL;
NPIAOUL=0.65*PIAOUL;
figure (8)
plot(Time,NPIFJLL,'g')
xlabel('24 Hours of the day')
ylabel('Power Imbalance in MW')
hold on
plot(Time,NPIAOLL,'b')
xlabel('24 Hours of the day')
ylabel('Power Imbalance in MW')
hold on
plot(Time,NPIFJUL,'c')
xlabel('24 Hours of the day')
ylabel('Power Imbalance in MW')
hold on
plot(Time,NPIAOUL,'b--o')
xlabel('24 Hours of the day')
ylabel('Power Imbalance in MW')
legend('model 2 Dispatch with 35% Reserve','model 2 dispatch with 35% reserve','model 1 dispatch with 40% reserve','Model 1
Dispatch with 40% Reserve')
%%SUSTAINED POWER IMBALANCES SWING CURVES%%
% Read data from IEEE modified 9 Bus System and Microgrid model
H1=2.6312; H2=4.1296;H3=4.768;%Inertia constants of the three generators
G1=512;G2=270;G3=125;%Machine ratings in MVA for the three generators
dt=0.05;
Gs=905.8; %Base MVA
E=1.0; %Equivalent Generator terminal voltage p.u
V=0.9;% Equivalent Receiving end voltage on infinite bus p.u
X=0.8983; % p.u line reactance
pmax=V*E/X;
Heq=(H1*G1/Gs)+(H2*G2/Gs)+(H3*G3/Gs);% dynamic equivalencing inartia constants to single machine - infinite bus bar
M=Heq/(pi*50);% equivalent moment of inertia in squared seconds per elecrtrical radian
Pe1=NPFJLL/Gs;
Pe2=NPAOLL/Gs;
Pe3=NPFJUL/Gs;
Pe4=NPAOUL/Gs;
Pe=vertcat(Pe1,Pe2,Pe3,Pe4);
Pmax1=max(Pe1);
Pmax2=max(Pe2);
Pmax3=max(Pe3);
Pmax4=max(Pe4);
Pmax=[Pmax1,Pmax2,Pmax3,Pmax4];
t1=0:30:3600;t2=3600:30:7200;t3=7200:30:10800;t4=10800:30:14400;t5=14400:30:18000;t6=18000:30:21600;
t7=21600:30:25200;t8=25200:30:28800;t9=28800:30:32400;t10=32400:30:36000;t11=36000:30:39600;t12=39600:30:43200;
t13=43200:30:46800;t14=46800:30:50400;t15=50400:30:54000;t16=54000:30:57600;t17=57600:30:61200;t18=61200:30:64800
;
t19=64800:30:68400;t20=68400:30:72000;t21=72000:30:75600;t22=75600:30:79200;t23=79200:30:82800;t24=82800:30:86400
;
t=horzcat(t1,t2,t3,t4,t5,t6,t7,t8,t9,t10,t11,t12,t13,t14,t15,t16,t17,t18,t19,t20,t21,t22,t23,t24);
%Rotor angle changes in each of the 24 hours
del1 = zeros(4,numel(t1));del2 = zeros(4,numel(t2));del3 = zeros(4,numel(t3));del4 = zeros(4,numel(t4));
del5 = zeros(4,numel(t5));del6 = zeros(4,numel(t6));del7 = zeros(4,numel(t7));del8 = zeros(4,numel(t8));
del9 = zeros(4,numel(t9));del10 = zeros(4,numel(t10));del11 = zeros(4,numel(t11));del12 = zeros(4,numel(t12));
del13 = zeros(4,numel(t13));del14 = zeros(4,numel(t14));del15 = zeros(4,numel(t15));del16 = zeros(4,numel(t16));
del17 = zeros(4,numel(t17));del18 = zeros(4,numel(t18));del19 = zeros(4,numel(t19));del20 = zeros(4,numel(t20));
del21 = zeros(4,numel(t21));del22 = zeros(4,numel(t22));del23 = zeros(4,numel(t23));del24 = zeros(4,numel(t24));

for u=1:4
del1(u,1)=(asin(Pe(u,1)));del2(u,1)=(asin(Pe(u,2)));del3(u,1)=(asin(Pe(u,3)));del4(u,1)=asin(Pe(u,4));
```

```
del5(u,1)=asin(Pe(u,5));del6(u,1)=asin(Pe(u,6));del7(u,1)=asin(Pe(u,7));del8(u,1)=asin(Pe(u,8));
del9(u,1)=asin(Pe(u,9));del10(u,1)=asin(Pe(u,10));del11(u,1)=asin(Pe(u,11));del12(u,1)=asin(Pe(u,12));
del13(u,1)=asin(Pe(u,13));del14(u,1)=asin(Pe(u,14));del15(u,1)=asin(Pe(u,15));del16(u,1)=asin(Pe(u,16));
del17(u,1)=asin(Pe(u,17));del18(u,1)=asin(Pe(u,18));del19(u,1)=asin(Pe(u,19));del20(u,1)=asin(Pe(u,20));
del21(u,1)=asin(Pe(u,21));del22(u,1)=asin(Pe(u,22));del23(u,1)=asin(Pe(u,23));del24(u,1)=asin(Pe(u,24));

 for ka=2:(numel(t1))
   del1(u,ka)=del1(u,(ka-1))+(((dt*dt)/M)*(Pe(u,1)-Pmax(u)*sin(del1(u,(ka-1)))));
 end
 for kb=2:(numel(t2))
   del2(u,kb)=del2(u,(kb-1))+(((dt*dt)/M)*(Pe(u,2)-Pmax(u)*sin(del2(u,(kb-1)))));
 end
 for kc=2:(numel(t3))
del3(u,kc)=del3(u,(kc-1))+(((dt*dt)/M)*(Pe(u,3)-Pmax(u)*sin(del3(u,(kc-1)))));
 end
 for kd=2:(numel(t4))
del4(u,kd)=del4(u,(kd-1))+(((dt*dt)/M)*(Pe(u,4)-Pmax(u)*sin(del4(u,(kd-1)))));
 end
 for ke=2:(numel(t5))
   del5(u,ke)=del5(u,(ke-1))+(((dt*dt)/M)*(Pe(u,5)-Pmax(u)*sin(del5(u,(ke-1)))));
 end
 for kf=2:(numel(t6))
del6(u,kf)=del6(u,(kf-1))+(((dt*dt)/M)*(Pe(u,6)-Pmax(u)*sin(del6(u,(kf-1)))));
 end
 for kg=2:(numel(t7))
del7(u,kg)=del7(u,(kg-1))+(((dt*dt)/M)*(Pe(u,7)-Pmax(u)*sin(del7(u,(kg-1)))));
 end
 for kh=2:(numel(t8))
del8(u,kh)=del8(u,(kh-1))+(((dt*dt)/M)*(Pe(u,8)-Pmax(u)*sin(del8(u,(kh-1)))));
 end
 for ki=2:(numel(t9))
del9(u,ki)=del9(u,(ki-1))+(((dt*dt)/M)*(Pe(u,9)-Pmax(u)*sin(del9(u,(ki-1)))));
 end
 for kj=2:(numel(t10))
del10(u,kj)=del10(u,(kj-1))+(((dt*dt)/M)*(Pe(u,10)-Pmax(u)*sin(del10(u,(kj-1)))));
 end
 for kk=2:(numel(t11))
del11(u,kk)=del11(u,(kk-1))+(((dt*dt)/M)*(Pe(u,11)-Pmax(u)*sin(del11(u,(kk-1)))));
 end
 for kl=2:(numel(t12))
del12(u,kl)=del12(u,(kl-1))+(((dt*dt)/M)*(Pe(u,11)-Pmax(u)*sin(del12(u,(kl-1)))));
 end
 for km=2:(numel(t13))
del13(u,km)=del13(u,(km-1))+(((dt*dt)/M)*(Pe(u,13)-Pmax(u)*sin(del13(u,(km-1)))));
 end
 for kn=2:(numel(t14))
del14(u,kn)=del14(u,(kn-1))+(((dt*dt)/M)*(Pe(u,14)-Pmax(u)*sin(del14(u,(kn-1)))));
 end
 for ko=2:(numel(t15))
del15(u,ko)=del15(u,(ko-1))+(((dt*dt)/M)*(Pe(u,15)-Pmax(u)*sin(del15(u,(ko-1)))));
 end
 for kp=2:(numel(t16))
del16(u,kp)=del16(u,(kp-1))+(((dt*dt)/M)*(Pe(u,16)-Pmax(u)*sin(del16(u,(kp-1)))));
 end
 for kq=2:(numel(t17))
del17(u,kq)=del17(u,(kq-1))+(((dt*dt)/M)*(Pe(u,17)-Pmax(u)*sin(del17(u,(kq-1)))));
 end
 for kr=2:(numel(t18))
del18(u,kr)=del18(u,(kr-1))+(((dt*dt)/M)*(Pe(u,18)-Pmax(u)*sin(del18(u,(kr-1)))));
 end
 for ks=2:(numel(t19))
del19(u,ks)=del19(u,(ks-1))+(((dt*dt)/M)*(Pe(u,19)-Pmax(u)*sin(del19(u,(ks-1)))));
```

```
 end
 for kt=2:(numel(t20))
del20(u,kt)=del20(u,(kt-1))+(((dt*dt)/M)*(Pe(u,20)-Pmax(u)*sin(del20(u,(kt-1)))));
 end
 for ku=2:(numel(t21))
del21(u,ku)=del21(u,(ku-1))+(((dt*dt)/M)*(Pe(u,21)-Pmax(u)*sin(del21(u,(ku-1)))));
 end
 for kv=2:(numel(t22))
    del22(u,kv)=del22(u,(kv-1))+(((dt*dt)/M)*(Pe(u,22)-Pmax(u)*sin(del22(u,(kv-1)))));
 end
 for kw=2:(numel(t23)-1)
del23(u,kw)=del23(u,(kw-1))+(((dt*dt)/M)*(Pe(u,23)-Pmax(u)*sin(del23(u,(kw-1)))));
 end
  for kx=2:(numel(t24))
del24(u,kx)=del24(u,(kx-1))+(((dt*dt)/M)*(Pe(u,24)-Pmax(u)*sin(del24(u,(kx-1)))));
  end
end
delbf=horzcat(del1,del2,del3,del4,del5,del6,del7,del8,del9,del10,del11,del12,del13,del14,del15,del16,del17,del18,del19,del20,de
l21,del22,del23,del24);
figure (9)
subplot(2,2,1)
plot(t,delbf(1,:))
subplot(2,2,2)
plot(t,delbf(3,:))
subplot(2,2,3)
plot(t,delbf(2,:))
subplot(2,2,4)
plot(t,delbf(4,:))
figure (10)
subplot(2,2,1)
plot(t1,del1(1,:))
xlabel('1 hour time in seconds')
ylabel('Coherent Swing Rotor Angle')
subplot(2,2,2)
plot(t1,del1(2,:))
xlabel('1 hour time in seconds')
ylabel('Coherent Swing Rotor Angle')
subplot(2,2,3)
plot(t1,del1(3,:))
xlabel('1 hour time in seconds')
ylabel('Coherent Swing Rotor Angle')
subplot(2,2,4)
plot(t1,del1(4,:))
xlabel('1 hour time in seconds')
ylabel('Coherent Swing Rotor Angle')
%PRIORITIZED LOAD SHEDDING SCHEME FOR THE MODEL RE MICROGRID
% Classification and Selection of Load combinations in the shedding scheme
% stages
IL=round([Nak(3) Kak(3) Ker(3) Kisu(3)]); %Industrial Loads
CL=round([Bun(3) Nan(3) Hom(3) Nar(3) TraZ(3) Kii(3)]); %Commercial loads
DAL=round([Bar(3) ElgM(3) WesP(3) Bus(3) Mig(3) Nyam(3) Sia(3) UasN(3) Bom(3) Vih(3)]); %Domestic Loads and
agricultural Loads
SF=DAL; % Shed First
SS=horzcat(DAL,CL); % If instability persists, Shed Second
ST=horzcat(DAL,CL,IL); % If instability persists, Shed Third, sparing non of the loads
%Classification and selection of Generation source combinations in the
%shedding scheme stages
SFG=[PVG(1) PVG(4) PVG(5) PVG(6) PVG(10) PVG(11)];%Solar PV generation will be removed first
SSG=[SFG WTG(4) WTG(5) WTG(6) WTG(7) WTG(8) WTG(9)];%If instbility persists, wind turbines will be removed
STG=[SSG HTG(6) HTG(7) HTG(8) HTG(9) HTG(10) HTG(11)];%If instability persists further hydro-turbines will be removed
%Load Shedding Process Module (Negative Power Imbalance)
LSM=round(horzcat(NPIFJLL,NPIAOLL,NPIFJLL,NPIAOLL));
```

```
idx=LSM<0;
LSMneg=(-1)*LSM(idx);
LSMpos=LSM(~idx);
LSM1=max(LSMneg);%Maximum negative power imbalance requires load shedding
LSM2=max(LSMpos);%Maximum positive power imbalance requires generator shedding
if LSM1>0 && LSM1<=sum(SF)
   VECL=SF;
n=length(VECL);
disp('Selected loads for 1st stage load shedding')
loadshed=zeros(2^n-1,n);
for i=1:(2^n-1)
   ndx=dec2bin(i,n)=='1';
   if (sum(VECL(ndx))>(LSM1-5) && sum(VECL(ndx))<(LSM1+5))
      L=length(VECL(ndx));
      VECL(ndx);
      loadshed(i,[1:L])=ans;
   end
end
end
if LSM1>sum(SF) && LSM1<=sum(SS)
   VECL=SS;
n=length(VECL);
disp('Selected loads for 2st stage load shedding')
for i=1:(2^n-1)
   ndx=dec2bin(i,n)=='1';
   if (sum(VECL(ndx))>(LSM1-3) && sum(VECL(ndx))<(LSM1+3))
      L=length(VECL(ndx));
      VECL(ndx);
      loadshed(i,[1:L])=ans;
   end
end
end
if LSM1>sum(SS) && LSM1<=sum(ST)
   VECL=SS;
n=length(VECL);
disp('Selected loads for 3st stage load shedding')
%loadshed=zeros(2^n-1,n);
for i=1:(2^n-1)
   ndx=dec2bin(i,n)=='1';
   if (sum(VECL(ndx))>(LSM1-3) && sum(VECL(ndx))<(LSM1+3))
      L=length(VECL(ndx));
      VECL(ndx);
      loadshed(i,[1:L])=ans;
   end
end
end
loadshed( ~any(loadshed,2), : ) = [];  %remove zero rows
loadshed( :, ~any(loadshed,1) ) = [];  %remove zero columns
loadshedd=loadshed.*1;
%Print Out the Possible Load Shedding Schemes/ Load Combinations
[fileID,message]= fopen('C:\Users\paulm\Documents\MATLAB\LoadSheddingSchemes.m','w');
fprintf(fileID,'%6s %6s %6s %6s %6s %6s %6s %6s %6s %6s %6s %6s
%6s\r\n','C1','C2','C3','C4','C5','C6','C7','C8','C9','C10','C11','C12','C13');
fprintf(fileID,'%6.1f %6.1f %6.1f %6.1f %6.1f %6.1f %6.1f %6.1f %6.1f %6.1f %6.1f %6.1f %6.1f\r\n',loadshedd);
fclose(fileID);

if LSM2>0 && LSM2<=sum(SFG)
   VECG=SFG;
n=length(VECG);
disp('Selected generators for 1st stage battery charging or gen shedding')
genshed=zeros(2^n-1,n);
for i=1:(2^n-1)
```

```
    ndx=dec2bin(i,n)=='1';
    if (sum(VECG(ndx))>(LSM2-5) && sum(VECG(ndx))<(LSM2+5))
        L=length(VECG(ndx));
        VECG(ndx);
        genshed(i,[1:L])=ans;
    end
end
end
if LSM2>sum(SFG) && LSM2<=sum(SSG)
    VECG=SSG;
n=length(VECG);
disp('Selected generators for 2nd stage battery charging or gen shedding')
genshed=zeros(2^n-1,n);
for i=1:(2^n-1)
    ndx=dec2bin(i,n)=='1';
    if (sum(VECG(ndx))>(LSM2-3) && sum(VECG(ndx))<(LSM2+3))
        L=length(VECG(ndx));
        VECG(ndx);
        genshed(i,[1:L])=ans;
    end
end
end
if LSM2>sum(SSG) && LSM2<=sum(STG)
    VECG=STG;
n=length(VECG);
disp('Selected generators for 3rd stage battery charging or shedding')
genshed=zeros(2^n-1,n);
for i=1:(2^n-1)
    ndx=dec2bin(i,n)=='1';
    if (sum(VECG(ndx))>(LSM2-3) && sum(VECG(ndx))<(LSM2+3))
        L=length(VECG(ndx));
        VECG(ndx);
        genshed(i,[1:L])=ans;
    end
end
end
genshed( ~any(genshed,2), : ) = [];  %remove zero rows
genshed( :, ~any(genshed,1) ) = [];  %remove zero columns

%OPIMAL LOAD SHEDDING USING HYBRID PARTICLE SWARM OPTIMIZATION/GENETIC
%ALGORITHM
sumoloadshed=sum(loadshed,2);
oloadshed=flip((sort(sum(loadshed,2)))/Gs);
ogenshed=flip((sort(sum(genshed,2)))/Gs);
ooloadshed=oloadshed(1:4);
oogenshed=ogenshed(1:4);
Peoo=Pe(:,1)-ooloadshed;
Pmaxoo=Pmax;
Hoo1=2.6312; Hoo2=4.1296;Hoo3=4.768;%Inertia constants of the three generators
Goo1=512;Goo2=270;Goo3=125;%Machine ratings in MVA for the three generators
dtoo=0.05;
Gsoo=905.8; %Base MVA
Eoo=1.0; %Equivalent Generator terminal voltage p.u
Voo=0.9;% Equivalent Receiving end voltage on infinite bus p.u
Xoo=0.8983; % p.u line reactance
pmaxoo=Voo*Eoo/Xoo;
Heqoo=(Hoo1*Goo1/Gsoo)+(Hoo2*Goo2/Gsoo)+(Hoo3*Goo3/Gsoo);% dynamic equivalencing inartia constants to single
machine - infinite bus bar
Moo=Heqoo/(pi*50);
%Pmaxoo=[1.2519 1.3448 1.2371 1.3245];
too1=0:30:3600;
deloo1 = zeros(4,numel(too1));
```

```
for uoo=1:4
    deloo1(uoo,1)=(asin(Peoo(uoo,1)));
    for kaoo=2:30
   deloo1(uoo,kaoo)=deloo1(uoo,(kaoo-1))+(((dtoo*dtoo)/Moo)*(Peoo(uoo,1)+Pmaxoo(uoo)*sin(deloo1(uoo,(kaoo-1)))));
    end
    for kaoo=31:(numel(too1))
   deloo1(uoo,kaoo)=deloo1(uoo,(kaoo-1))-(((dtoo*dtoo)/Moo)*(Peoo(uoo,1)+Pmaxoo(uoo)*sin(deloo1(uoo,(kaoo-1)))));
    end
end
swarm_size = 64;                % number of the swarm particles
maxIter = 50;                   % maximum number of iterations
inertia = 2.0;
correction_factor = 2.0;
% set the position of the initial swarm
a = 1:8;
[X,Y] = meshgrid(a,a);
C = cat(2,X',Y');
D = reshape(C,[],2);
swarm(1:swarm_size,1,1:2) = D;      % set the position of the particles in 2D
swarm(:,2,:) = 0;                   % set initial velocity for particles
swarm(:,4,1) = 1000;                % set the best value so far

plotObjFcn = 0;                     % set to zero if you do not need a final plot

%% define the objective funcion here (vectorized form)
objfcn =  @(x)(x(:,1) - (numel(GAO)-4)).^2 + (x(:,2) - (numel(GenModel))).^2;

tic;
%% The main loop of PSO
for iter = 1:maxIter
    swarm(:, 1, 1) = swarm(:, 1, 1) + swarm(:, 2, 1)/1.3;       %update x position with the velocity
    swarm(:, 1, 2) = swarm(:, 1, 2) + swarm(:, 2, 2)/1.3;       %update y position with the velocity
    x = swarm(:, 1, 1);                                 % get the updated position
    y = swarm(:, 1, 2);                                 % updated position
    fval = objfcn([x y]);                               % evaluate the function using the position of the particle

    % compare the function values to find the best ones
    for ii = 1:swarm_size
        if fval(ii,1) < swarm(ii,4,1)
            swarm(ii, 3, 1) = swarm(ii, 1, 1);              % update best x position,
            swarm(ii, 3, 2) = swarm(ii, 1, 2);              % update best y postions
            swarm(ii, 4, 1) = fval(ii,1);                   % update the best value so far
        end
    end

    [~, gbest] = min(swarm(:, 4, 1));                       % find the best function value in total

    % update the velocity of the particles
    swarm(:, 2, 1) = inertia*(rand(swarm_size,1).*swarm(:, 2, 1)) + correction_factor*(rand(swarm_size,1).*(swarm(:, 3, 1) ...
        - swarm(:, 1, 1))) + correction_factor*(rand(swarm_size,1).*(swarm(gbest, 3, 1) - swarm(:, 1, 1)));   %x velocity component
    swarm(:, 2, 2) = inertia*(rand(swarm_size,1).*swarm(:, 2, 2)) + correction_factor*(rand(swarm_size,1).*(swarm(:, 3, 2) ...
        - swarm(:, 1, 2))) + correction_factor*(rand(swarm_size,1).*(swarm(gbest, 3, 2) - swarm(:, 1, 2)));   %y velocity component


end
toc
%% plot the function
if plotObjFcn
    ub = 40;
    lb = 0;
    npoints = 1000;
    x = (ub-lb) .* rand(npoints,2) + lb;
```

```
    for ii = 1:npoints
        f = objfcn([x(ii,1) x(ii,2)]);
        plot3(x(ii,1),x(ii,2),f,'.r');hold on
    end
    plot3(swarm(1,3,1),swarm(1,3,2),swarm(1,4,1),'xb','linewidth',5,'Markersize',5);grid
end
figure (11)
subplot(2,2,1)
plot(too1,deloo1(1,:))
xlabel('1 hour time in seconds')
ylabel('Coherent Swing Rotor Angle')
subplot(2,2,2)
plot(too1,deloo1(3,:))
xlabel('1 hour time in seconds')
ylabel('Coherent Swing Rotor Angle')
subplot(2,2,3)
plot(too1,deloo1(2,:))
xlabel('1 hour time in seconds')
ylabel('Coherent Swing Rotor Angle')
subplot(2,2,4)
plot(too1,deloo1(4,:))
xlabel('1 hour time in seconds')
ylabel('Coherent Swing Rotor Angle')
function [child1 , child2] = crossover(parent1 , parent2, Pc, crossoverName)

switch crossoverName
    case 'single'
        Gene_no = length(parent1.Gene);
        ub = Gene_no - 1;
        lb = 1;
        Cross_P = round (  (ub - lb) *rand() + lb  );

        Part1 = parent1.Gene(1:Cross_P);
        Part2 = parent2.Gene(Cross_P + 1 : Gene_no);
        child1.Gene = [Part1, Part2];

        Part1 = parent2.Gene(1:Cross_P);
        Part2 = parent1.Gene(Cross_P + 1 : Gene_no);
        child2.Gene = [Part1, Part2];


    case 'double'
        Gene_no = length(parent1);

        ub = length(parent1.Gene) - 1;
        lb = 1;
        Cross_P1 = round (  (ub - lb) *rand() + lb  );

        Cross_P2 = Cross_P1;

        while Cross_P2 == Cross_P1
            Cross_P2 = round (  (ub - lb) *rand() + lb  );
        end

        if Cross_P1 > Cross_P2
            temp =  Cross_P1;
            Cross_P1 =  Cross_P2;
            Cross_P2 = temp;
        end

        Part1 = parent1.Gene(1:Cross_P1);
        Part2 = parent2.Gene(Cross_P1 + 1 :Cross_P2);
```

```
        Part3 = parent1.Gene(Cross_P2+1:end);

        child1.Gene = [Part1 , Part2 , Part3];


        Part1 = parent2.Gene(1:Cross_P1);
        Part2 = parent1.Gene(Cross_P1 + 1 :Cross_P2);
        Part3 = parent2.Gene(Cross_P2+1:end);

        child2.Gene = [Part1 , Part2 , Part3];
    end

    R1 = rand();

    if R1 <= Pc
       child1 = child1;
    else
       child1 = parent1;
    end

    R2 = rand();

    if R2 <= Pc
       child2 = child2;
    else
       child2 = parent2;
    end

    end
    function [child] = mutation(child, Pm)

    Gene_no = length(child.Gene);

    for k = 1: Gene_no
       R = rand();
       if R < Pm
          child.Gene(k) = ~ child.Gene(k);
       end
    end

    end
    function [parent1, parent2] = selection(population)

    M = length(population.Chromosomes(:));

    if any([population.Chromosomes(:).fitness] < 0 )
       % Fitness scaling in case of negative values scaled(f) = a * f + b
       a = 1;
       b = abs( min(  [population.Chromosomes(:).fitness] )  );
       Scaled_fitness = a *  [population.Chromosomes(:).fitness] + b;

       normalized_fitness = [Scaled_fitness] ./ sum([Scaled_fitness]);
    else
       normalized_fitness = [population.Chromosomes(:).fitness] ./ sum([population.Chromosomes(:).fitness]);
    end



    %normalized_fitness = [population.Chromosomes(:).fitness] ./ sum([population.Chromosomes(:).fitness]);

    [sorted_fintness_values , sorted_idx] = sort(normalized_fitness , 'descend');
```

```
742     for i = 1 : length(population.Chromosomes)
743         temp_population.Chromosomes(i).Gene = population.Chromosomes(sorted_idx(i)).Gene;
744         temp_population.Chromosomes(i).fitness = population.Chromosomes(sorted_idx(i)).fitness;
745         temp_population.Chromosomes(i).normalized_fitness = normalized_fitness(sorted_idx(i));
746     end
747
748
749     cumsum = zeros(1 , M);
750
751     for i = 1 : M
752         for j = i : M
753             cumsum(i) = cumsum(i) + temp_population.Chromosomes(j).normalized_fitness;
754         end
755     end
756
757
758     R = rand(); % in [0,1]
759     parent1_idx = M;
760     for i = 1: length(cumsum)
761         if R > cumsum(i)
762             parent1_idx = i - 1;
763             break;
764         end
765     end
766
767     parent2_idx = parent1_idx;
768     while_loop_stop = 0; % to break the while loop in rare cases where we keep getting the same index
769     while parent2_idx == parent1_idx
770         while_loop_stop = while_loop_stop + 1;
771         R = rand(); % in [0,1]
772         if while_loop_stop > 20
773             break;
774         end
775         for i = 1: length(cumsum)
776             if R > cumsum(i)
777                 parent2_idx = i - 1;
778                 break;
779             end
780         end
781     end
782
783     parent1 = temp_population.Chromosomes(parent1_idx);
784     parent2 = temp_population.Chromosomes(parent2_idx);
785
786     end
```

Appendix B: Two Papers Accepted for Publication in Conference Proceedings

Coherent Swing Under-Frequency Transient Stability for Renewable Sources Islanded Micro-Grid

Paul Muia Musyoka[1], Peter Moses Musau[2], Abraham Nyete[3]
Electrical and Information Engineering Department
University of Nairobi
pauilmuia80@gmail.com[1], pemosmusa@gmail.com[2], nsonorig@gmail.com[3]

Abstract---**Renewable Energy Sources micro-grids experience operational challenges due the unpredictable weather patterns, requiring continuous demand control schemes, which are detrimental to both customers and the micro-grid operator. Optimal unit commitment plans coupled with a synthetic inertia system, that is, distributed renewable energy storage (DRES), are considered to lower power imbalances and thus contributing to frequency transient stability. This research models a renewable energy micro-grid with solar PV, wind turbine, hydro and a geothermal power plant. The transient stability study during times of severe power imbalances shows the micro-grid is unstable during such a time. Particle swarm optimization is developed to commit the units in an optimal scheme that considers load flow power losses and DRES in a multi-objective function. This improves the control and operation of the micro-grid, minimizing frequency fluctuations caused by power imbalance, at times of severe shortage of generation from intermittent renewable sources.**

Index Terms---**coherent swing, rotor angle, transient stability, islanded micro-grid, renewable energy storage**

I. INTRODUCTION

Climate change campaign in different countries has led to development of numerous renewable energy micro-grids and thermal power plants shut down to lower carbon footprints and secure a clean environment for humanity. However, these developments come at a cost, since renewable energy grids depend on weather patterns that are intermittent and unpredictable. Frequency and voltage collapse in entirely renewable energy grids are therefore prevalent [1].

These challenges require compensation measures and beyond certain limits measures of last resort such as load shedding are deployed, hurting the economic benefit of both consumers and suppliers of the electricity. Optimal power harvesting, unit commitment schemes, least losses and distributed renewable energy storage systems, that closely assumes the load profiling, developed in this study, are necessary to ensure least amounts of loads are disconnected from micro-grid.

Intelligent techniques such as particle swarm optimization, genetic algorithm and artificial neural networks can be utilized to optimize dispatch and unit commitment, which reduces the amount of power imbalance, and hence sustaining loads that would otherwise have been disconnected from the network [2] [3] Advanced dynamic equivalency modeling techniques for coherent swing systems reduce the multi-objective function complexity and thus lowering computational time.

Primarily, this work involved a wide range of literature review, simulations in MATLAB code and results obtained indicate severe frequency collapse in the transient stability swing curve, which reduces with reduction of power imbalance on an optimized unit commitment, load flow and DRES micro-grid network. Key contributions addressed in this research include minimal power loss micro-grid modeling, power imbalance/ probable extra power outages reduction/ stabilization through DRES and recovery times thereof.

II. LITERATURE REVIEW

80% of the Kenyan national electricity demand is supplied by renewable energy generations such as hydro, geothermal, wind and solar making the power system vulnerable to unpredictable weather patterns. Reserve capacity at 35% ensures restoration within the specified time limits by the energy regulatory authority [4]. This setup informs selection of generation sources for the micro-grid model in this study.

[5] With interconnection to East Africa Power Pool and development of larger solar farms through the solar access project, the challenges are bound to soar higher even as the government stretches the high loss distribution network to last mile connections.

[6]Using scenario based method, Peter Moses Musau et al 2017, carried out simulations of multi-objective function with storage systems cost and frequency fluctuations as the key effects of power imbalances. This included a case study in which 180MW hyro-power generator tripping caused long hours of blackout before restoration of the network.

Rate of frequency changes and input frequency parameters were utilized for setting load shedding relays in [7], using particle swarm optimization for the computation of the parameters in the proposed model. Uncertainty in the setting of the system was solved by a fuzzy logic system model attaining least load disconnection for optimal operation at the standard frequency.

In [8] a model wind farm whose base load is carried on a diesel generator was investigated for under frequency collapse in which genetic algorithm in hierarchical forms were used to provide weighting factors, in largest peak loads and severe contingency, where an iterative process appending the fitness function, checking the problem constraints after population initialization, individual encoding, cross-over and mutation was simulated in the PSCAD software resulting in a more reliable solution, as compared to traditional methods.

Testing and validation of a hardware in the loop algorithm for predictive under-frequency instability was developed, providing a preventive measure to frequency collapse of micro-grids that are highly penetrated by the renewable energy sources [9]

In [10], fast-acting distributed energy storage system (DESS) to lower extra power outages in a case study of Guadeloupe electrical island in France is studied. The results show that DESS possess synthetic inertia that enhances frequency stability of the island, however, it failed to address voltage ride-through, forecast error and variability nature of renewable sources.

In [11], a multi-period load flows whose accuracy is higher and convergence time short, is studied by building a surrogate model using a combination of Latin hypercube sampling, Kriging and polynomial regression. The developed technique is more efficient when compared to voltage linearization or time sampling, with ten minutes power losses, bus currents and voltage profiles being computed within satisfactory time.

III. PROBLEM FORMULATION

a) Micro-Grid Model: Wind Turbines Generation

The output of wind turbine generation system is given in equation (1), explicitly defining MW output of the system as a function of velocity, turbine diameter and Euler/ power co-efficient

$$.P = \frac{1}{2}\pi\rho R^2 C_P\left(\frac{\omega R}{V}, \beta\right)V^3 \qquad (1)$$

In this equation, β= pitch angle of the turbine blade, Cp= power coefficient, V= measured wind velocity, R= radius of rotor, ρ= density of air flow, ωR / v = tip velocity ratio with angular speed of rotor as ω.

b) Micro-Grid Model: Geo-Thermal Generation:

Equation (2) gives the specific work output for a geothermal generation system, where Whpt = turbine pressure upper limit, Wlpt= lower limit output power, w =turbine specific work output

$$w = \frac{W_{tatol}}{m_1}:\ W_{tatol} = W_{lpt} + W_{hpt} \qquad (2)$$

c) Micro-Grid Model: Mini Hydro Power Plant

The real power output from a hydropower plant is characterized by equation (3), where f is a constant of conversion from ft pounds to kilowatts, Q is the volumetric flux release from all sources, θ is the elevation angle of the reservoir, H= net head, pi= power generated from the plant, γ = specific density of water and ε_I= efficiency.

$$P_i = \frac{H(Q,\theta)\varepsilon_I \gamma q_i}{f * 1000} \qquad (3)$$

d) Micro-Grid Model: Solar PV Farm Generation

Solar PV system power generation is characterized by

$$P.R = \frac{\sum P_{PV}}{P_{nom}} * \frac{G_s}{G_{ag}} = \frac{E_{pv}}{P_{nom}} * \frac{G_s}{H_{AG}} \qquad (4)$$

In which, Hag= solar irrandiance, Epv = Kwh output, Gag= gloabal radiation in per kW, Pnom= nameplate rating for nominal power, Rs= resistance in series arrangement, Ipv= output current, Vph= volltage at the termianl of the PV panel and Iph = solar panel current at output termianl

e) Objective Function

The underfrequency transient stability probem is formulated as shown in equation (5), in which NL= network losses, UCFF = Unit Commitment plan based Frequency Fluactions as a result of power imbalance and CRES is the cost of renewable energy storage. Each of these factors possess a weight φ_n, that is a range of a random value between 0 to 1, that is depended on extend to which the individual factor affects recovery of the system stability.Time sampling at intervals of 10 seconds is considered for evaluation of this function, to check for violations in frequency fluctuations.

$$Min\ F = \{\varphi_1 NL + \varphi_2 UCFF - \varphi_3 DRES\} \qquad (5)$$

Network losses (NL) contribute to power imbalances, widening the gap between the generation and the demand, thus contributing to network instability. These losses are obtained from the multi-period load flow equation (6), in which the symbols carry their usual meaning in a load flow study

$$NL = \sum_{j=1}^{M}\sum_{i=1}^{M}\{V_j V_i(G_{ji}\cos\theta_{ji} + B_{ji}\sin\theta_{ji})\} \qquad (6)$$

Unit Commitment Frequency Fluctuations are derived from swing equation, as shown in equation (7), considering RES commitment plan for the outputs of equations (1 to 4). A renewable energy sources commitment plan, whose $Pm_n \neq Pe_n$, contributes to network instability.

$$UCFF = \sum_{n=1}^{N_g} Pm_n - \sum_{n=1}^{N_g} Pe_n = \frac{2\sum_{n=1}^{N_g}\left\{H_n \frac{df_n}{dt}\right\}}{f_0} \qquad (7)$$

Where LHS = power imbalance for commited N units, with mechanical power Pm_n and demand Pe_n. The RHS gives the frequency fluctuations resulting from the power imbalance, considering rate of change of frequency $\frac{df_n}{dt}$ and inertia constant H_n, in which f0 = standard frequency.

Distributed Renewable Energy Storage (DRES) formulation is illustrated in equation (8), considering charging time (T), storage system rating P_{gt} and total energy (E) available during positive power imbalance of the renewable energy source generation i.e. when available mechanical power is greater than demand ($Pm_n \geq Pe_n$)

$$DRES = \sum_{t=1}^{T} \Delta t P_{gt} \leq E \qquad (8)$$

IV. METHODOLOGY: PARTICLE SWARM OPTIMIZATION ALGORITHM

a) Justification and Mapping of problem formulation to PSO algorithm

Selection of this method ensures mininum number of iterations is constituted to achieve the convergence criterion for the optimum under frequency commitment of the units, for minimal power loss, maximum renewable energy storage and least power imbalances that correspond to minimal frequency fluctuations. When applied to deficit contingencies and losses for medium, small and large systems, PSO adapts well with the system dynamics. Table 1.0 illustrates mapping of the problem formulation of equation 5, into the PSO algorithm.

Table 1.0 Problem –Method Mapping

No.	PSO Parameters	Prob. Formulation
1.	Fittness Function	Equation (5)
2.	inertia weight	0.4
3.	acceleration coefficient	0.2
4.	Population	1000 Particles
5.	No. of Iterations	200
6.	Constraints	E, Pm, Pe and $\frac{df_n}{dt}$

b) Optimization Algorithm Pseudo code

PSO algorithm in steps as utilized in optimization of the objective function given in equation (5) is outlined as follows;

1. Initialization of population (size of population, swarm and individual acceleration constants, number of partitions, partition variables and solutions etc.)
2. Fitness function evaluation for search agents
3. Application of PSO on the population
4. Partitioning of the whole population in Sub partitions/ sub-populations
5. Update the global best and individual best positions and iterate until the convergence criteria is met

V. RESULTS

a) Algorithm calculation time, Convergence and response times

Expected response time is highly dependent on the size of a disturbance/ power imbalance that micro-grid is recovering from. For extreme faults, causing frequency fluctuations such that f>51.50 or f<47.75, where f= operational frequency, frequency response is expected in 20 seconds or less [12]. Other bearable faults should have time response in 10 seconds or less. The developed simulation algorithm computes the fitness function using particle swarm optimization in 0.3575 seconds, converging within first 50 iterations on core i3 processor, 2.50GHz machine.

b) Output variables of the fuel constraint generation models

The renewable energy generation capacities are illustrated in table 2.0, where the wind turbine generation model has 3 input variable parameters/ data sets i.e. Wind Turbine Output Coefficient (WTOp), Wind Turbine diameter (WTd) and variable wind velocity (Wv) with a single output (WTG). Hydro-turbine model has 3 input variables i.e. hydraulic head (HTh), Volumetric Flux (HTQ) and Hydro-turbine efficiency (HTeff), with a single output (HTG). Solar PV Model has 3 input variables i.e. Solar Radiation (H), output co-efficient (OpCoef) and Area (A) with one output (PVG). The geothermal generation model carries the base load with a capacity of 175 MW. The four generation models give a total output variable (TotalGen) as shown in table 2.0.

Table 2.0 Output variables of the fuel constraint generation models

WTG	HTG	PVG	GTG	TotalGen
0.220	0.078	0.250	175	175.549
1.554	4.010	3.152	175	183.716
5.074	12.624	6.900	175	199.598
12.867	26.165	11.600	175	225.632
28.299	44.879	17.363	175	265.541
56.509	69.013	24.302	175	324.825
105.020	98.813	32.537	175	411.371
184.465	134.524	42.194	175	536.183
309.458	176.392	53.399	175	714.250
499.602	224.664	66.288	175	965.554
780.655	279.585	81.000	175	1316.239

c) A sample ideal load curve for load profiling

An ideal load curve that consists of loads from the Kenya national grid, (western region) as illustrated in fig. 1 is used to examine the difference between generation and demand.

d) Optimal generation commitment curve

From the optimization of unit commitment suitable for the load profile, the 2 optimal generation models shown in fig. 2 are used to examine the power flow. At the times of severe power deficiency, the generators can be dispatched optimally in 2 different models 1 and 2, in order to track the load curve closely, depending on available generation.

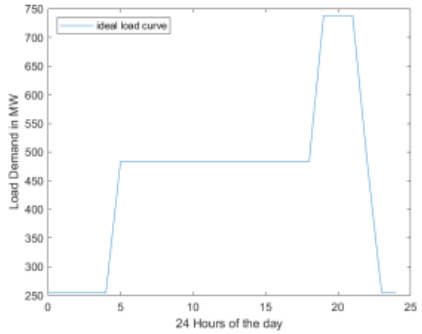

Fig. 1 Load profile curve for the model micro-grid

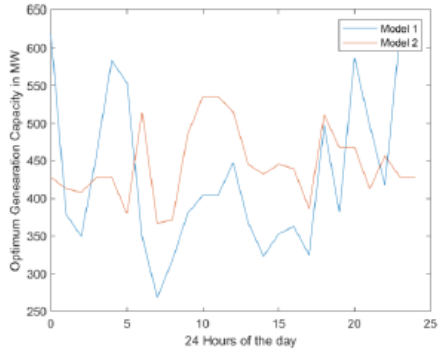

Fig. 2 Optimal generation commitment curve

e) Power imbalances for each of the optimal generation commitments

Power imbalances are derived, considering two models of generation reserves for power borrowing, resulting in a set of 4 similar power imbalance curves illustrated in fig. 3. A net power imbalance is eminent, as a result of unpredictable renewable energy source generation and probable load switching by consumers. The renewable energy micro-grid remains resilient for short periods of low net power imbalances, since the inertia constant of the wind, geothermal and hydro plants provides the self-restoration although with larger swings in the swing curve. A positive power imbalance is economically desirable since the operator will not incur the cost of energy not supplied.

For large negative net power imbalances, which occur majorly at the peak demand periods, it's necessary to take remedial measures of the last resort such as load shedding, by treating the loads as faults and disconnecting the feeders. This leads to economic losses on both sides of network i.e. to consumers and to operator in pursuit for a secure grid.

f) Transient Stability swing curve for the RE Micro-grid

The coherent transient swing curve for the highest power deficiency, investigated for a period of 1 hour (3600 seconds), at intervals of 10 seconds shows (in fig. 4), unstable system, requiring an under frequency load shedding for restoration of system stability. Investigation of the transient frequency stability is carried out, for the largest power imbalances, at intervals of 30 seconds which show that the system is unstable with swing curve increasing its swing amplitudes continuously

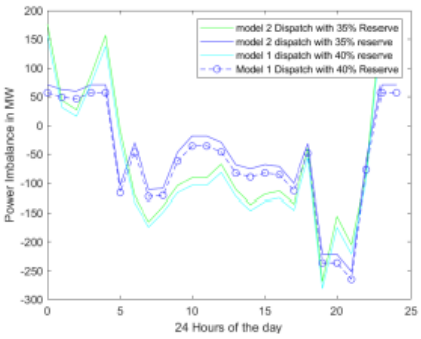

Fig. 3 Power imbalance curves considering generation reserves

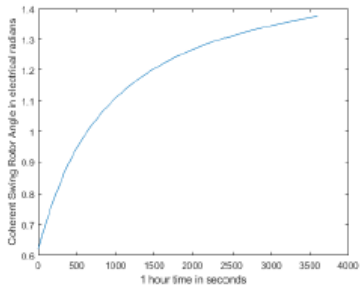

Fig. 4 Transient stability – coherent swing curve for the RES Micro-grid

c) CONCLUSION AND RECOMMENDATION

A highly penetrated RES islanded micro-grid exhibits both sessions of extra power potential generation and power deficiency. Optimization of the unit commitment using intelligent search PSO algorithm indicates improvements in net power imbalance and thus lower amounts of load will be affected by demand control measures. Connecting the micro-grid to national grid/ power pool solves these challenges in a smart metering power system. However, in the advent of climate change campaign, the national grids will be highly penetrated by renewable energy sources, multiplying the effect of instability. Although optimal unit commitment and dispatch lower the impact of demand control, an optimal under frequency load shedding (OUFLS) still necessary to restore the grid from frequency collapse. A localized OUFLS scheme at the islanded micro-grid levels would easily stabilize the overall network with consideration for primary feeder prioritization.

REFERENCES

[1] Salah Kamel and Omar Abdel Rahim Fatma Sayed, "Load shedding solution using multi-objective teaching learning based optimization," in *international conference on inovative trends in computer engineering (ITCE)*, 2018.

[2] A.I Isa, Z.Mat Yasin, N.A Salim and N.N. mOHD Rahim H. Mohamad, "Use of genetic Algorithm for Evalaution and control of Technical problems due load shedding in Power systems," in *International conference on power generation systems and renewable energy technologies*, 2017.

[3] M.K Gray and W.G Morsi, "Application of PSO and Fuzzy Logic for Under frequency load shedding," in *IEEE Electrical Power and Energy Conference (EPEC)*, 2013.

[4] ERC, KenGen, KPLC, REA, KETRACO, GDC, "updated least cost power development plan," Energy Regulatory commission, Nairobi, ERC, KenGen, KPLC, REA, KETRACO, GDC Study Period, 2011 to 2031, 2011.

[5] Kenya Power and Lighting Co. and Rural Electrification Authority, "Kenya off-grid solar access project (KOSAP) for underserved counties," 2017.

[6] Terry Lumbasi Chepkania, Abungu Nicodemus Odero and Cyrus Wekesa Moses Peter Musau, "Effects of renewable energy on Frequency stability: A proposed case study of Kenya Grid ," in *IEEE PES- IAS power Africa*, 2017.

[7] Gunjan Dashora and Payal Awwal, "Adaptive particle swarm optimization employing fuzzy logic ," in *International conference on recent advances and innovations in Engineering (ICRAIE)*, 2017.

[8] Ying-yi Hong and Shih-Fan Wei, "Multi-objective Under frequency load shedding in an autonoumous system using hierarchical genetic algorithms," in *IEEE transactions on power delivery*, 2010.

[9] Shiyou Yang and Peihong Ni Jiagiang Yang, "A vector tabu search algorithm with enhanced searching ability for pareto solution and its application to multi-objective optimizations," *IEEE*, vol. 52, no. 3, pp. 1-5, 2016.

[10] Bruno François, Gilles Malarange Gauthier Delille, "Dynamic Frequency Control Support by Energy Storage to Reduce the Impact of Wind and Solar Generation on Isolated Power System's Inertia," *IEEE TRANSACTIONS ON SUSTAINABLE ENERGY*, vol. 3, no. 4, October 2012.

[11] Gauthier Delille, Bruno Francois, Julien Bect, Marjorie Cosson, Dutrieux Baraffe, "A novel non-intrusive approximation method to obtain fast and accurate multi-period load-flows for distribution network planning," *HAL*, August 2017.

[12] Energy regulatory commission of kenya, "Kenya national grid transmission code," Nairobi, 2013.

HYPERLINK "mailto:pauilmuia80@gmai

Optimal Load Shedding Scheme for a Model Renewable Energy Micro-Grid

Paul Muia Musyoka[1], Peter Musau[2], Abraham Nyete[3]
Department of Electrical and Information Engineering
University of Nairobi
pauilmuia80@gmail.com[1], pemosmusa@gmail.com[2], nsonorig@gmail.com[3]

Abstract---Optimization of demand control in renewable energy micro-grids involves developing load shedding schemes and searching for the most optimum. With climate change campaign in favor of renewable energy micro-grids or integration to national grids, the stability of the systems becomes more unpredictable. Its therefore justified, technically and economically, to optimize both unit commitment plans to track the load curve closely and design load-shedding schemes that attain the voltage and frequency limits, while retaining maximum load on the grid. The study shows that through load-shedding, renewable energy micro-grids can be operated in the stable state at the expense of loads during times of severe power imbalances. Optimization of the load-shedding using PSO-GA technique ensure optimum amount of load is shed from the grid with each possible load shedding scheme getting evaluated first and selection of most effective scheme with priority for loads is accomplished.

Index Terms: **load shedding, under-frequency stability, renewable energy micro-grid, transient stability, shedding scheme**

I. INTRODUCTION

Highly penetrated renewable energy grids or purely renewable energy micro-grids exhibit higher frequencies of network instabilities due to stochastic nature of loading and chaotic generation of power from unpredictable sources. These system instabilities are solvable by compensation techniques for voltage and frequency, which only apply when the available generation is capable of powering the connected loads, without violating the limits thereof. In cases where the generation is insufficient and power imbalances lead to violation of voltage and frequency limits, demand control is deployed as a measure of last resort.

According to Kenya National Grid Transmission Code/ Eastern Africa Power Pool, frequency fluctuations are regulated, such that when the grid is operating in the normal conditions, the frequency of operation ranges at ±1%, about the nominal frequency of 50Hz, i.e. between 49.5Hz to 50.5Hz. This frequency band is expanded to ±2% i.e. a range of between 49.0Hz to 51.0Hz about the nominal frequency, upon occurrence of disturbance in the network [1]. Once a major disturbance such as disconnection of large loads, failure of a major element in the transmission network or tripping of generating unit occurs, the frequency band can be expanded further up to ±2.5%, to range between 48.75 Hz to 51.25Hz. Extreme operational measures are taken after allowing a simultaneous occurrence of 2 or more major disturbances to operate with frequency ranges of -5%/+3% about the nominal frequency for a maximum of 20 seconds before extreme measures are initiated.

The main objective in this study was to model a purely renewable energy sources micro-grid, investigate its transient frequency stability and optimize the under-frequency load shedding scheme to achieve required levels of frequency and voltage fluctuations with minimum load disconnection and least cost for power storage, as formulated in the multi-objective function.

For a stable operation of a renewable energy micro-grid, controllable wind turbine/ solar plants need be resilient in fault ride through. The plants must provide active power that's proportional to retained voltages and maximizes reactive current supply during voltage dip while operating within its declared limit for at least 600 milliseconds or until voltage recovery to normal operating range. The plant should provide 90 percent of its maximum active power within 1 second upon voltage recovery.

Hybrid Particle Swarm-Genetic Algorithm is utilized to optimize the process of load shedding, in which the optimum possible combination of loads is selected, considering priority for the various types of loads i.e. industrial, commercial and domestic loads [2]. The renewable energy source generating units must remain connected for limits of: 0.5 Hz, rate of change of frequency, 20 seconds for frequency range of 47.0 to 47.5 Hz, 60 minutes for frequency ranges of 49.0 to 51.0 Hz and continuously operate at frequency range of 49.5 Hz to 50.5 Hz. Power imbalances that violate these conditions even after exhausting energy reserves option and compensation measures, will automatically initiate the prioritized load-shedding process [3].

Major contributions in this work included considering the five components/ causes of demand

control in a multi-objective formulation, as opposed to the single measurements of either voltage deviations, frequency fluctuations, energy storage, load flow/ losses and amount of disconnected load in restoring the grid into its normal operating conditions.

This paper is organized into five main sections: The first section, introduction, gives a background on the research while the second section describes related works (literature review) from different authors. A multi-objective problem formulation is outlined in third section with 5 sub-functions. In the fourth section, a detailed methodology, where an hybrid PSO-GA optimization technique is mapped into the problem, and on the last section, the results obtained from this study are analyzed and a conclusion is made on the sixth section.

II. LITERATURE REVIEW

[4] presented a fuzzy logic based demand control technique for shedding loads in an islanded distribution network, considering a major disturbance such as generator tripping. The developed fuzzy logic system technique utilizes load prioritization, rate of change of frequency and frequency levels to determine the most optimum loads for disconnection. Satisfactory stabilization is achieved, during generator tripping and on islanding operation.

[5] developed an under frequency load shedding scheme combining intelligent and adaptive techniques for both response based (frequency and its rate of change in the swing equation) and event based (power imbalance). The scheme is implemented in a islanded distribution network, whose investigations demonstrates improvements in frequence response of the network, with significant reduction of power deficiency effects during island transitions [6].

[7] considered parameters such as settling time, frequency deviation, nadir frequency and rate of change of frequency, in modelig the response of renewable energy power plants and developing frequency stabilization strategies. A thyristor switched lag compensator is used for improvemennts of frequency stability and optimization of the process is carried out using fire-fly algorithm. The results from this study indicate that frequency of parralled generation plants falls out of sychronism upon disturbance and low inertia turbine plants have least settling time and experience huge ROCOF and high frequency fluctuations.

[8] demonstrated the operation of an islanded mode grid, using intelligent load-shedding for power imbalances to stabilize voltage and frequency levels. Digisilent software is used in simulation of PLCs, in which the functions are embedded. The results affirm an efficient demand control for contingencies that are severe. [9] formulates a multi-objective function for restoration of voltage, considering cost of demand control, voltage deviations and power losses.

[10] Particle swarm optimization and its vectored form are used solution searches and comparatively found that EPSO has higher precision in shedding loads as compared to its conventional form. [11] analyzed challenges of high penetration of renewable energy sources in a grid and the required load shedding processes for stability restoration. The study considered multi-country approach for interconnected power systems, with high ranges of frequency dips. The main functions with respect to renewable sources included UFLS, primary control and system inertia. ENTSO-E guidelines were used.

III. PROBLEM FORMULATION

The multi-objective problem formulation is illustrated in equation (1), with five major sub-functions.

$$Min\ F = \{\varphi_1 VD + \varphi_2 LS + \varphi_3 FF + \varphi_4 NL + RE\} \quad (1)$$

The sub-functions include:

i) Energy storage for supply in times of deficiency (RE)
ii) Voltage Deviation Effects (VD)
iii) Frequency Deviation Effects (FF)
iv) Transmission and Distribution Losses (NL)
v) Disconnected Load for frequency recovery (LS)

The extent to which individual factors are co-related and magnitude with which they affect system stability is weighted using φ_n; where n = 1, 2, 3, 4 and 5.

Each of the sub-objectives is formulated as follows;

A. Disconnected Load for frequency recovery (LS)

Once power imbalances occur, such that demand exceeds supply, an optimal amount of load will have to be connected from the grid to ensure stability is restored. Equation (2) shows addition of individual power imbalances for the n generators in the network.

$$\sum_{n=1}^{n} Pm_n - \sum_{n=1}^{n} Pe_n = \frac{2\sum_{n=1}^{n}\left\{H_n \frac{df_n}{dt}\right\}}{f_o} \quad (2)$$

In equation (2), ΔP_{ls} = disconnected load until frequency recovery, Hn = N^{th} generator inertia constant, and n= Number of generating machines in the network.

B. Voltage Deviations (VD)

In order to minimize destruction of equipment resulting from voltage violations the model micro-grid is developed with insulation levels according to IEC

60071-1 standard code, as indicated in table 1.0 below. Equation (3) constitutes the formulation of the sub-objective, in which V_m and V_j are the respective swing and j^{th} bus voltage levels during abrupt swings, VD= fluctuations in voltage and M is number of nodes.

$$VD = \sum_{j=1}^{M} \frac{(V_j - V_m)^2}{V_m^2} \quad (3)$$

Table 1.0 Insulation levels for model micro-grid equipment

Nominal/Rated Voltage	50 Hz, 1 minute WV	Lighting Surge	Highest operating voltage
220kV	395kV	950kV	245kV
132kV	275kV	650kV	145kV
66kV	140kV	325 kV	72.5kV

C. *Transmission and Distribution Network Power Losses (NL)*

Using the modified IEEE 9 Bus system with 3 renewable energy generators, a power flow solution based on equations (4) is carried out for power loss using NR method for transmission system. An additional distribution technical and non-technical power loss is provided for, ranging between 15 to 18 percent as per the World Bank 2019 report on energy efficiency for Kenya national grid systems. Active and reactive power losses in the network are formulated as in equation (4), where B = susceptance, G= conductance, M= total no. of network nodes and NL = network power losses

$$NL = \sum_{j=1}^{M} \sum_{i=1}^{M} \{V_j V_i (G_{ji} \cos\theta_{ji} + B_{ji} \sin\theta_{ji})\} \quad (4)$$

D. *Frequency Fluctuations (FF)*

During times of severe power imbalance, frequency fluctuations violating the specified limits of secure operation occur and are formulated in equation (5), in which H= inertia constant, PD= power demand, PG= available generation, f= frequency denotations nrm and f represent normal and faulty operation periods.

$$FF = 2\left[\left(\frac{H_{nrm}\frac{df_{nrm}}{dt}}{PG_{nrm} - PD_{nrm}}\right) - \left(\frac{H_f\frac{df_f}{dt}}{PG_f - PD_f}\right)\right] \quad (5)$$

E. *Renewable Energy Storage Cost (CRE)*

Renewable energy micro-grids utilize batteries for power supply during times of power imbalances. The facilities for storage and power conversions are, therefore, key in system stability. Their cost function is shown in equation (6), where C_{RESi}= Reduced cost of power not supplied due to available storage, C_{EAi}= Storage bank capital costs, C_{PGi}= fuel cost for supply storage power supply, P_i= Stored power, T= time period of study, CRE= cost of renewable energy storage.

$$CRE = \{\sum_{i=1}^{T} P_i (C_{EAi} - C_{RESi} + C_{PGi})\} \quad (6)$$

The multi-objective function of equation (1) is subject to constraints for load flow, generation capacity for active and reactive power, network node voltage levels, feeder current limits, optimum load shedding scheme constraints, allowable frequency limits, load priorities and capacity of battery banks and assumptions for coherence and dynamic equivalency, reducing the complexity of the transient stability analysis, the n-machine system is assumed coherent and reduced using equation (7), in which the inertia constants of individual machines are ramped together.

$$H_{eq} = \frac{H_1 G_1}{G_S} + \frac{H_2 G_2}{G_S} + \cdots + \frac{H_N G_N}{G_s} \quad (7)$$

Where Heq= Equivalent inertia constant, H1= Inertia constant of machine 1, G1= MVA rating of machine 1 and Gs = base rating and N denotes the number of machines.

IV. HYBRID PARTICLE SWARM – GENETIC ALGORITHM OPTIMIZATION

This hybridized version reaps three main benefits: first application of PSO for fitness function evaluation balances the exploration and exploitation processes in each iterations; second, high probability of crossing over in the partitioned sub-populations reduces the dimensionality and provides diversity and third, mutation operation rides through pre-mature convergence and snares of local minima. The adopted algorithm for optimization of the multi-objective function subject to constraints is outlined as follows;

i) Step 1: Initialize the population (partition variables, number of partitions, crossover and mutation probabilities, acceleration constants for the swarm and individual chromosomes and size of population)
ii) Step 2: Evaluate the fitness function for possible solutions/ search agents
iii) Step 3: Apply particle swarm optimization on whole population
iv) Step 4: Apply selection operator of genetic algorithm on the population

v) Step 5: Partition the whole population into smaller sub-populations
vi) Step 6: Apply arithmetical crossover to each sub-population
ⁱii) Step 7: Apply genetic algorithm mutation operator to the swarm
iii) Step 8: Update individual and global best positions
ix) Step 9: Iterate until the convergence criteria is met
x) Step 10: Print the solution and stop

The position and velocity of each particle is updated in every iteration according to equations (8) and (9), in which x represents the position of the particle, v represents the particle velocity, pb is the best position achieved by the particle, gb is the global best position, j denotes the iteration number, 0 denotes the previous iteration and 1 denotes the current iteration.

$$x_j^1 = x_j^0 + v_j^1, \quad j = 1, 2, 3, 4 \ldots P \tag{8}$$

$$v_j^1 = v_j^0 + \epsilon_1 r_{j1}\left(pb_j^0 - x_j^0\right) + \epsilon_2 r_{j2}\left(gb - x_j^0\right) \tag{9}$$

The crossover operation is done by first choosing a random set of β such that $\beta \in [0\ 1]$

Two offspring are generated from parents such that;

$$OS_j^1 = \beta pop_j^1 + (1-\beta) pop_j^2 \tag{10}$$

$$OS_j^2 = \beta pop_j^2 + (1-\beta) pop_j^1 \tag{11}$$

In equations (10) and (11), OS = offspring, pop= population and j denotes the iteration.

V. RESULTS AND ANALYSIS

A. *Model Micro-grid Transmission and Distribution (TD) Losses*

The transmission and distribution losses model considers load flow studies for the transmission network using the IEEE 9 Bus system, and considers distribution losses of 15 to 18 percent of the generation, according to distribution distances and voltage levels, as per the World Bank energy efficiency survey 2019. The resultant power loss profile is illustrated in the graphs of figure 1.0

B. *Transient Stability Swing Curve before Load Shedding*

Examining the transient stability of the renewable

micro-grid with power imbalances as the key system disturbances, the swing curves of figure 2.0 are derived. These swing curves indicate severe instability that needs immediate load shedding to secure the system from frequency collapse.

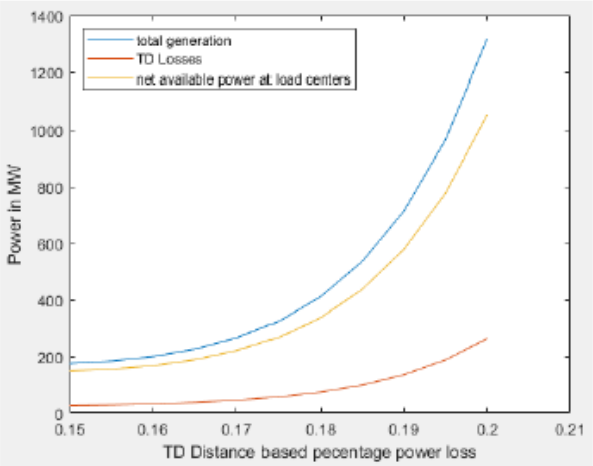

Figure 1.0 TD network losses for micro-grid model

C. *Prioritized Load Shedding Scheme*

After simulation, there are about 1500 possible combinations of loads, forming the population for optimization. These populations of possible solutions are evaluated using PSO-GA and the population which has best swing curve is selected and implemented. For a maximum power imbalance of 269MW, the optimum load combination constitutes of 12 loads and falls in the second stage of load shedding i.e. combines loads in domestic, agricultural and commercial categories and spares industrial category of loads as per the prioritization schedule. The total load disconnected for this imbalance is 295MW, consisting of 5MW, 6MW, 8MW, 10MW, 14MW, 16MW, 18MW, 23MW, 25MW, 31MW, 42MW and 97MW feeders.

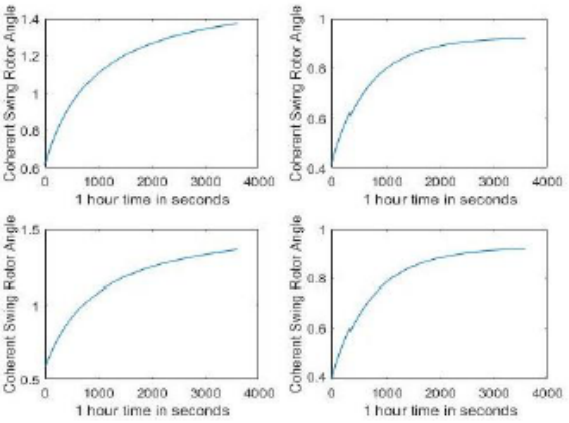

Figure 2.0 Severe power imbalance operation Swing

D. *Transient Stability Swing Curve after Load Shedding*

The PSO-GA method is utilized to find the most optimal load shedding combinations. These optimal load combinations are then treated as faulty feeders and disconnected by switching off respective relays, thus relieving the micro-grid from adverse effects. The optimally restored stable system swing curves are indicated in figure 3.0.

VI. CONCLUSION AND RECOMMENDATIONS

An ideal solution for renewable energy micro-grids stability is to provide energy reserves sufficient enough to take up loads immediately after shedding, to avoid violation of consumer rights to universal access to energy for long periods. However, these reserves will increase cost of energy even during times of sufficient supply. A compromise is, therefore, required to ensure forecasting for availability of energy is integrated with reserve schemes and agreements in form of time and amount of energy with a trade-off for load-shedding in short periods of scarcity, as the only option of last resort, in securing the grid from collapse.

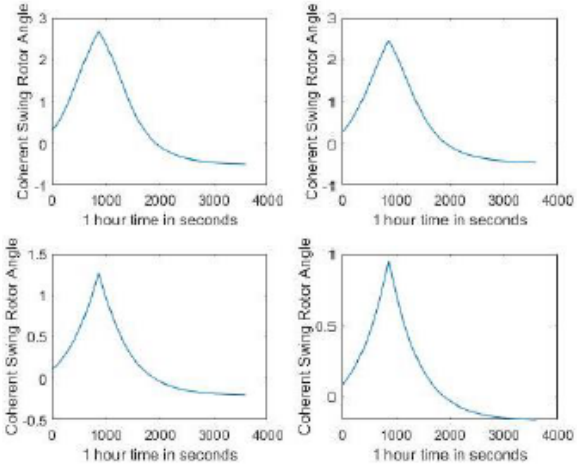

Figure 3.0 PSO-GA Optimized frequency recovery swing curves

References

[1] Energy regulatory commission of kenya, "Kenya national grid transmission code," Nairobi, 2013.

[2] Ardash TV HL Suresh, "PLC based Load Shedding Mechanism using Battery SOC in Micro Grids," in *IEEE International Conference on Power, Control, Signals and Instrumentation Engineering*, India, 2017, pp. 386-0814.

[3] KPLC, "Kenya distribution network master plan," Nairobi, 2012.

[4] Hazlie Mokhlis, "A Fuzzy based load shedding scheme for an islanded distribution network," in *Power and Energy Systems (AsiaPES 2013)*, Thailand, 2013, pp. P2013/800-088.

[5] M. Karimi, "Under-Frequency Load Shedding scheme for islanded distribution network connected with mini-hydro," *Electrical Power and Energy Systems*, pp. 127-138, 2012.

[6] Kumar Manoj Maharana K Shanti Swarup, "Particle Swarm Optimization based Corrective Strategy to Alleviate Overloads in Power System," in *World Congress on Nature & Biologically Inspired Computing*, India, 2009, pp. 4244-5612.

[7] B.O Ojwang, M. Kiprotich, Musau P, "Improving Frequency Stability for Renewable Energy Power Plants with Disturbances," in *Proceedings of the 2019 IEEE PES GTD Asia*, GTD Asia, 2019, pp. 5386-7434.

[8] Shahab Dehghan, Rasoul Moradtalab, Parizad Ali Hamid Khoshkhoo, "An Intelligent Load and Generation Shedding Procedure in an Islanded Network Using a Smart Power Management System," in *Smart Grid Conference*, SGC, 2017, pp. 4279-5386.

[9] Muhammad Muneer Azam, H. Mokhalis, Muhammad Usman Adil Amin, "Optimal Under Voltage Load Shedding Scheme for a Distribution Network Using EPSO Algorithm," in *Energy conference*, Malaysia, 2018, pp. 5386-5482.

[10] Z Matyasin, N.A Salim, NNA mohd Rahim, H. Mohamad Aimd Isa, "Optimal Load Shedding Technique for an Islanding Distribution System by Using Particle Swarm," in *Energy Conference*, Pakistan, 2017, pp. 5090-5353.

[11] Andre Richter Martin Wolter, "Under-Frequency Load Shedding in the European Interconnection System," in *Energy Conference*, uk, 2018, pp. 5386-3669.

Multi-objective Load Shedding Scheme for RE Micro-grids

Peter Moses Musau[1], Abraham Nyete[2], Paul Muia Musyoka[3]
Department of Electrical and Information Engineering
University of Nairobi
pemosmusa@gmail.com[1], nsonorig@gmail.com[2], pauilmuia80@gmail.com[3]

***Abstract*— RE micro-grid operators experience a number of challenges while planning for unit commitments in the context of intermittent RE generation sources, whose reliability is purely probabilistic. However, the current worldwide focus on environmental ambience and climate change campaigns are influencing policies in favor of RE generation and integration on existing power systems, with a vision to wipeout conventional generation. This research provides a model RE micro-grid optimization to increase their reliability in energy harvesting, through application of distributed RE storage system for provision of synthetic inertia, and deployment of a multi-faceted load shedding scheme that secures the micro-grid from voltage and frequency collapse, as a measure of last resort, while economically dispatching the available energy sources. The formulated multi-objective problem is solved by use of a hybrid particle swarm-genetic algorithm. The results illustrate improvements in aspects of frequency fluctuations, with minimal power imbalances during times of severe shortage of RE generation, and hence optimum operational controls. Once adopted in industry, this model load-shedding scheme will enable system operators to accurately weigh options on quality of service vs. grid security vs. profitability of their network.**

***Index Terms*— RE micro-grid, frequency collapse, load shedding, rotor angle stability, fault ride through, voltage collapse, multi-objective**

I. BACKGROUND

Universal access to clean and affordable energy with insistence on climate action are worldwide Sustainable Development Goals (SDGs), which every individual is striving to attain, in person, either by partnership or in business. In this setup, environmentally securing conventional power plants vs. developing renewable energy sources ends up as weighted functions, whose ultimate decision by power system operators is, most a times, based on profitability indices implied by either option.

Government and institutional regulations play a vital role, aligning public and private sector players towards attaining SDGs. In the Eastern Africa Power Pool's (EAPP) grid transmission code, a nominal frequency of 50 Hz is adopted with specific percentages of operational frequency ranges, as shown in Table A. EAPP's recommended nominal voltages include; 400kV, 500kV, 230kV, 132kV, 220kV, 110kV and 66kV, with 3 operating ranges based on prevailing conditions of voltage drops as indicated in Table B.

Table A: EAPP's Grid Operations Frequency Limits

No.	Operating Frequency Limits	Operational Condition
1.	Under system disturbance	49 to 51
2.	Operating in extreme fault	$47.75 > f \geq 51.50$ for max. of 20 seconds
3.	Large fault condition	48.75 to 51.25
4.	Normal operation	49.5 to 50.5

Table B: EAPP's recommended voltage swings for steady state operations

No.	Allowable p.u. voltage swing limit	Operational Condition
1.	0.90 to 1.10	N-1 contingency
2.	0.95 to 1.05	Normal Operation
3.	0.85 to 1.20	Multiple Contingency

This research focuses on RE micro-grids operational planning and control, aiming at highest Quality of Service (QoS) for consumers. Key factors featured in the model priorities include intermittence of weather patterns for RE generators, voltage fluctuations, frequency deviations, rate of change of frequency, cost of Distributed Renewable Energy Storage System (DRESS), amount of load shed from grid and power losses. System stability measures considered include load shedding as a measure of last resort, optimal unit commitment for minimum power imbalances and DRESS for synthetic inertia.

II. LITERATURE HIGHLIGHTS

[7] Proposes a load shedding model, in which computation of parameters such as rate of change of frequency and input frequencies are carried out using PSO and applied to set load shedding relays. A fuzzy logic model solves the uncertainty experienced in systems

setting. The results illustrate that minimum amount of load is disconnected during severe power imbalances, with optimum operations at the nominal frequency.

[8] Examined frequency collapse of a model wind farm, providing weighting factors for severe contingencies and large peak-loads, through hierarchical forms of genetic algorithm, where a diesel generation system is utilized as the base load carrier. An iterative process is constituted to perform a number of functions, including initialization of population, appending of fitness function, problem constraint checks, mutation, individual encoding, and cross over. The PSCAD simulation results indicate higher reliability of this solution, contrast to conventional approaches.

[9] Provides micro-grids with a preventive strategy against frequency collapse, that is based on instability predictions using a hardware-in-the-loop algorithm. A high rate of renewable energy penetration in the micro-grid model is considered during model validation and testing.

[10] Carried out a case study in France's Guadeloupe electrical island, in which power blackouts are lowered by use of a Distributed Energy Storage System (DESS) that is fast-acting. From this study, it is concluded that synthetic inertia possessed by DESS provides the electrical island with sufficient frequency enhancement. The model system failed to consider renewable energy sources variability, forecasting error and did not address voltage ride-through.

[11] Built a surrogate model for multi-period load flow studies, where sampling is done by use of a Latin hypercube. Polynomial and Kriging regressions for a fast convergence and highly accurate load flow solution. Compared to time sampling and voltage linearization, the model technique resulted to an efficient and satisfactory time computation of voltage profiles, bus currents and ten minute power losses.

[4] Determines optimum loads that should be shed from grid for stabilization, using a fuzzy logic technique, that takes into account frequency levels, ROCOF and load prioritization. Main disturbances i.e. generator tripping are modeled as major faults in the distribution network island, where the demand control schemes are executed based on the presented fuzzy logic model. On islanding operation and in generator tripping, satisfactory system stability is achieved.

[5] Combined adaptive and intelligent approaches and used them to develop under-frequency demand control schemes for power imbalance (event based) and swing equation based standard frequency/ ROCOF (response based) faults. The demand control scheme is applied on a distribution network island and its performance investigated. The results showcase islanding transition power deficiency reduction, and a significant improvement in terms of network frequency response.

[7] Develops a compensator (thyristor switched), for enhancing frequency stability, in which fire-fly algorithm is applied in optimizing stabilization process. Factors that were included in the model strategy for improving stability response of renewable energy power plants were; nadir frequency, settling time, ROCOF and frequency deviation. Simulation results indicate falling out of synchronism of paralleled generators due to large disturbances. High frequency deviations, higher ROCOF and least settling time characterized the turbine plants experiencing low inertia.

[8] Stabilizes voltage and frequency levels caused by power imbalances, by applying intelligent load-shedding on an islanded micro-grid's operational plan. During restoration of voltage, power losses, voltage deviations and cost of demand control are considered in a multi-objective function application.The PLC embedded functions are simulated on a Digisilent software, whose results affirm efficiency of severe contingency-demand control.

[10] Compared conventional PSO approaches of load shedding with vectored EPSO based demand controls, from where a conclusion is drawn to assert the superior precision of vectored EPSO with reference to its conventional form, in searching optimal solutions for load shedding problem.

[11] Studied under frequency load shedding for interconnected power systems in a multi-country approach, where frequency dips in high ranges were modeled. Analysis of load shedding requirements for restoration of stability and high penetration of RES in the model grid was carried out as per the ENTSO-E guidelines. System inertia, primary control and UFLS functions were modeled with respect to renewable energy sources, resulting into a highly effective demand control scheme.

III. MODELNG OF RES MICRO-GRID GENERATION SYSTEMS

a) Hydro Power Generation System

Energy harvesting from a hydropower plant is modeled according to equation (1), in which factors such as net head (H), water reservoir elevation angle (θ), summation of instantaneous volumetric flow rates from all sources (Q), efficiency (ε_t) and specific water density (γ) are considered.

$$P_i = \frac{\gamma \varepsilon_I q_i * H(\theta, Q)}{fpk * 1000} \quad (1)$$

In this equation, fpk is conversion constant for converting units of energy from feet-pound to KW

b) Wind Farm Generation System

Explicit definition of MW output of a wind farm generation system is given in equation (2), where Euler/ power co-efficient, turbine diameter and a wind velocity function are considered.

$$P = 0.5 * C_p \rho \pi R^2 * V^3 * \left(\beta, \frac{R\omega}{V}\right) \quad (2)$$

Where ω is rotor's angular velocity, (Rω/ v) is tip velocity ratio, V is velocity of wind measured, ρ is air flow density, Cp is Euler's coefficient for turbine power generation and R is rotor radius

c) Solar Photo-Voltaic Farm System

Computation of power generation from a solar PV system is achieved through application of equation (3), where nominal power (Pn) and solar irradiance (Hag) are considered.

$$P_v = \frac{G_s}{H_{ag}} * \frac{E_{pv}}{P_n} \quad (3)$$

In equation (3), Epv represents kilowatt-hour output of the system, Gs is the total conductance in series and Pv is the output electrical power from the system

d) Geo-Thermal Generation power plant

An open system for geo-thermal generation is described by equation (4), giving specific work output (sw).

where Whpt = turbine pressure upper limit, Wlpt= lower limit output power, sw =turbine specific work output

$$sw = \frac{W_{tt}}{m_1} : W_{tatol} = W_{lpt} + W_{hpt} \quad (4)$$

For equation (4), Wlpt= output power lower-limit and Whpt = maximum allowed pressure of the steam turbine, m1 = mass flux of the steam

IV. MULTI-OBJECTIVE LOAD SHEDDING SCHEME MODELING

Five main factors were considered in the development of the load shedding scheme, as shown in equation (5). These included amount of loads disconnected from the grid (LS), power losses in the distribution and transmission networks (NL), frequency fluctuations (FF), squared voltage deviations (VD) and Distributed Renewable Energy Storage System (DRESS).

$$Min\ F = \{\varphi_1 NL + \varphi_2 LS + \varphi_3 VD + \varphi_4 FF + \varphi_5 DRESS\} \quad (5)$$

The magnitude and co-relation of each individual factor's effect on system stability is weighed by weighting factors denoted by φ_n, in equation (1).

Each of these five sub-functions is formulated as per the following equations (6-10) ;

A. Distributed Renewable Energy Storage System (DRESS)

Distributed Renewable Energy Storage Systems (DRESS) provide power supply during times of severe imbalances, enhancing system stability with a synthetic inertia. However the storage system capacity and cost are limiting factors in the network design. Equation illustrates the DRESS model that considers capacity based costs for charging fuel C_{PGi}, capital equipment (C_{EAi}), reduction of power not supplied by the grid during severe shortage (C_{RESi}), amount of stored energy(P_i) and DRESS system based supply periods (T).

$$DRESS = \{\sum_{i=1}^{T}(C_{PGi} - C_{RESi} + C_{EAi}) * P_i\} \quad (6)$$

B. Frequency Fluctuations (FF)

Occurrence of frequency deviations that violate the specified operational limits of Table A are prevalent during power shortages in the RES. Equation (7) models these fluctuations from swing curve derivation. In this equation, fs denotes a quantity in the faulty operation state while n denotes a quantity in the allowed normal operation state. PGA is the available power generation, CPD is connected demand at the instant while H is the inertia constant.

$$FF = 2\left[\left(\frac{\frac{df_n}{dt} * H_n}{PGA_n - CPD_n}\right) - \left(\frac{\frac{df_{fs}}{dt} * H_{fs}}{PGA_{fs} - CPD_{fs}}\right)\right] \quad (7)$$

C. Voltage Deviations (VD)

Operating the micro-grid at voltages without the limits provided in Table B stress the system insulation beyond expected IEC 60071-1 standard

limits. Squared voltage deviations are minimized as per equation (8), where Vi and Vp are voltage leves in jth bus and the reference/ swing bus respectively, during abrupt voltage swings. In this equation, the total number of nodes is considered as P

$$VD = \sum_{i=1}^{P} \frac{(v_i - v_p)^2}{v_p^2} \quad (8)$$

D. Amount of Load Disconnected from grid to recover frequency (LS)

During operational periods where available power supply is less than power demand, an optimum (least) amount of load has to be disconnected from the network to restore system back to stability. The power discrepancy is formulated in equation (9), according to swing equation. Hn is inertia constant of Mth generator, M = total number of generators available the power system network, pm is available mechanical power in the turbine, Pe = electrical load and fo= standard operating frequency.

$$LS = \sum_{m=1}^{m} Pm_m - \sum_{m=1}^{m} Pe_m = \frac{2\sum_{m=1}^{m}\left\{H_m \frac{df_m}{dt}\right\}}{f_0} \quad (9)$$

E. Distribution / Transmission Network Losses (NL)

Equation (10) provides the power flow that is run on a modified IEEE 9 bus system, to derive the power losses resulting from the micro-grid transmission network, while a 15 to 18 percent power loss is provided for the distribution network, according to energy efficiency report of the world bank 2019 for Kenyan grids. From equation (10), reactive and active power losses are obtained. In this equation, G represents conductance and B is the susceptance while P is the total number of network nodes in the study model network.

$$NL = \sum_{n=1}^{p}\sum_{m=1}^{p}\{(B_{nm}\sin\theta_{nm} + G_{nm}\cos\theta_{nm})V_n V_m\} \quad (10)$$

F. *Multi-objective Function constraints*

Constraints considered in the MoF formulation included: Maximum generator's active and reactive power, bus voltages, allowable frequency limits, load priority and storage capacity of the DRESS.

V. SIMULATION METHOD

To escape local minima snares and ride through immature convergences, a mutation operation was prescribed in the iterative process required to solve the multi-objective function. To provide diversity, cross-over operation was considered while a reduced dimensionality was achieved by partitioning the populations, with higher crossover probability. Individual iterations required exploitation and exploration of a balanced fitness function evaluation, which would optimally be achieved by applying particle swarm optimization algorithm. These beneficial requirements led to selection of the hybrid particle swarm – genetic algorithm method for solving the multi-objective function, subject to outlined constraints.

The MATLAB Simulation algorithm was developed as per the following sequence of steps, solving the formulated problem

a) Initialization of variables such as size of population, mutation and crossover probabilities, number of partitions, swarm's acceleration constants, partition variables and individual chromosomes
b) Generation of search agents through evaluation of fitness function (MoF)
c) PSO application over the populations
d) Carry out GA selection operation on the population
e) Population partitioning into small size populations
f) Crossover application on every partitioned population
g) Carry out mutation operation the swarm
h) Best positions update for both global and individual
i) Check if the convergence criteria is met and iterate until the condition is met
j) Stop and print simulated solution

During application of PSO, velocities and positions of particles are updated as per equations (11) and (12). In these equations, glob = global best position, z particle position, j = iteration number, pos = best particle position attained and s = particle velocity,

$$z_j^1 = z_j^0 + s_j^1, \quad j = 1, 2, 3, 4 \ldots P \quad (11)$$

$$v_j^1 = s_j^0 + \epsilon_1 r_{j1}(pos_j^0 - z_j^0) + \epsilon_2 r_{j2}(glob - z_j^0) \quad (12)$$

A pair of γ such that $\gamma \in [0\ 1]$ is selected randomly, for the crossover operation, generating the two offspring from parents such that;

$$ch_j^1 = \gamma parent_j^1 + (1-\gamma) parent_j^2 \quad (13)$$

$$ch_j^2 = \gamma parent_j^2 + (1-\gamma) parent_j^1 \quad (14)$$

In equation (13) and (14), ch = offspring, parent= population and j is number of the iteration

VI. ANALYSIS OF RESULTS

a) Response time, convergence and Algorithm calculation time

Specification for the response time during recovery, were largely determined by size of power imbalances present in the micro-grid. Utmost 20 seconds were specified for extreme power imbalances, whose magnitudes initiate frequency swings such that operating frequency is less 47.75 Hertz, or greater than 51.50 Hertz. Algorithm computation time for the fitness function was observed to be 0.3575 seconds, and convergences within first 50 iterations. An utmost time period of 10 seconds was specified for bearable faults whose frequency swings do not exceed the lower and upper limits of Table A.

b) load profiling curve for the model micro-grid

Western Kenya region typical load curve was utilized for the examination of potential deficits between demand and generation, as shown in Fig. 1.

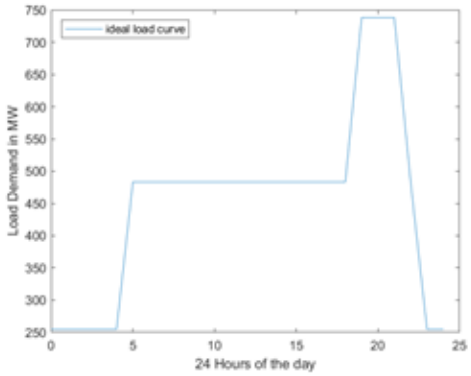

Fig. 1 Model micro-grid Load profiling curve

c) Commitment curve at the optimal generation points

Depending on available generation, load curve tracking was considered for optimization of the dispatch, with 2 best solutions as illustrated in Fig. 2. The committed units are utilized in power flow study. The commitment curves with minimum discrepancy between generation and load are considered optimal solutions.

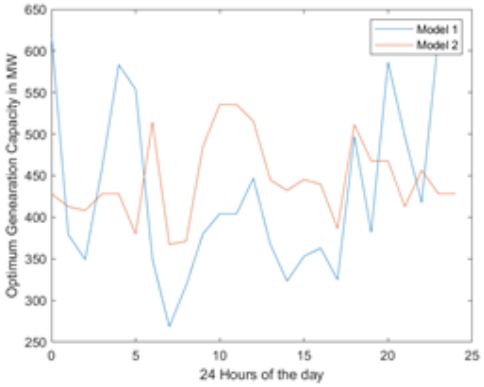

Fig. 2 Optimized commitment curves

d) Model Micro-grid Transmission and Distribution (TD) Losses

Equivalent IEEE 9 bus system was modeled for examination of the losses, in which the transmission losses are obtained from the load flow, while the distribution losses are considered at 15% on the lower limit and 18% on the upper limit, as per the united nations energy efficiency survey 2019. Power loss profile curves are shown in the diagram of Fig. 3

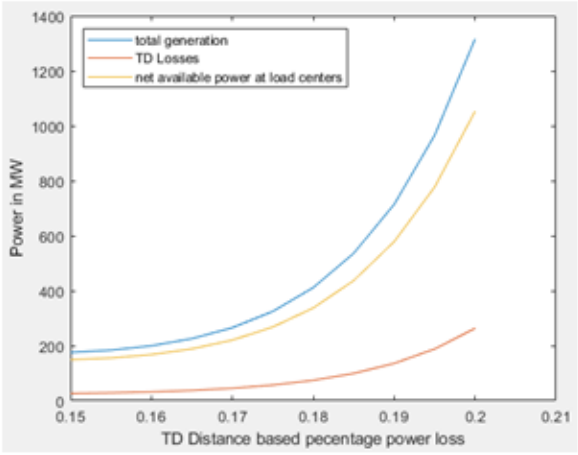

Fig.3 Model micro-grid Transmission and Distribution network losses

e) *Pre-load shedding swing curve upon Transient Stability study*

Considering power imbalances as the renewable micro-grid system disturbances, a transient stability study was carried out, with the results indicated in Fig. 4. Severe instabilities are experienced, requiring immediate load shedding as a measure of last resort, towards achieving recovery from frequency collapse

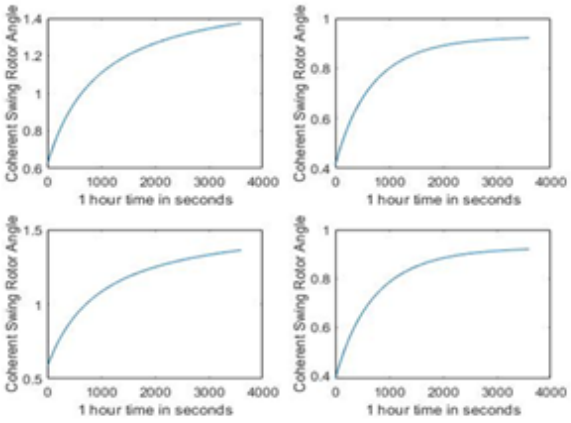

Fig. 4 pre-load shedding Swing Curves

f) Transient Stability Swing Curve after Load Shedding

To relieve micro-grid from overloads, the respective relays are selected based on the load combinations computed by the PSO-GA algorithm. The optimally restored stable system swing curves are given in Fig. 5. Optimum selection is based on the tendency towards zero point criterion, which is the most stable rotor angle.

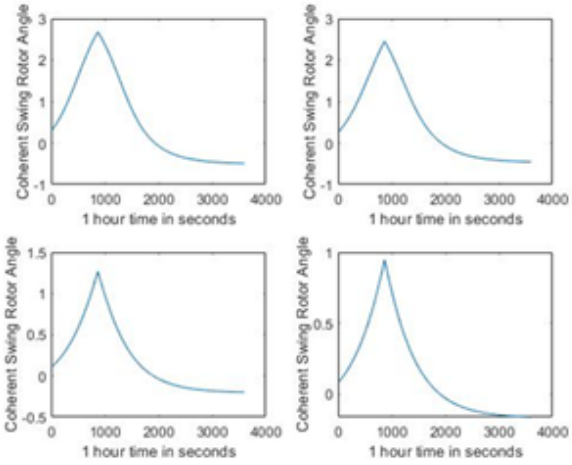

Figure 3: Optimum Frequency Swing Curves based on PSO-GA

VII. CONCLUSION AND RECOMMENDATIONS

Adoption of the optimal load shedding scheme developed in this thesis, will definitely assure operators of off-grid systems, of a full exploitation of opportunities and options available in a load shedding process. These opportunities are composed of the five objective components, i.e. frequency fluctuations, voltage deviations, battery storage, amount of loads shed and power losses. Once adopted in power systems operation, the optimized load shedding scheme will provide minimal interruptions/ blackouts, for minimal periods, while maintaining a secure operational margin, for a highly profitable power network operation during severe power imbalance. It is therefore necessary for off-grid operators to adopt the developed optimal load shedding scheme.

Intelligent search using PSO-GA algorithm for optimal load shedding scheme results into minimum load sheds to attain required transient stability levels. However the amount of load disconnected from the grid may be slightly larger due feeder sizing. Loads tapping from a feeder are uncontrolled from the power station and only the whole feeder can be switched on or off.

However, in such a study the equivalent network consists of "virtual" machines whose stability may not reflect the real behavior of the multi-machine system, where some machines will retain synchronism and others fall out of step, in times of power imbalances. More accurate equivalent networks that can be extended backwards to tell the behavior of each machine's transient stability according to individual inertia constants is necessary.

References

[1] Gunjan Dashora and Payal Awwal, "Adaptive particle swarm optimization employing fuzzy logic," in International conference on recent advances and innovations in Engineering (ICRAIE), 2017.

[2] Ying-yi Hong and Shih-Fan Wei, "Multi-objective Under frequency load shedding in an autonoumous system using hierarchical genetic algorithms," in IEEE transactions on power delivery, 2010.

[3] Shiyou Yang and Peihong Ni Jiagiang Yang, "A vector tabu search algorithm with enhanced searching ability for pareto solution and its application to multi-objective optimizations," IEEE, vol. 52, no. 3, pp. 1-5, 2016.

[4] Bruno François, Gilles Malarange Gauthier Delille, "Dynamic Frequency Control Support by

Energy Storage to Reduce the Impact of Wind and Solar Generation on Isolated Power System's Inertia," IEEE TRANSACTIONS ON SUSTAINABLE ENERGY, vol. 3, no. 4, October 2012.

[5] Gauthier Delille, Bruno Francois, Julien Bect, Marjorie Cosson, Dutrieux Baraffe, "A novel non-intrusive approximation method to obtain fast and accurate multi-period load-flows for distribution network planning," HAL, August 2017.

[6] M. Karimi, "Under-Frequency Load Shedding scheme for islanded distribution network connected with mini-hydro," Electrical Power and Energy Systems, pp. 127-138, 2012.

[7] Kumar Manoj, Maharana K and Shanti Swarup, "Particle Swarm Optimization based Corrective Strategy to Alleviate Overloads in Power System," in World Congress on Nature & Biologically Inspired Computing, India, 2009,

[8] Shahab Dehghan, Rasoul Moradtalab, Parizad Ali, Hamid Khoshkhoo, "An Intelligent Load and Generation Shedding Procedure in an Islanded Network Using a Smart Power Management System," in Smart Grid Conference, SGC, 2017

[9] Muhammad Muneer, Azam, H. Mokhalis, Muhammad Usman, Adil Amin, "Optimal Under Voltage Load Shedding Scheme for a Distribution Network Using EPSO Algorithm," in Energy conference, Malaysia, 2018,

[10] Z Matyasin, N.A Salim, NNA mohd Rahim, H. Mohamad, Aimd Isa, "Optimal Load Shedding Technique for an Islanding Distribution System by Using Particle Swarm," in Energy Conference, Pakistan, 2017

[11] Andre Richter and Martin Wolter, "Under-Frequency Load Shedding in the European Interconnection System," in Energy Conference, uk, 2018

Appendix C: IEEE 9 Bus System Data

Section 1: Machine Data

IEEE 9-BUS MODIFIED TEST SYSTEM MACHINE DATA

Type	GENROU	GENROU	GENROU
Operation	Sync. Gen.	Sync. Gen.	Sync. Gen.
Default Unit no. (New Unit no.)	1(12)	2(10)	3(11)
Rated power (MVA)	512	270	125
Rated voltage (kV)	24	18	15.5
Rated pf	0.9	0.85	0.85
H (s)	2.6312	4.1296	4.768
D	2.000	2.000	2
r_a (p.u)	0.004	0.0016	0.004
x_d (p.u)	1.700	1.700	1.220
x_q (p.u)	1.650	1.620	1.160
x'_d (p.u)	0.270	0.256	0.174
x'_q (p.u)	0.470	0.245	0.250
x''_d (p.u)	0.200	0.185	0.134
x''_q (p.u)	0.200	0.185	0.134
x_l or x_p (p.u)	0.160	0.155	0.0078
T'_{d0} (s)	3.800	4.800	8.970
T'_{q0} (s)	0.480	0.500	0.500
T''_{d0} (s)	0.010	0.010	0.033
T''_{q0} (s)	0.0007	0.0007	0.070
$S(1.0)$	0.090	0.125	0.1026
$S(1.2)$	0.400	0.450	0.432

Section 2: Exciter Data

IEEE 9-BUS MODIFIED TEST SYSTEM EXCITER DATA

Type	IEEET1	IEEET1	IEEET1
Default Unit no. (New Unit no.)	1(12)	2(10)	3(11)
Rated power (MVA)	512	270	125
Rated voltage (kV)	24	18	15.5
T_r (s)	0.000	0.000	0.060
K_a (p.u)	200	30	25
T_a (s)	0.395	0.400	0.200
V_{Rmax} (p.u)	3.840	4.590	1.000
V_{Rmin} (p.u)	-3.840	-4.590	-1.000
K_e (p.u)	1.000	-0.020	-0.0601
T_e (s)	0.000	0.560	0.6758
K_f (p.u)	0.0635	0.050	0.108
T_f (s)	1.000	1.300	0.350
E_1 (p.u)	2.880	2.5875	2.4975
$SE(E_1)$	0.000	0.7298	0.0949
E_2 (p.u)	3.840	3.450	3.330
$SE(E_2)$	0.000	1.3496	0.37026

Section 3: Governor Data

IEEE 9-BUS MODIFIED TEST SYSTEM GOVERNOR DATA

Type	BPA_GG	BPA_GG	BPA_GG
Default Unit no. (New Unit no.)	1(12)	2(10)	3(11)
Rated power (MVA)	512	270	125
Rated voltage (kV)	24	18	15.5
P_{max} (p.u)	0.8984	0.8518	1.056
R (p.u)	0.00976	0.01852	0.040
T_1 (s)	0.150	0.100	0.083
T_2 (s)	0.050	0.000	0.000
T_3 (s)	0.300	0.259	0.200
T_4 (s)	0.260	0.100	0.050
T_5 (s)	8.000	10.000	5.000
F	0.270	0.272	0.280

Section 4: Modified IEEE 9 Bus System Layout Diagram

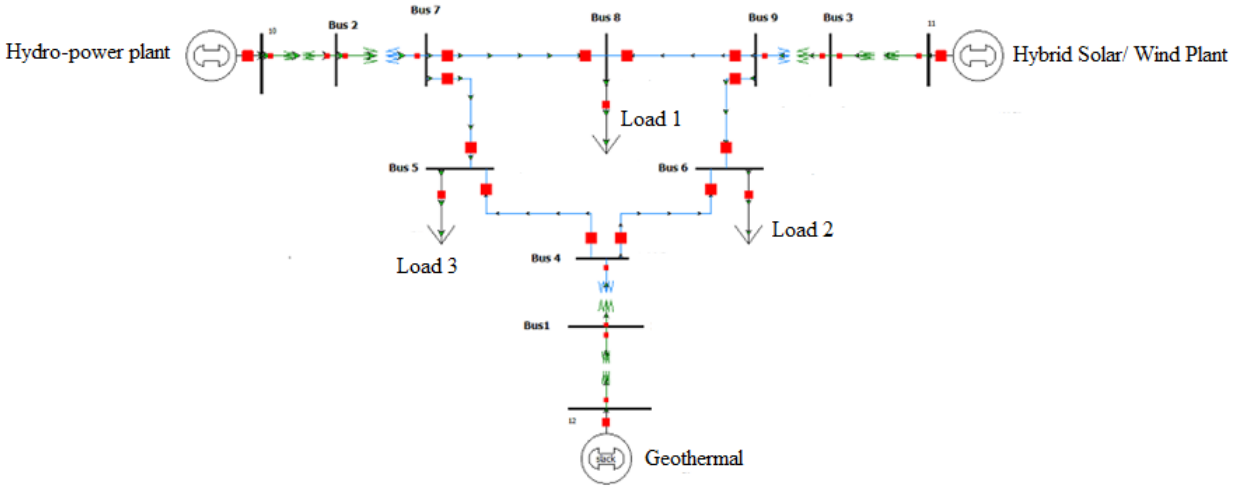

Appendix D: Plagiarism Report - Similarity Index

Plagiarism Report - Similarity Index

Name: Paul Muia Musyoka

Reg. No: F56/6984/2017

Topic: Development of Optimal Under-Frequency Load-Shedding Scheme With Renewable-Energy Student

Turnitin has been used to do a fully inclusive scan for similarity index (including all sections of thesis i.e. cover page, preliminary pages, references page and appendix). In overall, the similarity index is 13% which is composed of 6% internet sources (corporate reports), 8% from published articles and 11% from student papers (depositories of different universities).

MSC Thesis

ORIGINALITY REPORT

13%	6%	8%	11%
SIMILARITY INDEX	INTERNET SOURCES	PUBLICATIONS	STUDENT PAPERS

PRIMARY SOURCES

1	studentsrepo.um.edu.my Internet Source	1%
2	Submitted to Poornima University Student Paper	1%
3	Submitted to Nanyang Technological University, Singapore Student Paper	1%
4	Submitted to University of Nairobi Student Paper	<1%
5	Submitted to Universiti Teknologi MARA Student Paper	<1%
6	Submitted to University of Edinburgh Student Paper	<1%
7	Submitted to Monash University Student Paper	<1%
8	Submitted to Universiti Putra Malaysia Student Paper	<1%
9	Alshammari Fahad, El-Refaie Ayman.	

Dr P Musau : Signature: **Date: ....05th May, 2020**

DEAN
SCHOOL OF ENGINEERING
UNIVERSITY OF NAIROBI
P. O. Box 30197, NAIROBI

26.02.24